FRACTURE SURFACES OF GLASS

Being a thesis on

"The physical significance of the presence of the mirror, mist and hackle morphology on glass fracture surfaces".

by

J.W. Johnson, B.A.

Presented to the University of Keele for the Degree of Ph.D.

Department of Physics,
University of Keele,
KEELE,
Staffordshire,

October 1963.

BEST COPY AVAILABLE.

VARIABLE PRINT QUALITY

MISSING PRINT

SYNOPSIS

Glass specimens tested in simple tension, bending, or torsion, with breaking strengths up to approximately 100 Kg/mm^2, develop a characteristic morphology of the fracture face which has become known as "mirror, mist and hackle". This general pattern and some variants have been observed in the fracture of other materials. Smekal (1) has defined a quantity called the "reduced tensile strength" based upon this fracture pattern. During an unsuccessful experimental reexamination of Smekal's parameter, an empirical relationship between breaking strength and the "mirror" depth was observed. This relationship, arising from an independent observation, was later found to have been used by several workers (Levengood (2) Shand (3), (4), but had not been examined in any detail by them. The relationship may be expressed in the form

$$Zc^{\frac{1}{2}} = \text{constant}$$

where Z is the breaking strength,

and c is the "mirror" depth (a term fully defined later).

The experiments described in this thesis have yielded information on the numerical value of the constant in the above relationship and on the significance of the characteristic morphological fracture pattern itself.

Chapter 1 describes the gross features of the mirror, mist and hackle pattern and defines some of the terms in constant use throughout the work.

The second chapter describes the apparatus and techniques used to measure the numerical value of $Zc^{\frac{1}{2}}$ for some common glasses under various experimental conditions.

The results are reviewed briefly in Chapter 3. The main conclusions are that at a given temperature of test the value of $Zc^{\frac{1}{2}}$ for any one glass is constant, but different for different glasses. The constant appears to be unaffected by the surrounding media and is relatively insensitive to the fibre drawing method. For one glass a variation in the value of $Zc^{\frac{1}{2}}$ with temperature seems likely. Particular attention is paid to the results of tensile and bend tests on "as received" soda glass rods which suggest a method of determining the mirror shape to be expected from tests conducted with different stressing systems. Also in this chapter is a review of previous observations of the empirical fact that $Zc^{\frac{1}{2}}$ = constant.

Chapter 4 describes the qualitative examination of detail in the mist zone with the aid of optical microscopy. This examination showed the presence of stopped sub-surface micro-cracks in the mist zone which correlate with surface features. It is proposed that the morphological elements making up the mist zone can be classified by introducing two generalised types of mist feature. A discussion concerning the possibility of explaining the formation of these features in terms of micro-crack interaction follows. Finally this chapter closes with a discussion of possible mechanisms of micro-crack formation during crack growth and the acceptance of secondary nucleation as a working hypothesis.

Chapter 5 contains a review of theoretical work having a bearing on the problem of the formation of the mirror, mist and hackle morphology.

Chapter 6 discusses the energetics of brittle fracture in real materials with reference to the work of Griffith (5) and Mott (6).

Using a critical energy criterion for the bifurcation condition and utilising the work of Culf (7), a form of Mott's equation is proposed which gives theoretical $Zc^{\frac{1}{2}}$ values for glass approaching those found in practice. This criterion associates the value of $Zc^{\frac{1}{2}}$ with the fracture energy of the material. Further discussion is given to the possibility of extending these principles to include other materials. The theoretical value for $Zc^{\frac{1}{2}}$ in perspex is predicted on this basis. The postscript gives a brief account of further experiments performed to check this latter value. Preliminary results show encouraging agreement between theory and experiment even for this material.

ACKNOWLEDGEMENTS

I should like to thank:-

Professor D.J.E. Ingram	-	for the use of laboratory and research facilities
Dr. D.G. Holloway	-	for his advice, discussion and careful supervision
Mr. W. Brearley	-	for practical assistance as specified in the postscript
Mr. F. Rowerth and Mr. G. Dudley	-	for the use of technical and workshop facilities
Rolls-Royce Limited	-	for their financial support
The Typist	-	for care in typing this thesis

CONTENTS

LIST OF FIGURES

Facing Page

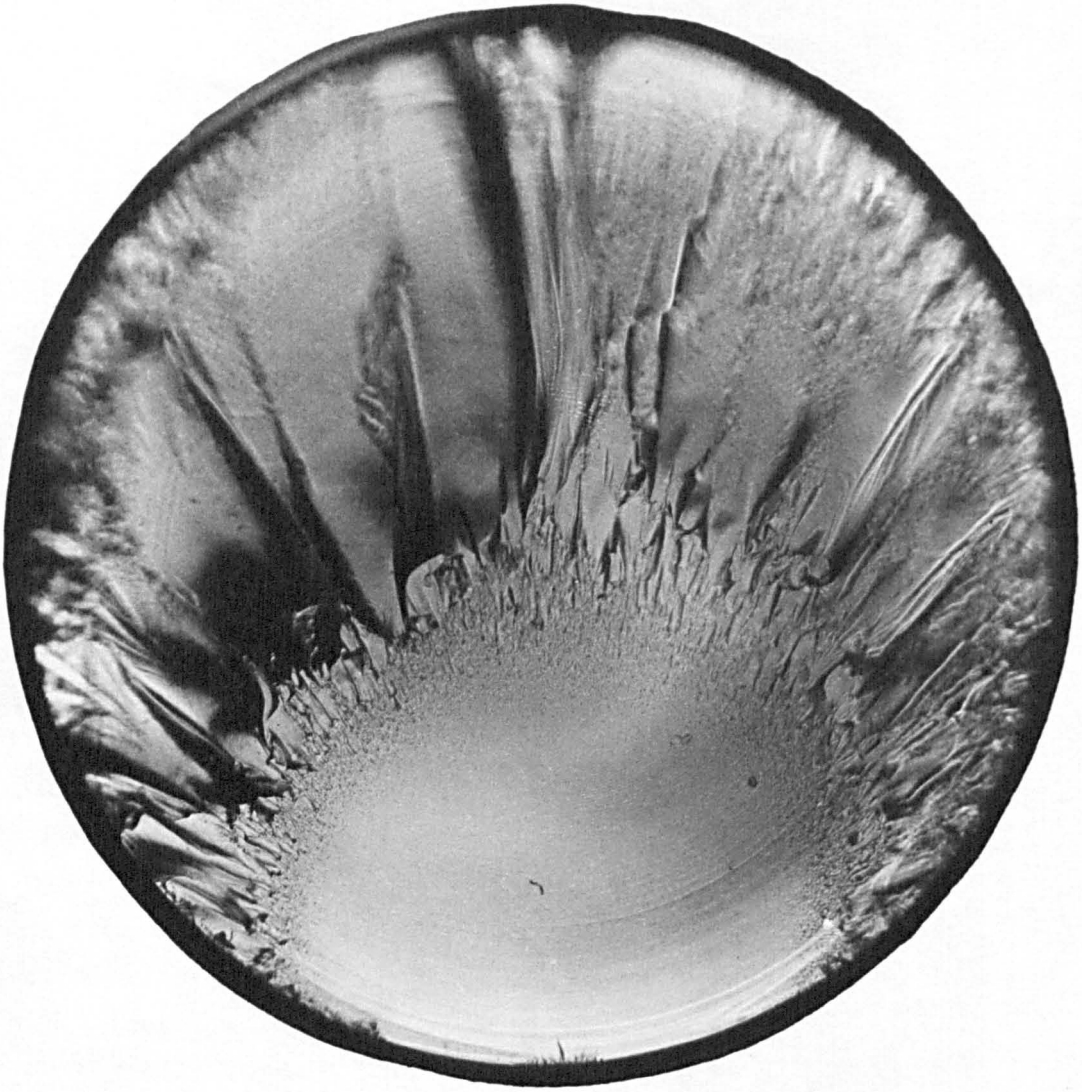

Fig. 1

Typical mirror, mist and hackle. Annealed X8 rod broken in tension. Magnification x 45. Vertical incident illumination.

CHAPTER 1 THE CHARACTERISTICS OF "WEAK" FRACTURE OF GLASS RODS AND FIBRES

1.1 Introduction

The study of complex fractures is of considerable practical importance to glass technology. Often an analysis of the fracture system together with a study of the fracture faces makes it possible to draw conclusions concerning the origin and cause of fracture. Preston (8) has given what is probably the most comprehensive general survey of the field of fracture phenomena for the failure of sheets of glass, and other glass objects and masses under a variety of mechanical and thermal stresses. Recently interest in this type of study has increased and widened to include a variety of different materials e.g., single crystals, polymers, polycrystalline metals etc. Probably this is because there are many associated fracture phenomena which are able to provide a certain amount of information on the physical and mechanical properties of the material. As far as glass is concerned, experiments which involve the examination of fracture faces are usually confined to instances in which the specimens have been induced to fracture at relatively low stress levels, i.e., a few tens of Kg/mm^2. This is because a specimen failing at, for example, 360 Kg/mm^2 is usually reduced to fragments, many of the pieces acquiring considerable velocities. There is therefore little left to examine after such a fracture. It must be borne in mind that anything which is said concerning the fracture process subsequently, cannot at the moment be proved to have equally valid application to fracture in such high strength material.

Attention will be largely confined in this work to the fracture characteristics of glass tested in tension or bending

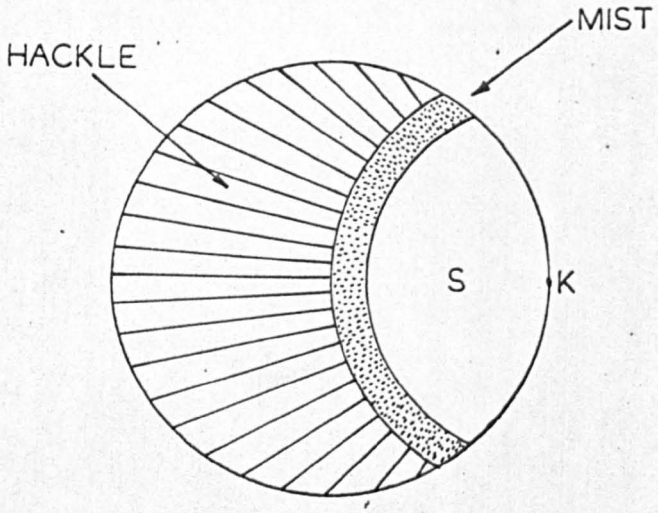

(a)

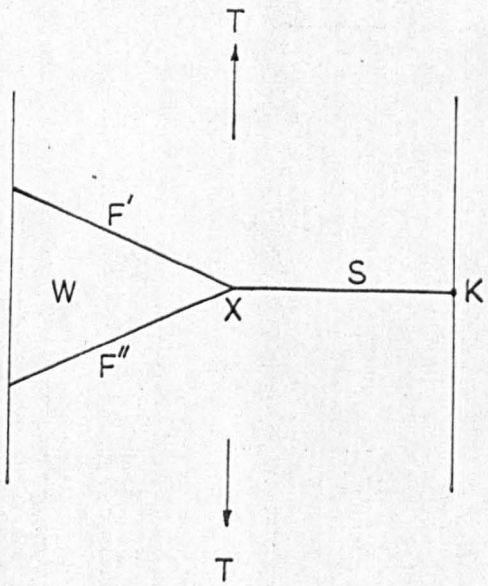

(b)

Fig. 2

Diagrammatic plan and elevation of a fracture surface.

when failure is induced at low stress levels (i.e., 3 - 70 Kg/mm^2). Under these conditions a specific and constant type of morphological pattern appears on the fracture surface. A typical example of one such pattern is shown in Fig. 1. It is convenient at this point to give an account of the typical features of fracture surfaces, using the fracture pattern of Fig. 1 as the archetype, and define some terms which will be in continuous use throughout the text.

1.2 Fracture of weak glass rods and fibres in tension

If a glass rod or fibre, of low strength (i.e., 3 - 70 Kg/mm^2), is broken by means of an axial pull, then the fracture surfaces always develop the same morphological features. One such surface is shown in Fig. 1. The most important points are, that fracture commences in a direction approximately at right angles to the direction of maximum tension, and subsequent events take place in a characteristic order, this order always remaining the same. The crack is nucleated at a local flaw K (diagrams a, b - Fig. 2) existing usually on the surface of the rod and propagates perpendicularly to the tensile axis as shown at S (diagram b - Fig. 2). The crack continues in this direction for some part of the way across the specimen, how far, in this simple case, depends to some extent on the severity of the flaw existing on the glass surface before fracture since this determines the external applied stress at which the specimen fails. If the rod has been heavily damaged the fracture may continue right across in the same plane. Usually however, after breaking through the area S, the primary crack branches at X and two cracks F' and F'' are subsequently propagated. As a result of this a wedge of glass W of crescent shape is thrown out during the fracture

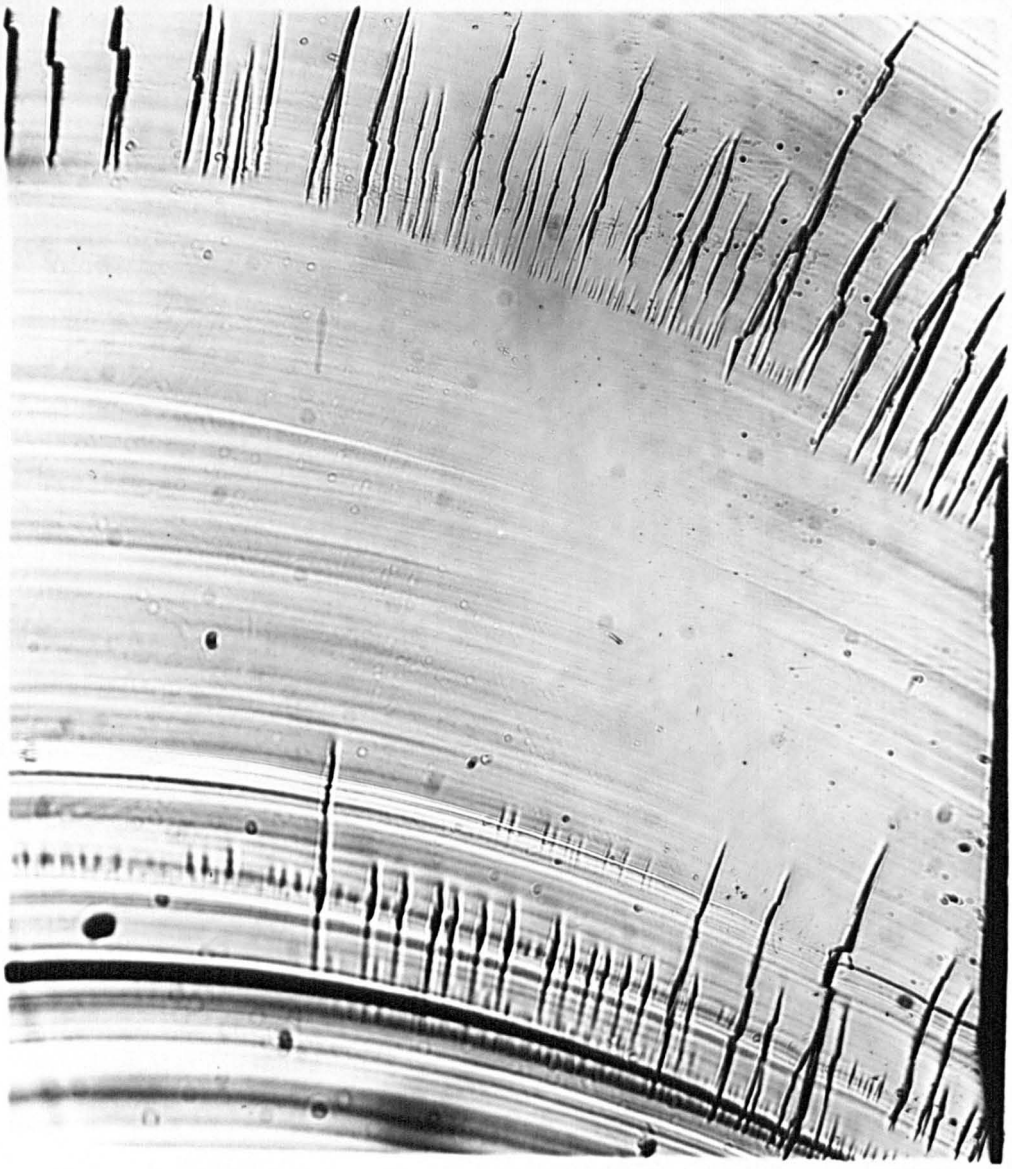

Fig. 3

Photomicrograph of ribs and striae in an X8 fracture surface (see text). Magnification x 75. Transmitted light.

process, Three more or less distinct and separate zones can be indicated on the resultant fracture surface, The separation into three zones was originally due to Poncelet (9) and the nomenclature used here is that of Andrews (10). A part of the surface is optically smooth and perpendicular to the tensile axis, this is usually called the mirror, and is the area S as shown in Fig. 2a. It is surrounded by an arcuate area with a stippled surface appearance when observed under a low power optical microscope. This second zone is called mist. The third zone consists of the remaining part of the fracture surface and is called hackle*. The surface of the hackle area consists of macroscopic furrows directed radially towards the fracture origin, but the surface of individual furrows is smooth. The transition area between the zones of mist and hackle is detected as an irregular arc more or less concentric with the mist arc (see Fig. 1 and Fig. 2a). It is at points along this irregular arc that the initial crack bifurcates by some mechanism, and two independent cracks are propagated (F' and F'') in two planes forming a small angle with each other. The dividing line between the mirror zone and the mist zone (the inner locus), cannot be placed with the same certainty as that

---

* Footnote: the term hackle used here defines an area of the fracture surface. It has been used previously by Murgatroyd (11) to denote certain surface features associated with rib markings. The rib and hackle features of Murgatroyd are called here ribs and striae - see Fig. 3.

between mist and hackle (the outer locus). In fact, assigning a position to the inner locus is an entirely arbitrary process and is nearly always dependent on a set of subjective conditions being satisfied. Often, especially when the mirror is small, a new formation of mist can be seen within the furrows of the hackle area. This precedes a second bifurcation of both cracks (F' and F'') and sometimes, in favourable cases, further instances of crack bifurcation can be seen.

Although the description given above refers to fracture surfaces produced in tensile tests on glass, in fact it is also possible to produce the mirror, mist and hackle morphology in bending and torsion as well. When complete mirrors are formed it is possible to see that each separate stressing system produces characteristic changes in the shape or profile of the mirror area. An attempt to unify the whole problem of the variation in mirror profiles will be included in Chapter 3.

Attention will be largely confined in this work to the mirror, mist and hackle pattern produced in glass when tested in tension or bending, and the morphological features to be considered are those associated with this fracture pattern. The existence of surfaces bearing other types of fracture face (e.g., see Fig. 3) is recognised. Usually these features develop in complex stressing systems and will not be considered further except insofar as they enter the general discussion.

The mirror, mist and hackle pattern is not confined to glass, a wide variety of brittle or semi-brittle materials show broadly similar features on their fracture surfaces. These materials can vary both

in homogeneity, e.g., pitch and rubber at low temperature, and in structure, e.g., ceramics, and crystalline materials like LiF and NaCl. The similarity of these fracture patterns in different materials indicates that they may have a common basis for their production. Following the considerations of the fracture process in glass given in the final discussion, an attempt will be made to generalise the arguments advanced there to include a wider variety of materials.

In addition to various qualitative studies (8), (9), (10), Smekal (1) has been responsible for a quantitative examination of the mirror mist and hackle phenomenon.

1.3 The relationship $Zc^{\frac{1}{2}}$ = constant

Smekal (1) has given an expression which shows that, for tensile test producing the mirror, mist and hackle morphology, the ratio of the load at fracture to the area occupied by the hackle should be constant. This ratio was called by Smekal "the reduced tensile strength". The very early experimental phase of the work reported in this thesis was performed to examine the reproducibility of Smekal's parameter, which naturally depends upon the development of the mirror, mist and hackle morphology. The work was soon abandoned since no sensibly constant value could be obtained for the "reduced tensile strength". In addition the limits on the acceptable mirror size set by Smekal diminished the usefulness of this parameter for experimental purposes. However, another empirical relationship was observed to hold true for the same specific morphological pattern. This relationship, subsequently found to have been recorded by a number of workers (Levengood (2), Shand (3), (4), Terao (12)), can be most easily stated as follows,

$$Zc^{\frac{1}{2}} = \text{constant} \qquad 1.3.1$$

where Z is the tensile stress at fracture,

and c is the mirror depth.

A full definition of what is meant by these terms is given later. The relationship represented by Eq. 1.3.1 had apparently not been examined in any detail previously. Such an examination forms the substance of Part I of this work. The experimental work described refers in the main to determinations of the value of $Zc^{\frac{1}{2}}$ for different glasses under various conditions of test. The results show that the value of $Zc^{\frac{1}{2}}$ is constant for any one glass, but different for different glasses. The value of the constant is apparently unaffected by specimen drawing conditions except where these lead to real mechanical stresses in the material, in which case the value of the constant is affected. In addition, a variation in the value of $Zc^{\frac{1}{2}}$ as a function of temperature has been found for one glass. The results are given a preliminary discussion, but full interpretation is not possible until the phenomenological evidence presented in Part II is properly evaluated.

CHAPTER 2 EXPERIMENTAL TECHNIQUES AND RESULTS

2.1 Introduction

The present chapter is devoted to an account of the experiments performed to measure the value of $Zc^{\frac{1}{2}}$ for glasses and determine the variation of this value with changes in the experimental testing conditions and changes in the methods of specimen production. It should be emphasised that these experiments are in the nature of a preliminary survey and the extension of some of the experiments performed to embrace a wider range of glass types would be both profitable and desirable.

2.2 Specimens and glasses used to measure the value of $Zc^{\frac{1}{2}}$

Glasses used were:-

1. Vitreosil - Thermal Syndicate Limited.
2. X8 - G.E.C., soda-lime-silica glass, Mg. pt. 560°C, nominal composition as given below,

SiO_2	"	70.5%	Na_2O	"	16.3%
Al_2O_3	"	2.6%	K_2O	"	1.2%
CaO	"	5.7%	B_2O_3	"	0.5%
MgO	"	2.9%	SO_3	"	0.2%

3. L1 - G.E.C., lead glass, Mg. pt. 470°C, nominal composition.

SiO_2	"	56%	K_2O	"	8.0%
PbO	"	30%	Na_2O	"	4.6%
Al_2O_3	"	1.3%			

Tests were conducted in bending and tension on 3mm and 5mm rod, and in tension on fibres (diameters from 0.5mm to 1mm). In forming the rod specimens for tensile tests, lengths of 3mm or 5mm cane were cut into pieces 8 - 12cms long and these were wiped with a clean cloth to remove

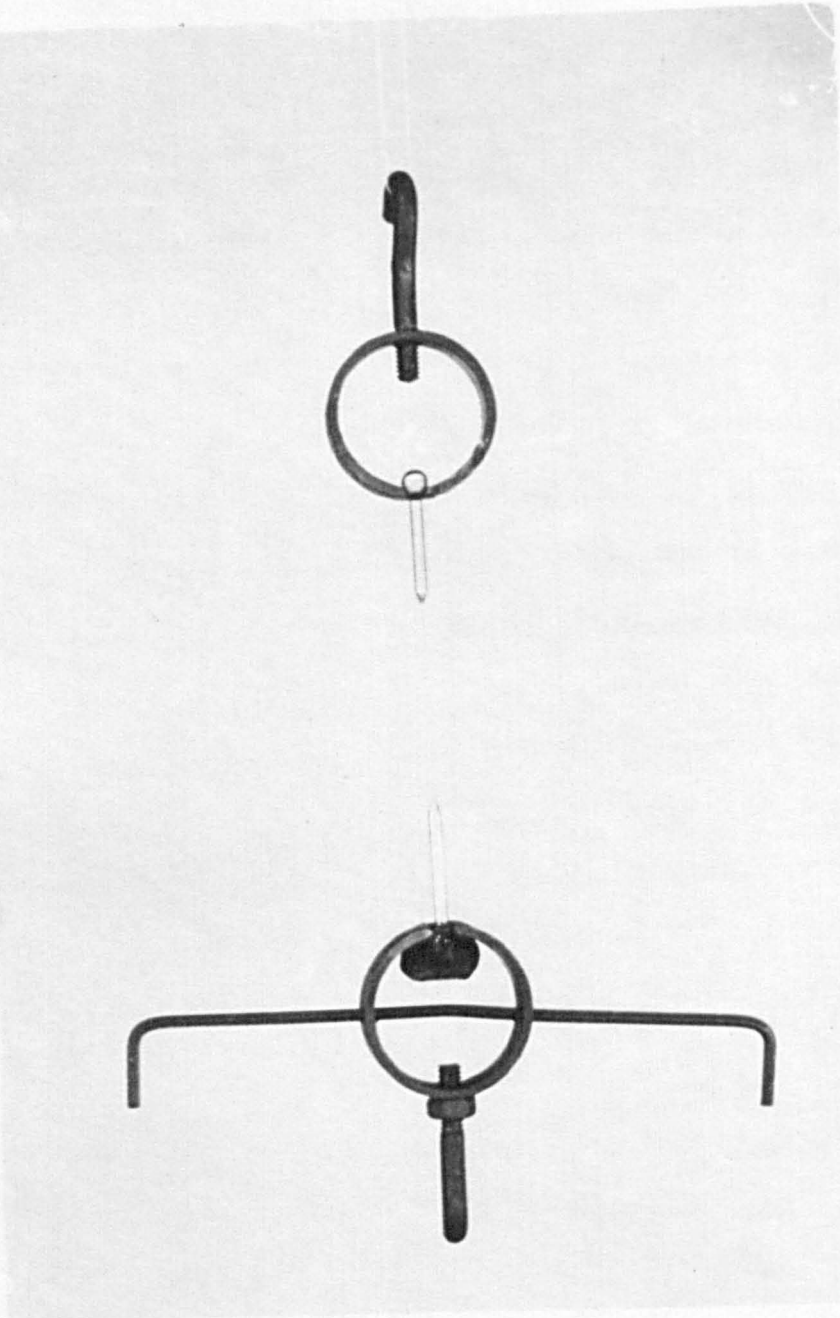

Fig. 4

Slotted ring-grips. Magnification x $\frac{1}{2}$.

excess grease and dirt. By heating a small length of each rod-end in an oxy-coal-gas flame and rotating the rod whilst cooling, a symmetrical glass ball was formed on each end of the rod. These balls provided the means of holding the specimen for test in slotted ring grips, as in Fig. 4. To form fibres, the central portion of a rod specimen was heated in a fairly hot flame with simultaneous rotation of the specimen; this hot zone was then removed from the flame and pulled by hand to the desired diameter.

It was found that pre-treatment of the specimens was required to give a useful distribution of mirror sizes, and this was accomplished by damaging the samples by one of two methods. The 3mm and 5mm rods were simply scratched with fine emery paper. Fibres were damaged by dropping fine silica sand onto them from a pre-determined height. These treatments were found to give a satisfactory range of mirror sizes.

2.3 Mirror Criteria and Measurement

The presence of the two more or less distinct loci, i.e., the mist and hackle arcs previously described, raises the problem of how to define the end of the mirror for the purposes of measurement, the first appearance of mist normally forms quite a regular boundary, but the position of this boundary depends upon the lighting and the magnification at which it is seen. Under inspection by an electron microscope, mist can be resolved in what is seen under optical conditions as the mirror zone, but gradually falls below the resolution of even this instrument in a direction towards the origin of the crack. The boundary of the hackle is much less ambiguous in position but is very much less regular. For this reason the mirror radius was measured to the inner locus as defined under a given set of subjective conditions.

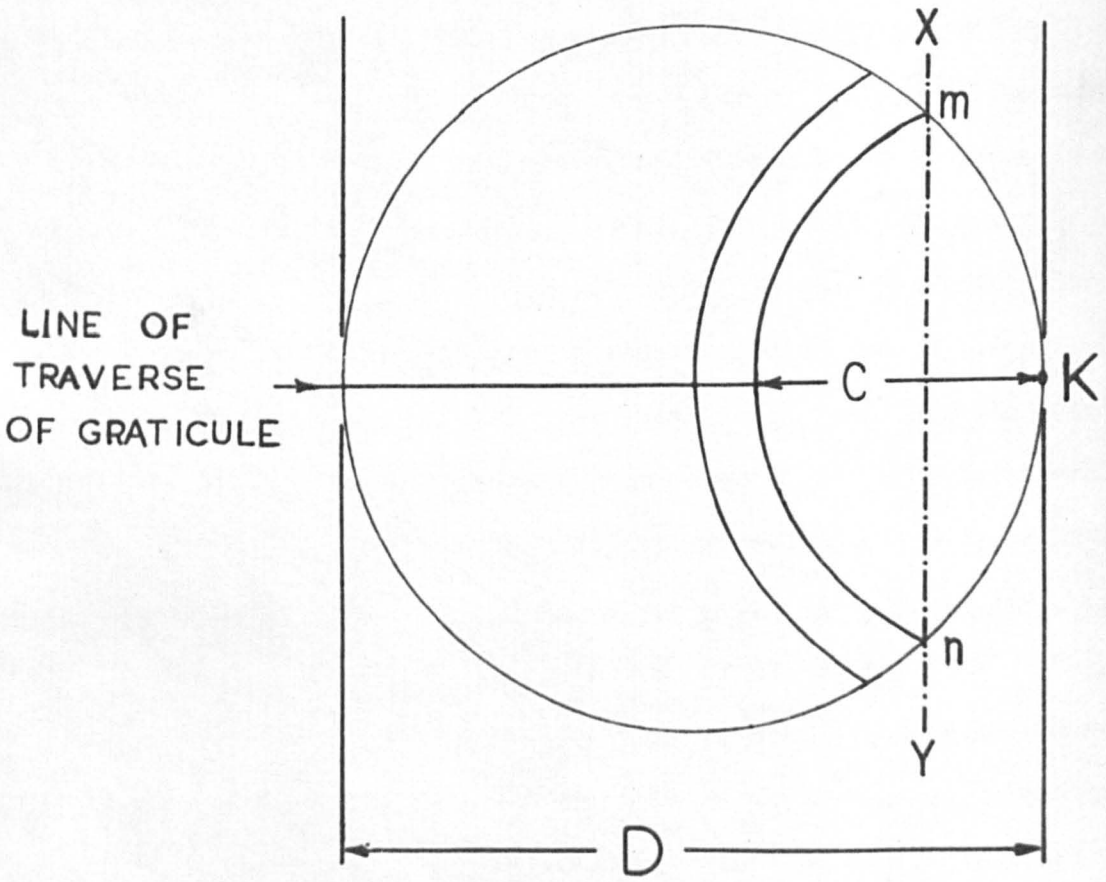

Fig. 5

Illustration of mirror measurement,

(see text).

The reproducibility of these measurements has been checked from time to time by examining results taken by a number of observers in this laboratory. The independent observations have usually agreed within 3 - 4%.

For the purposes of measuring c and D (see Fig. 5) a direct method of observation was employed using a micrometer eyepiece attached to the microscope. In this method, a length of about 2 cms was cut off the specimen after testing and this piece was set up vertically on the microscope stage, so that light was transmitted through the fracture surface of interest. Both portions of the broken specimen were set up on the microscope stage in this manner and the diameter of both pieces measured. Mirrors of good symmetry usually resulted from the pure tension tests, and by setting the intersections of the mist arc with the rod or fibre surface, on the vertical cross-wire in the eye-piece (as m, n on cross-wire xy in Fig. 5), a fairly accurate measure of c could be obtained along the diameter perpendicular to the chord mn as shown. The diameter D, was measured on both pieces, as noted above, along the same diameter perpendicular to the chord mn, and between the tangents to the circumference of the specimen, formed by traversing the cross-wire xy.

The first appearance of mist using constant magnification and subjectively the same lighting conditions was chosen as the criterion for the end of the mirror zone. The mist zone in fibre fractures is usually quite narrow and in this case it is not particularly difficult to decide upon a position for the end of the mirror. There is usually a somewhat broader mist zone on the fracture faces of 3mm and 5mm rods, it then becomes rather more difficult to define a beginning to the mist.

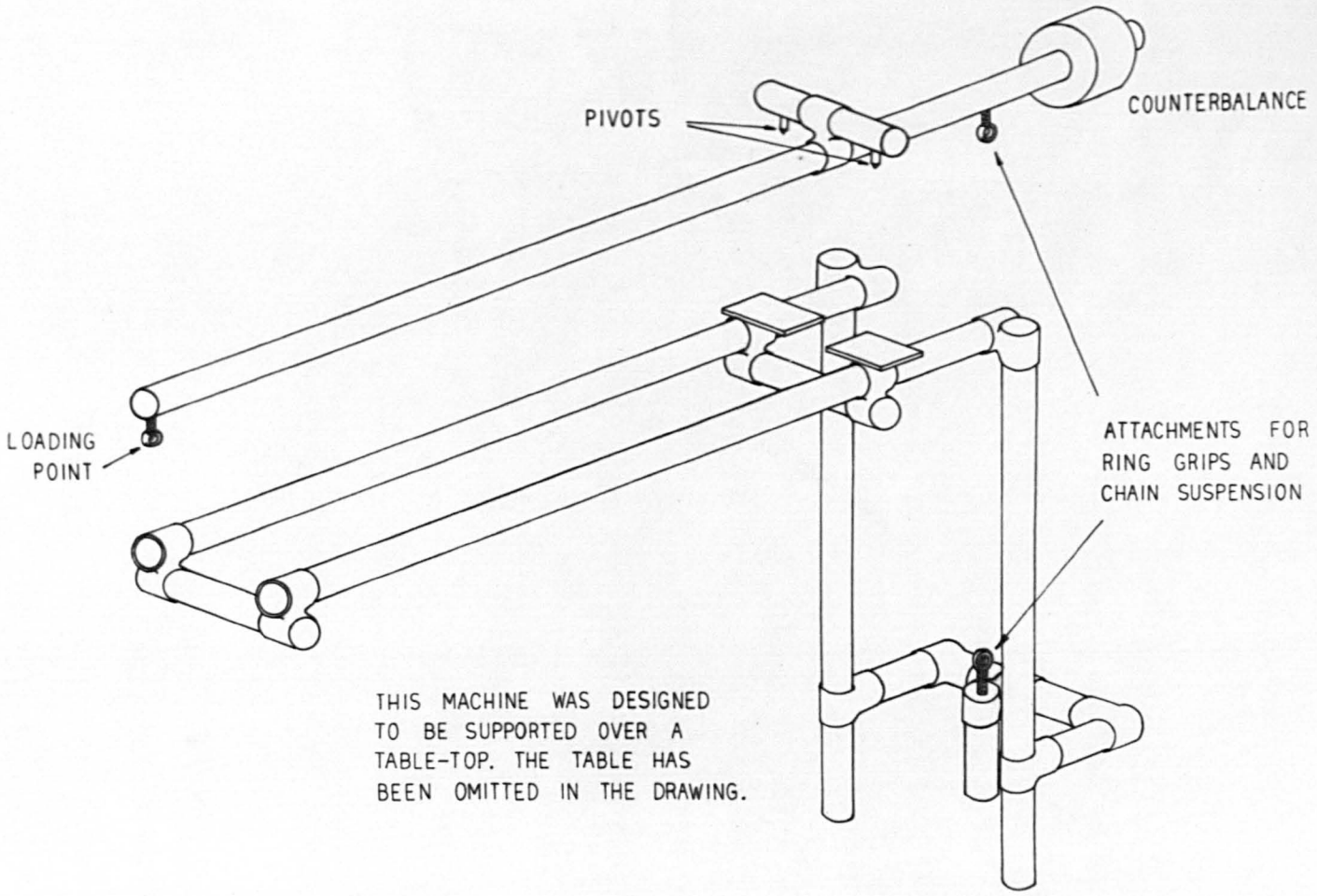

Fig. 6

Sketch of beam tensile tester in orthographic projection.
Not to scale.

In the early experiments it was found that a slight de-focussing of the microscope or, alternatively, of the eye, showed up this position as a slightly roughened arc.

During the course of the work, access to a Vickers Projection Microscope was obtained, so that when large numbers of 3mm and 5mm specimens were being tested a different method of mirror measurement was used.

In this case an image of the fracture surface was projected onto the screen of the microscope using oblique incident illumination. With the light falling obliquely on the fracture surface (parallel to mn in Fig. 5) a limit to the extent of the mirror surface could quite clearly be seen on the screen. By calibrating the latter with a graduated slide the mirror radius was easily obtained. This method however had the effect of reducing the value of c slightly for any given specimen when compared with the value obtained in direct observation, so that the numerical values of the later 3mm and 5mm results are slightly less than the early values.

2.4 Testing devices

I The Beam Machine

A tensile testing machine was constructed from 5cm steel scaffolding. As shown diagrammatically in Fig 6 the basis of this machine was a counter-balanced first order lever having a mechanical advantage completely variable from 1 to 7. Loading was accomplished by pouring lead shot into a tin-plate can suspended from the end of the beam. The beam itself was mounted between two flat steel platforms and pivoted on two case-hardened steel points, one resting on each platform. A steel tube, sliding inside a scaffolding clamp attached to a rigid mount, provided a simple means of accommodating specimens of different sizes.

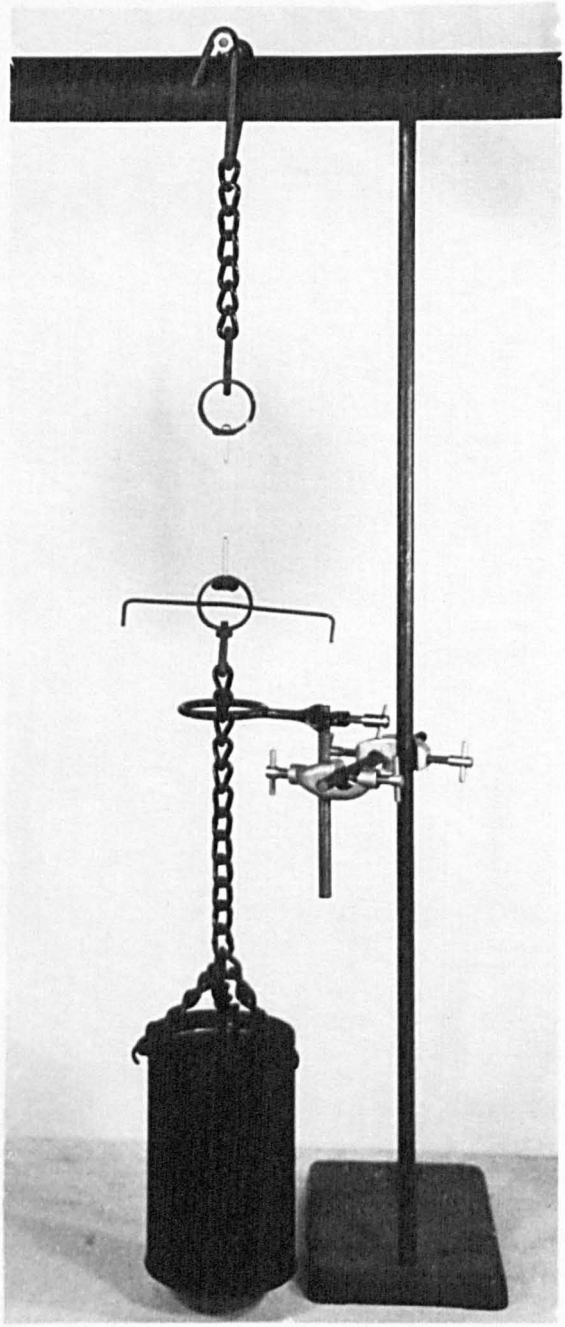

Fig. 7

Direct loading apparatus. Magnification x 1/6.

Several different types of grip were tried out with this machine including some with tapered polythene inserts designed to prevent failure at the balled-ends when applying loads in the region of 50 Kgms to rod specimens. However, the most successful arrangement was found to be the simple ring-grips shown in Fig. 4, used in conjunction with a sheet lead "ruff" fitted below the ball on each end of the rod. The lead ruffs were 1cm squares cut from 2mm thick lead sheet with a 3mm or 5mm hole punched in the centre and a cut from one side to the hole. The ruffs could then be easily fitted to a specimen by forcing the latter down the cut and into the central hole. The lower grip was fitted with an "outstretched arms" attachment enabling the grip to be arrested in its fall almost immediately by a retort ring. In order to prevent the two halves of the specimen from being thrown from the grips on fracture, small plasticine caps were fixed over the ends of the specimen where these were held by the grips.

II Direct Loading Apparatus

The direct loading apparatus was a simple arrangement used only for testing fibres in tension. The grips were the same as those used in the beam tensile-testing device and the upper grip was suspended by a short length of chain from a rigid overhead support. The lower grip again had an "outstretched Arms" attachment and a retort ring was used as the catching device to reduce the fall of the lower grip to a minimum. From the lower grip a light tin-plate can was freely suspended into which was poured the lead-shot used as a loading material. Any tendency for the can to swing under the influence of air currents was reduced by shielding the lower half of the apparatus with a box. By careful shot-pouring the can was prevented from swinging under the impact of the shot.

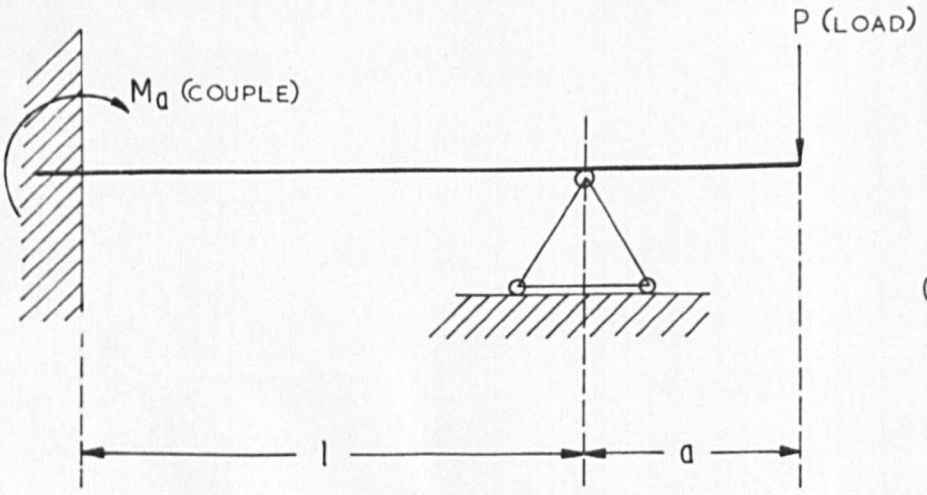

(a)

Diagrammatic representation of cantilever bending machine.

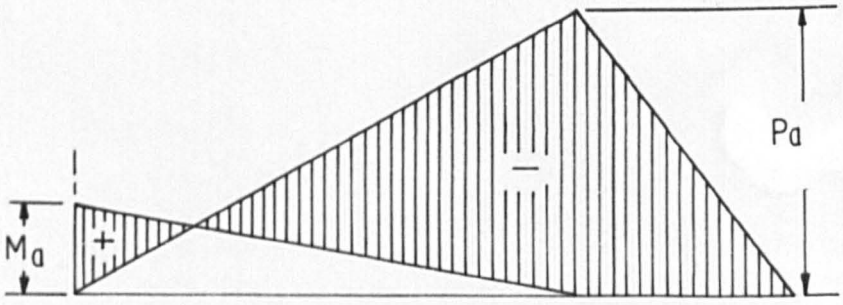

(b)

Bending moment distribution for the arrangement of Fig. 8(a) above.

Fig. 8

In loading a specimen by this method, a small extra quantity of loading material unavoidably entered the can due to the time lag in the experimenters reaction to the completion of the fracture process. It was demonstrated by simple subsidiary experiments that the resulting error in measuring the load was approximately compensated by the small additional force exerted on the specimen due to the loss in momentum of the lead-shot on striking the can.

A photograph of the apparatus is shown in Fig. 7. The draught shield is removed and the specimen is shown in place retained, as in the tests, by small pieces of plasticine.

In this apparatus a specimen occasionally fractured into more than two pieces. If the breaks took place close together it was possible to lose small pieces of the original fibre and have left two non-matching fracture surfaces. Rather than take steps to eliminate or account for the sporadic appearance of this effect at this stage it was decided to measure the total length of all specimens before and after test, rejecting those measuring less than their original length after test.

III Cantilever Bending Device

The cantilever bending device was designed partly to determine the value of $Zc^{\frac{1}{2}}$ in bending and partly to attempt to impose the high stresses on 3mm and 5mm rods which could not be attained in pure tension because of ball failures. Basically, as shown in Fig. 8a, the beam (consisting of the glass rod under test) was built in at one end and supported with an overhang at the other. The support conformed to the requirements of a "hinged movable support". So that, neglecting friction, the reaction at the support must act through the centre of the hinge and

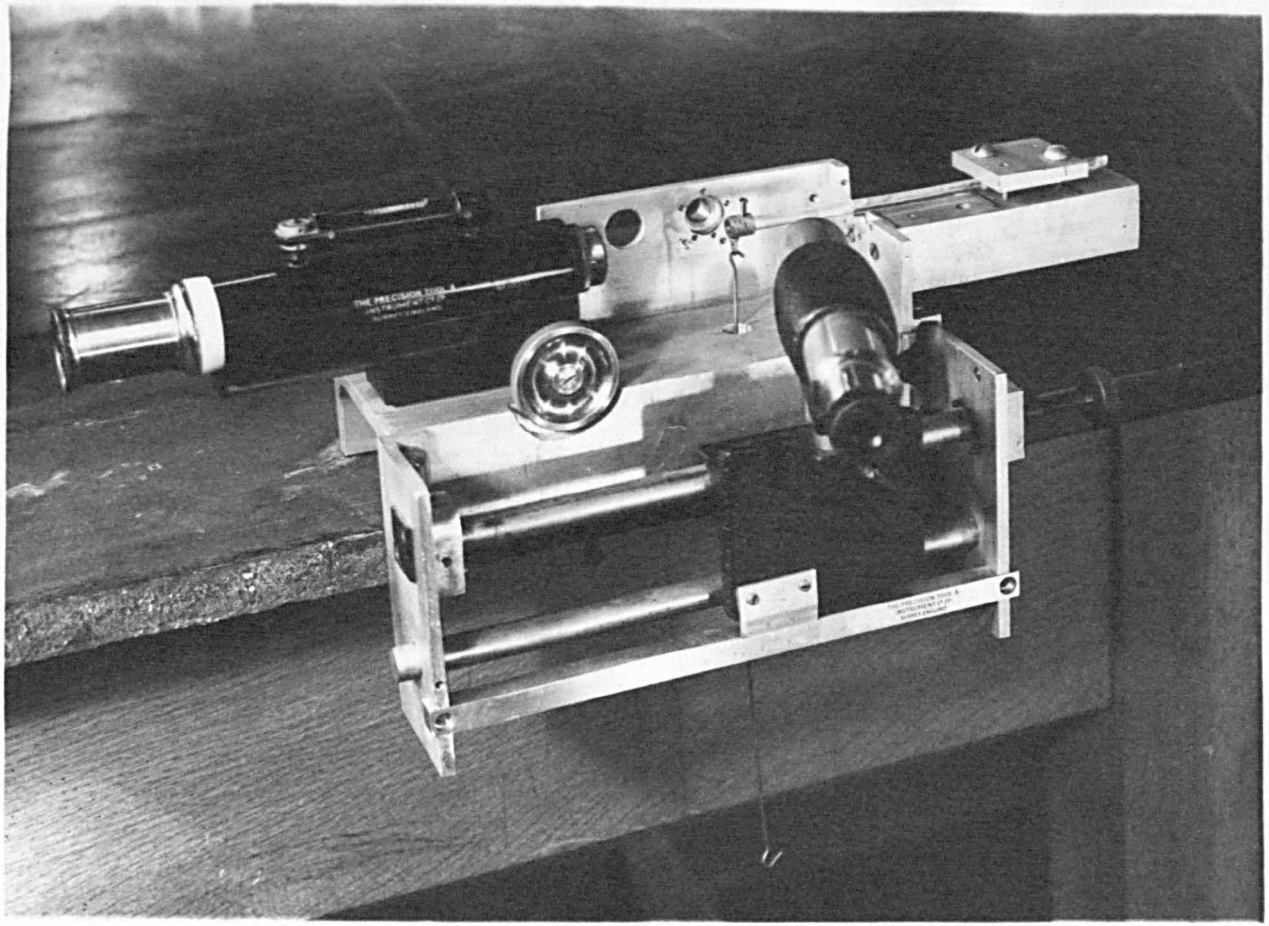

Fig. 9

Photograph of cantilever bending machine

be perpendicular to the plane on which the support rests (Timoshenko (13)). With a fixed non-hinged support an unknown longitudinal tension can develop during the test in that section of the rod between the support and the built-in end. A movable hinged support is necessary to eradicate this source of error. The load was applied at P by suspending a tin-plate can from this point and filling it with lead shot. The bending moment distribution for this complex cantilever arrangement is shown in Fig. 8b. It can be seen that the bending moment distribution attains a maximum value at the support and falls away to either side. Thus by damaging the rod in the area of the support it could be induced to fail preferentially in a region where the bending moment could be calculated. The actual value of the bending moment at the point of fracture was computed from the load and bending beam formulae (see Timoshenko). A prototype device embodying only a simple cantilever gave a great deal of trouble in that a large proportion of fractures took place flush with the built-in end.

A photograph of the apparatus is shown in Fig. 9. In the foreground of the photograph can be seen a travelling microscope. This was used to measure the distance from either the support or the built-in end to the point at which fracture took place. The second microscope which can be seen pointing down the axis of the glass rod was used for a preliminary examination of the fracture surface. In many tests the point of origin of the fracture was not located on the line of maximum stress at the top of the rod (see Fig. 10), but was displaced from it some distance around the circumference of the glass rod. The amount of this displacement was estimated by measuring the angle between two imaginary lines. One drawn between the point of maximum surface stress

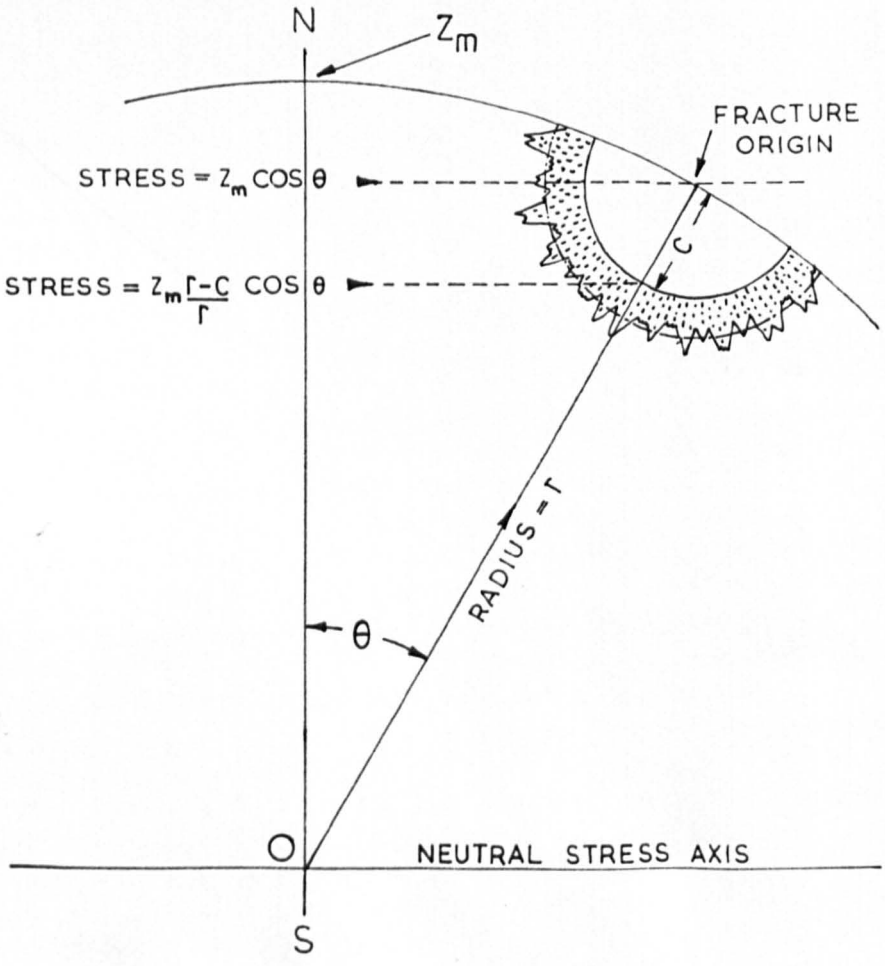

Fig. 10

Sketch of a fracture face produced in bending
(see text for explanation)

and the geometrical axis of the glass rod, the other between the point of origin of the fracture and the geometrical axis of the glass rod. That is, the lines defining the angle θ in Fig. 10. Practically this was accomplished by fitting the second microscope with rotatable cross-wires attached to a polythene ring graduated in degress. The cross-wires were brought to coincidence with the geometrical axis of the glass rod (C in Fig. 10), and the angle θ by which the fracture was judged to be "off axis" was determined by rotating the N - S cross-wire from the point of maximum surface stress until it intersected the fracture origin. The angle θ in degress was then read off the polythene ring against a fiducial mark.

Fractures which originated at points more than about ten degrees off axis were rejected since they produced mirror shapes or profiles which appeared to be distorted. The question of mirror profiles in general and the phenomenon of "break-through" also found in bending fractures is discussed later.

2.5 The value of $Zc^{\frac{1}{2}}$ in air

X8 Glass

The value of $Zc^{\frac{1}{2}}$ in air was measured for a group of X8 3mm rods and also for a group of flame-drawn X8 fibres. Both groups were heat-treated for one hour at 530°C, and cooled initially at a rate of 1.5°C, per minute for the first 200°C. The results from these experiments are shown in Fig. 11 where the breaking strength Z is given as a function of $c^{-\frac{1}{2}}$, the relationship between these two quantities over the range of specimen diameters and mirror sizes encountered, is a linear one.

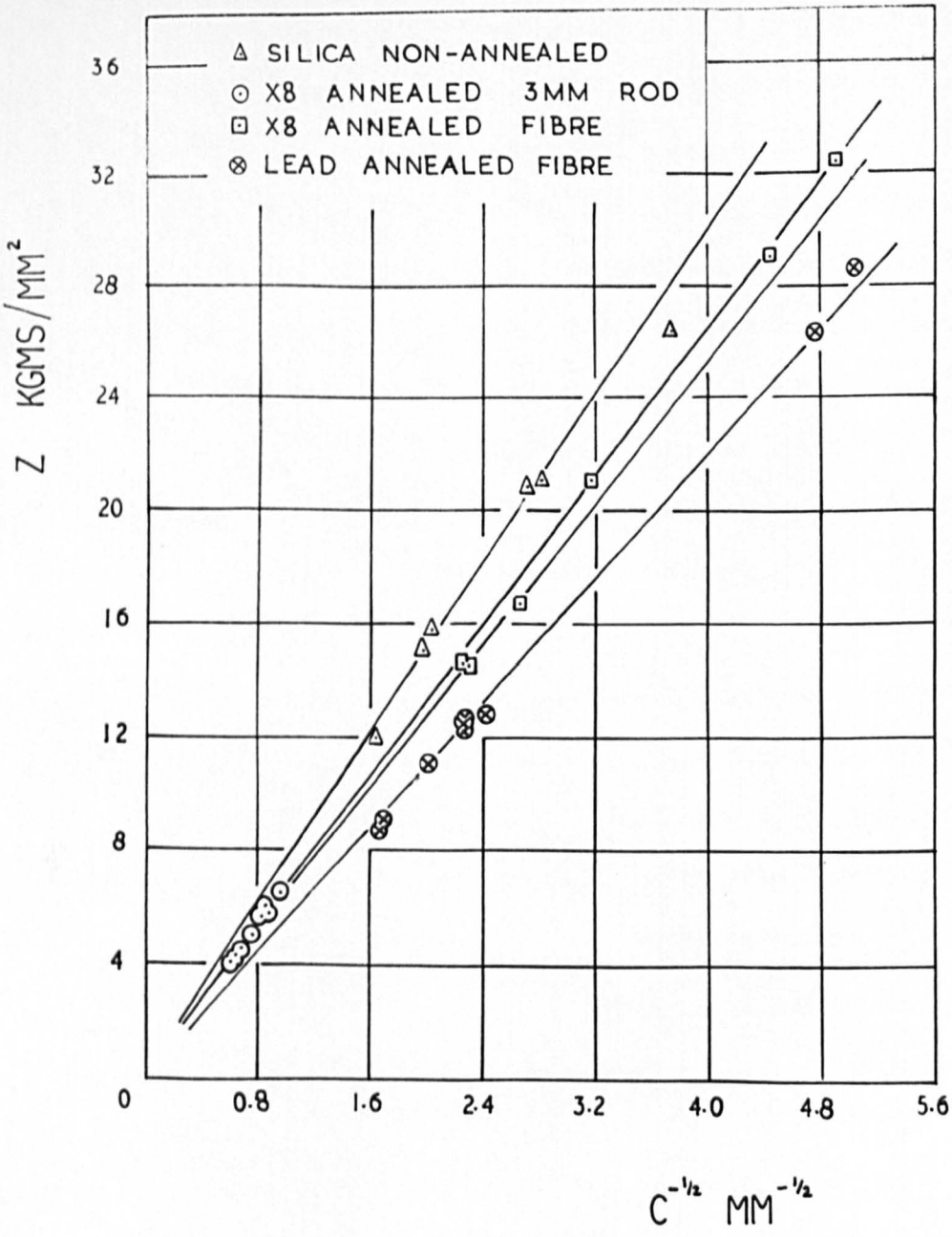

Fig. 11

Showing the breaking stress Z as a function of the reciprocal of the square root of the mirror depth for Silica, X8 and lead glasses.

Silica Glass

A group of flame drawn silica fibres had been produced during the experimental work on Smekal's parameter. The results for this group, shown plotted in Fig. 11, were obtained by re-analysing the photographic record which was kept of the fracture surfaces from specimens tested at that time. It should be noted that the mirror radii obtained for this group may have been slightly different had the method of direct observation been used, but it is thought that this difference would not reduce the value of $Zc^{\frac{1}{2}}$ by more than about 2 - 3%.

Lead Glass

The value of $Zc^{\frac{1}{2}}$ in air was determined for lead glass fibres also, the glass having the composition outlined in Section 2.2. A batch of flame-drawn lead-glass fibres was annealed for one hour at 420°C., and tested in the usual manner in the direct loading apparatus. The results for these fibres are given in Fig. 11.

2.6 Tests in Liquids

Two groups of X8 fibre specimens were tested, one under water and the other under methyl alcohol. These tests were performed on the beam machine with the mechanical advantage reduced to 1.

A water-tight perspex box 6cms by 7cms by 18cms was constructed with the top end open. Through the perspex base plate was a screwed brass rod arranged so that a short length projected into the box, and a short length projected below the box, thus facilitating its attachment to the rigid support of the tensile-tester. The inside projection carried a ring grip of the same type as those used previously. Thus when the box was mounted vertically on the machine and filled with

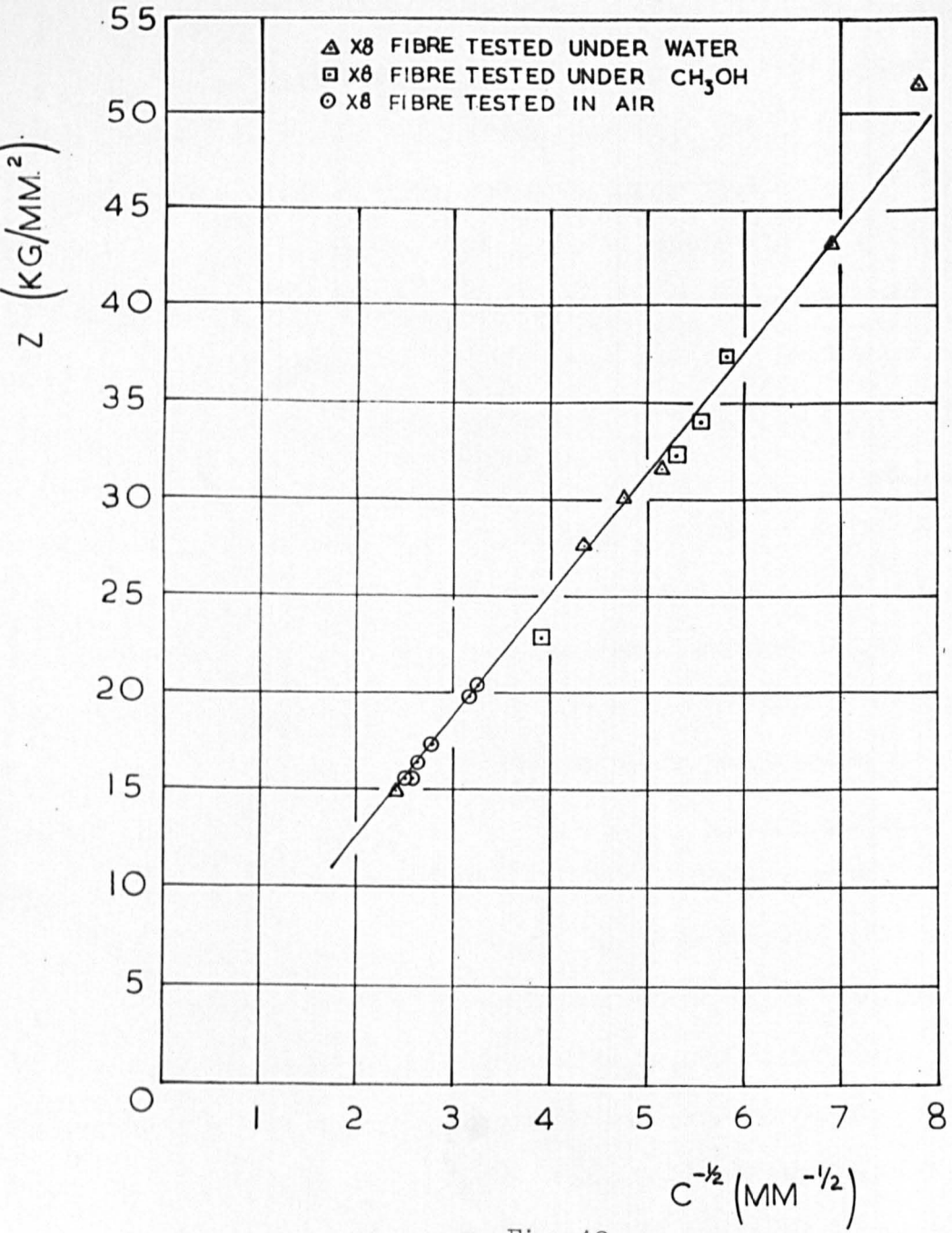

Fig. 12

Showing the breaking stress Z as a function of the reciprocal of the square root of the mirror depth for X8 fibres tested in tension under water, and methyl alcohol.

water or alcohol, the upper end of the specimen just projected from the surface of the liquid and could be held by the upper ring-grip. For these tests the specimens were not pre-damaged as described in Section 2.2.

The results for the two groups are shown in Fig. 12 and are compared with an air tested batch. There is no apparent change in the value of $Zc^{\frac{1}{2}}$. The distribution of the water and methyl alcohol points in the small mirror range is a reflection of the fact that these specimens were not pre-damaged.

2.7 Electrical-drawing and flame-drawing

The possibility of a difference between electrically-drawn and flame-drawn fibres led to a cursory examination of the value of $Zc^{\frac{1}{2}}$ given by such specimens.

The production of flame-drawn fibres has already been described (Section 2.2). In producing electrically-drawn fibres, a rod of 3mm x 8 with "balled" ends was suspended vertically, held by its upper end, inside a coil of Nickel wire through which a current of 200amps at 5 volts could be passed. A 20 gm weight attached to the lower end of the rod was used as the drawing load.

Six flame-drawn and six electrically-drawn X8 specimens were broken in air in the direct loading apparatus. These fibres were not heat-treated in any way after drawing. In addition, six flame-drawn and six electrically-drawn X8 specimens were heat-treated together at 530°C., for three hours and cooled at a rate of less than 1°C per minute for the first 200°C.

X8 FIBRE

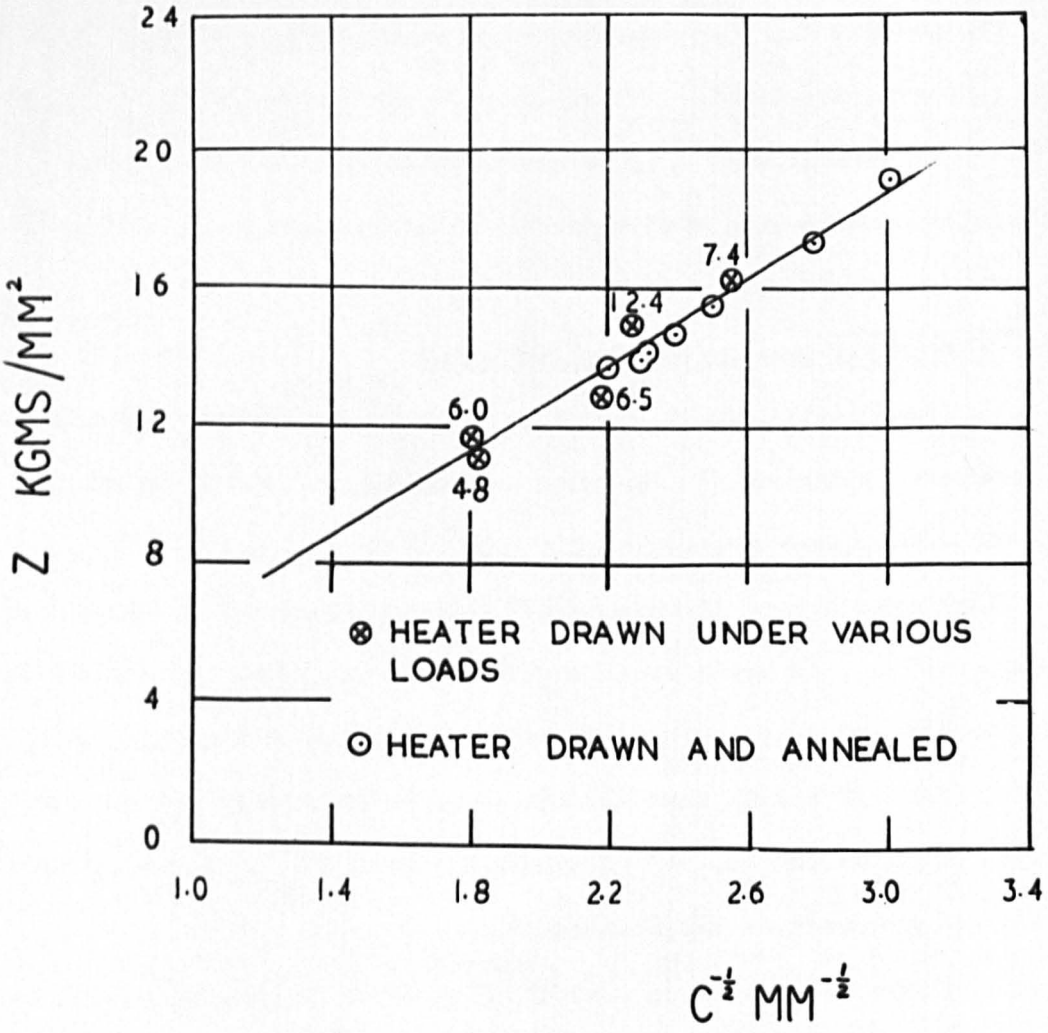

Fig. 13

Showing the breaking stress Z as a function of the reciprocal of the square root of the mirror depth for fibres containing "frozen" strains and for annealed fibres.

The results are given in Table 2.7.1 below

Table 2.7.1

	Non heat-treated		Heat-treated	
	Flame-drawn	Electrically drawn	Flame-drawn	Electrically drawn
Mean $Zc^{\frac{1}{2}}$ (Kg/mm$^{\frac{1}{2}}$)	6.06	6.16	6.23	6.27
Total spread	0.57	0.87	0.25	0.45

2.8 Electrical-drawing under large loads

The sensitivity of the value of $Zc^{\frac{1}{2}}$ to the presence of strains within the glass was examined for two types of strain. Under this section-heading, the strain concerned is of the type arising out of the stress applied during the fibre-drawing process and was originally described by Stirling (14). These "frozen" strains induced in the specimen during drawing are considered further in Chapter 3, Section 3.2.

Fibres were drawn by hanging weights up to 4 Kgms. on the lower end of a rod suspended in the electrical heater described in the previous section. Upon observing that extension of the rod had been initiated, the current was switched off and the drawing process allowed to come to completion. By this method up to 12 Kg/mm^2 drawing stress was obtained on the final fibre cross-section. The results from a batch of X8 fibres made by this method are shown in Fig. 13 together with the results from a batch of X8 fibres heater-drawn and annealed at 530°C. The figures recorded by the side of each point representing a fibre containing "frozen" strain indicate the value of the stress applied during drawing as calculated using the cross-sectional area of the fracture surface.

2.9 Variation in the value of $Zc^{\frac{1}{2}}$ with temperature

In order to investigate the high temperature variation in the value of $Zc^{\frac{1}{2}}$, a small electrically-heated oven was made in which specimens could be broken whilst held at a given temperature. This oven was constructed in the following manner.

A silica tube 9 cm in length and 8 mm internal diameter was wound with two layers of wet asbestos paper. About 50 turns of 28 S.W.G nichrome wire were wound onto the asbestos paper while it was still damp. This winding was then in turn covered by a further five thicknesses of asbestos paper and set aside to dry.

The oven was used in conjunction with the direct loading apparatus and was held in position around the fibre by a laboratory clamp and stand. Current was supplied to the oven by means of a"Variac"variable transformer connected to the mains supply. The time taken for the oven to reach thermal equilibrium was determined from a series of time-temperature curves, with a thermocouple in place of the fibre and the Variac settings in 10% steps from 40% to 100% of the output voltage. The time taken for the oven to attain a maximum temperature was found to be about 15 minutes. The time allowed for the specimen to reach the temperature of the oven was fixed at 30 minutes from the moment the Variac was advanced to its pre-determined position.

The specimens for these tests were fibres flamedrawn from 3mm X8 rods. The length of the fibre section was 4 - 5 cms and the overall length was such that the balled-ends of the rods projected a little way beyond the ends of the oven enabling the specimen to be easily fixed in the grips of the direct loading apparatus. Before testing, the specimens were

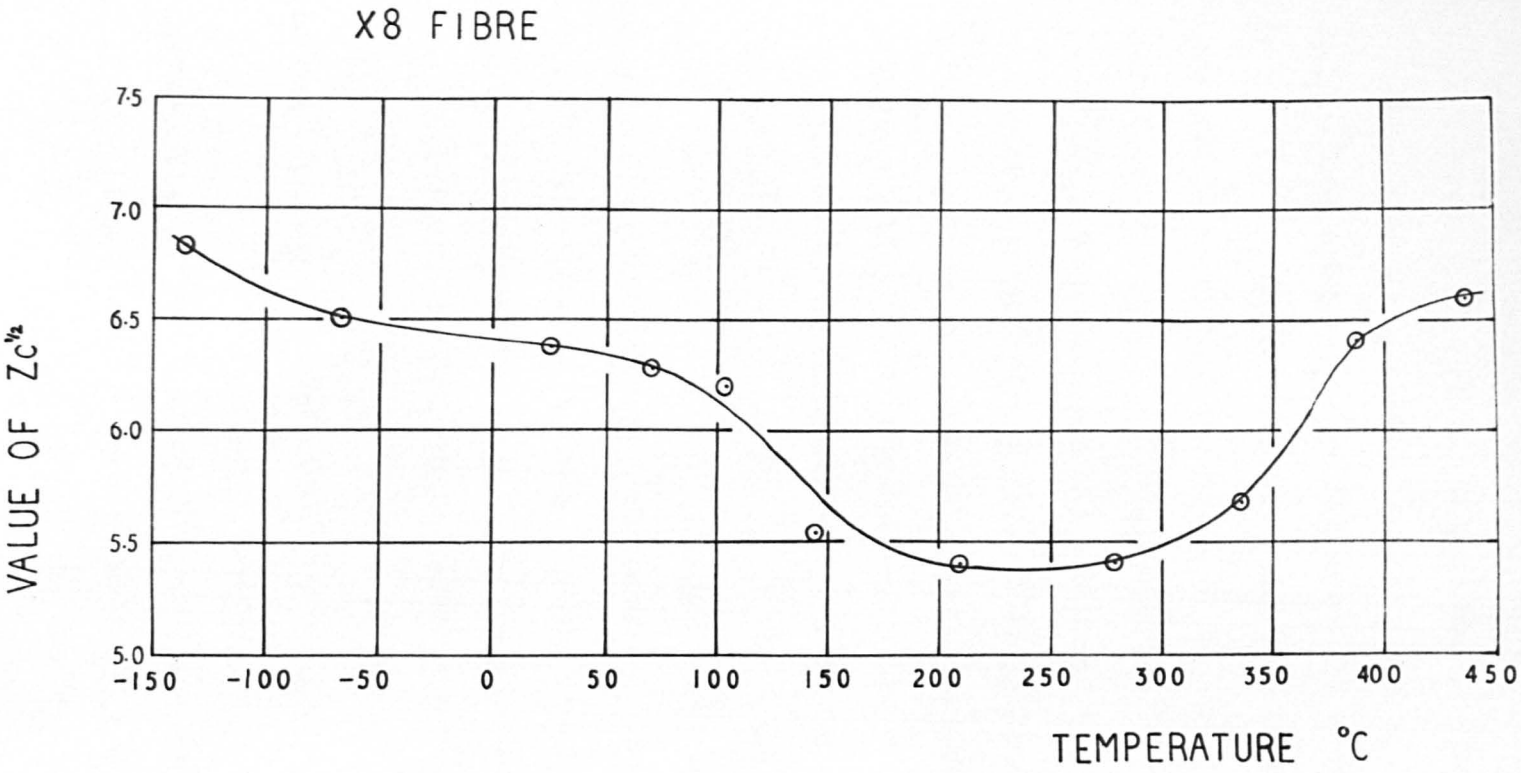

Fig. 14

The value of $Zc^{\frac{1}{2}}$ ($Kg/mm^{3/2}$) as a function of tempeature.

annealed together for one hour at 530°C., and cooled initially at a rate of 1°C. per minute. Each specimen was damaged (see Section 2.2) before testing and a note was made of the initial fibre length so that tests in which multiple breaks occurred could be eliminated (Section 2.4 II).

Fig. 14 shows the results of eight high temperature tests up to 435°C, and the mean of fibres tested at room temperature from the same batch. These high temperature results should be rechecked since each point represents only one specimen.

Two experiments were performed to determine the value of $Zc^{\frac{1}{2}}$ for X8 at temperatures below 0°C. In order to do this a container was constructed similar in form to that shown diagrammatically in Fig. 15. The container was held in place around the fibre by a laboratory clamp and stand, the fibre being held as before in the ring grip of the direct loading apparatus.

In the first experiment liquid nitrogen was allowed to evaporate from the annular cavity marked "liquid N_2" in Fig. 15. Ice was prevented from forming on the specimen by passing gaseous nitrogen through a copper helix immersed in liquid nitrogen and then into the copper cylinder surrounding the specimen. The gas was then allowed to seep through the space between the end caps and the specimen. The temperature of a specimen in the copper enclosure was estimated before each test by means of a chromel p-alumel thermocouple enclosed in a glass envelope. The temperature attained by this arrangement was found to be fairly constant at about - 136°C.

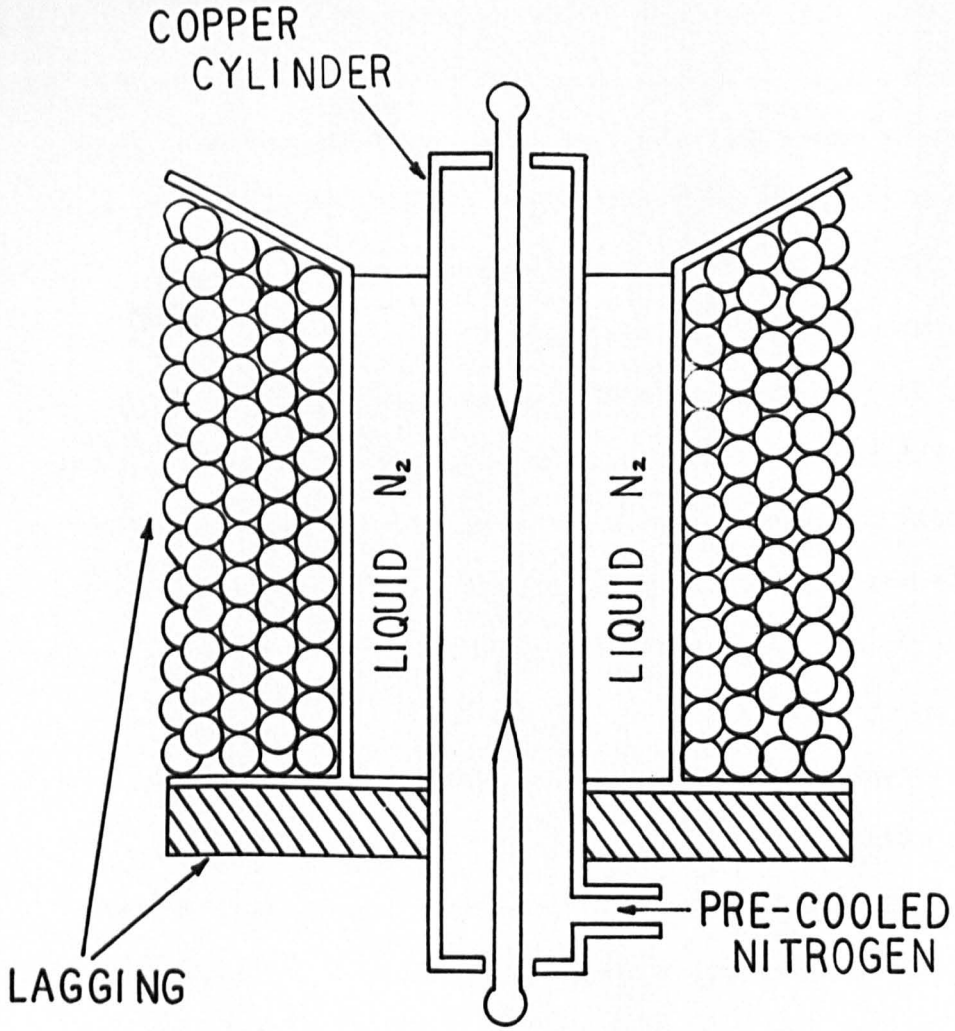

Fig. 15

Drawing of a section through
the liquid nitrogen container.
Approx. full size.

The second experiment was identical in its details with that above but in this case finely crushed solid carbon dioxide was packed into the annular space which previously held liquid nitrogen. The temperature of fibres in the copper enclosure was this time estimated to be about $-68^{\circ}C$.

The means of the results of tests at these two temperatures are also shown in Fig. 14.

2.10 Value of $Zc^{\frac{1}{2}}$ for "as received" 3mm and 5mm X8 rod

As noted in Section 2.8 the effect of two types of internal strain in glass on the value of $Zc^{\frac{1}{2}}$ was examined. Here the interest was concentrated on the effect of thermally induced strains, resulting in real mechanical stresses, in the glass. These stresses will be considered further in Chapter 3, it is sufficient for the moment to state that it is well known that when produced under specific conditions, the distribution of these stresses in a glass object follows a parabolic law. This series of experiments constituted an attempt to measure the value of $Zc^{\frac{1}{2}}$ as a function of the penetration achieved by the crack into a stress field of this type before the occurrence of crack bifurcation. This will be referred to below as a measurement of the value of $Zc^{\frac{1}{2}}$ as a function of c.

Fig. 16 shows the results of 10 specimens of "as received" 3mm X8 rod tested in the beam tensile tester. In addition the results from five tensile tests on annealed 3mm X8 specimens are also shown. It was found to be very difficult to obtain mirrors with radii less than approximately 0.4mm from rods tested in tension because of failure at the balls. In order to obtain mirror radii smaller than this it

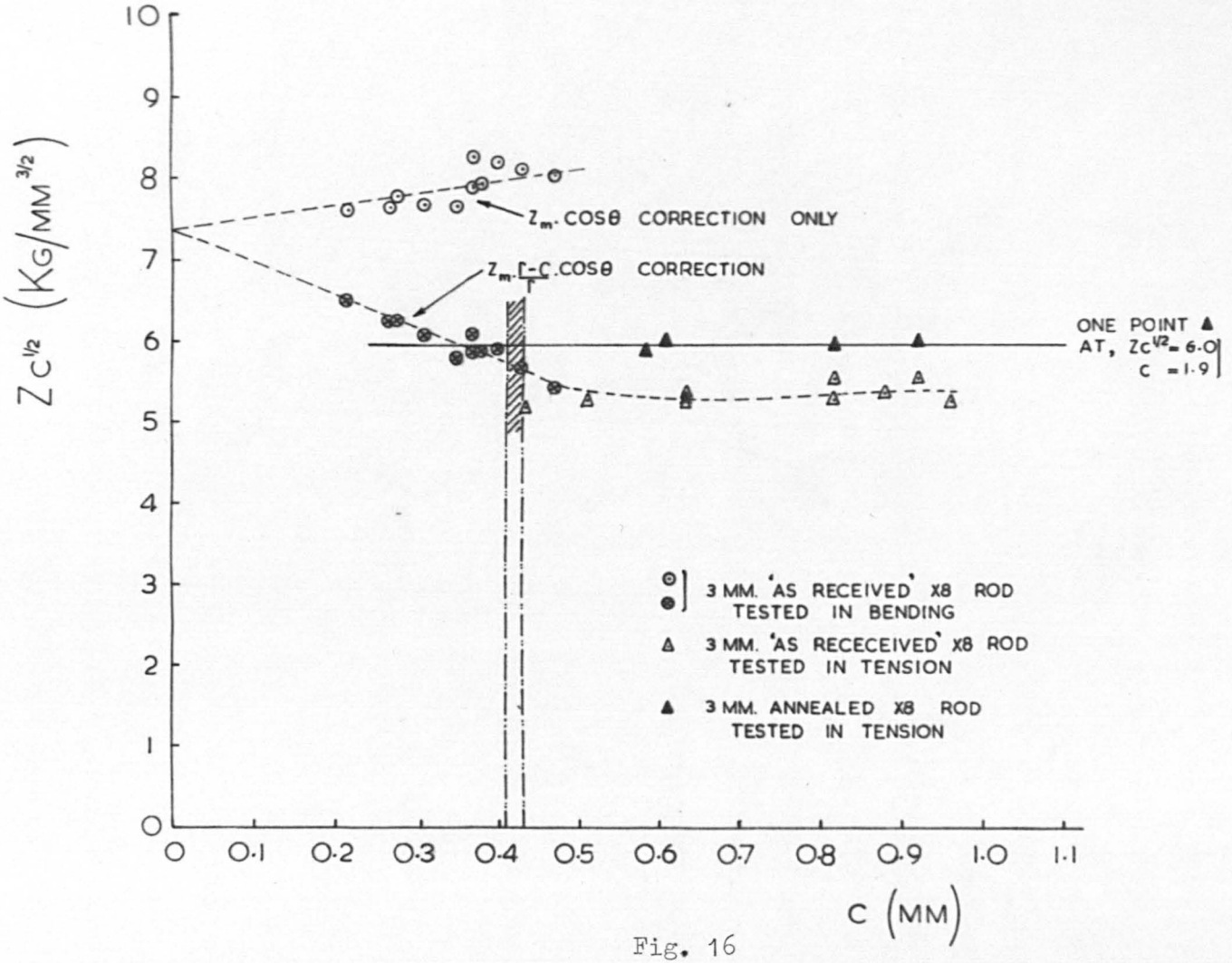

Fig. 16

Showing the value of $Zc^{\frac{1}{2}}$ as a function of mirror depth for 3 mm "as received" and annealed X8 glass rod.

was necessary to go to bending and for this purpose the cantilever bending device described in Section 2.4 III was built.

The results of 11 tests in this machine on "as received" 3mm X8 rod are shown in Fig. 16. In fact this batch also contains a few results obtained from a prototype simple cantilever system. As described in Section 2.4 III the simple cantilever system was replaced by the arrangement of Fig. 8 which allowed virtually all specimens to be included in the results. The breaking stress Z used for these $Zc^{\frac{1}{2}}$ values was the surface stress as determined for the fracture origins, i.e., $Z_m \cos \theta$ and the curve obtained for these specimens is so marked. This figure is discussed fully in Chapter 3.

In addition to the 3mm rods described above, two batches of 5mm X8 rods were also tested in the cantilever bending device. One batch was tested "as received", the other batch was heat-treated at 530°C for three hours and cooled at about 1°C per minute. The results from these two groups are shown in Fig. 17, where the results referred to at this stage are the curves marked "$Z_m \cos \theta$ correction".

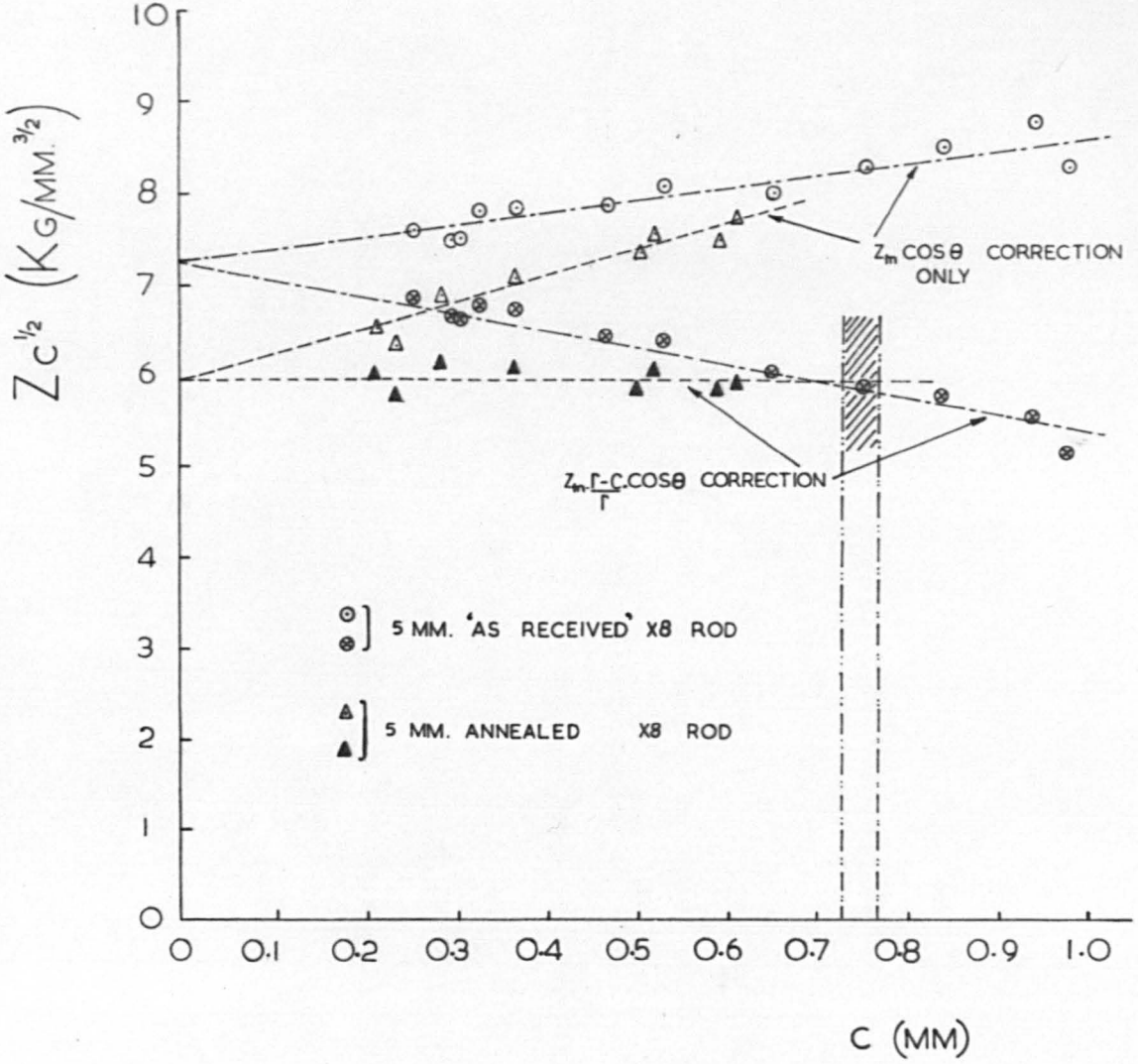

Fig. 17

Showing the value of $Zc^{\frac{1}{2}}$ as a function of mirror depth for 5 mm "as received" and annealed X8 glass rod.

CHAPTER 3 PRELIMINARY ANALYSIS AND DISCUSSION OF RESULTS

3.1 Introduction

The experimental work described in the previous chapter has yielded a body of factual information on the value of $Zc^{\frac{1}{2}}$ for various glasses under different conditions. In this chapter it is intended to examine some of the interesting points arising immediately out of these experiments, although a comprehensive interpretation of this information cannot be made until the full physical significance of the value of $Zc^{\frac{1}{2}}$ is known. This is discussed in a later chapter. A comparison of the numerical values obtained in the experiments just described and the results obtained by other workers is also made under this heading, although for convenience this latter section is held over from its conventional position at the head of the chapter until later.

3.2 Some points arising from the results

It is apparent from Figs. 11, 12, 13 and Table 2.7.1 that at a given temperature of test, the value of $Zc^{\frac{1}{2}}$ for any one glass is constant, but different for different glasses, is unaffected by the surrounding media and is relatively insensitive to the fibre-drawing method. Fig. 14 shows that for X8 the value of $Zc^{\frac{1}{2}}$ depends upon the temperature. The value of $Zc^{\frac{1}{2}}$ is constant over a wide range of mirror sizes and specimen diameters.

The experiments of Stirling (14) showed that fibres drawn under loads exhibited optical activity proportional to the stress applied in drawing them. The optical activity was shown to be uniform across the specimen and indicated a strain of one sign only, in the case of fibres drawn as described in Section 2.8 a tensile strain. Clearly there can be no real internal stresses associated with this type of "strain" since the specimens would not be able to maintain static equilibrium. An examination of Fig. 13

shows that there is no major change in the value of $Zc^{\frac{1}{2}}$ due to the presence of Stirling's "frozen" strains in X8 fibres. The slight increase in scatter does not vary in a regular manner with the amount of strains if the value of the applied drawing stress is taken as a measure of the strain induced in any one sample.

However the most interesting results at this stage are those obtained from the experiments described in Section 2.10. These experiments were conducted on "as received" 3mm and 5mm rod which can be shown under the polarizing microscope to contain mechanical stresses. It is useful to record briefly how these stresses arise.

Unless the cooling rate of the glass is carefully controlled during the drawing process (or for that matter during any heat-treatment - but for the stresses to be permanent the glass must attain the softening temperature), the surface cools more quickly than the interior and temperature gradients are set up in the glass. The removal of these gradients results finally in the generation of compressive stresses in the surface of the specimen and balancing tensile stresses in the centre. When the specimens are cylindrical in shape, provided that the cooling rate over the whole surface layer is the same, the locus of all points subsequently having the same compressive or tensile stress is a cylindrical shell concentric with the axis of the rod. The stress distribution along a diameter of the cross-section of a rod may be represented by a parabola, the exact shape of which depends upon the temperature range over which the rapid cooling takes place and the rate of cooling within this range. The presence of stress distributed in this manner can easily be detected in the 3mm and 5mm X8 rod used in these experiments by means of a polarising microscope.

For a cylindrical specimen in which the stress distribution of the statically balanced stresses over any cross-section may be represented by the rotation of a parabola as described above, there is, at some distance below the surface of the cylinder, a layer with no stress, that is, a neutral zone. If a section could be made across the rod perpendicular to its axis without disturbing the stress distribution, the sum of the tensile stresses acting within the neutral zone would be balanced by the sum of the compressive stresses acting over the area around the neutral zone. Also if some of the surface of the specimen is removed by some method, for example chemical etching, these stresses are re-distributed until a new equilibrium is reached.

Assuming a paraboloidal distribution of stresses within the rods and assuming also that the stresses within the specimens are in equilibrium with each other, it is possible to calculate, using a simple approach, the position of the neutral stress zone for any rod. The calculation is given in Appendix I, but the result is that the distance of the neutral layer from the axis of the rod is $r/\sqrt{2}$, where r is the radius of the rod. The vertical cross-hatched zones in Figs. 16 and 17 represent the maximum and minimum values calculated for the neutral layer for both 3mm and 5mm rods within the diameter variation encountered in the experiments.

The results of the two series of tensile tests shown in Fig. 16 indicate that the presence of these internal stresses exercise a distinct influence on the value of $Zc^{\frac{1}{2}}$. It is clear that the "as received" rods giving mirrors falling inside the neutral zone yield a value of $Zc^{\frac{1}{2}}$ which is consistently lower than the value given by annealed rods.

However, by comparing the results of these tensile tests with the results from the "as received" 3mm rod ($Z_m \cos\theta$ curve Fig. 16) tested in bending, it is immediately apparent that an incompatibility exists between the two. It was found that the bending results could be reduced to give values consistent with the tensile results if the meaning given to the quantity Z in Eqn. 1.3.1 was altered slightly, as follows. Suppose that the stress Z used in the equation was regarded as being the applied stress acting locally, immediately prior to fracture, at that point in the material where bifurcation of the crack subsequently took place, no alteration in the values of $Zc^{\frac{1}{2}}$ for annealed specimens tested in tension would be required. However, in the case of the bend values for $Zc^{\frac{1}{2}}$ the Z used in Eqn. 1.3.1 would not now be Z_m or $Z_m \cos\theta$ (depending on the position of the fracture origin) but $Z_m \cos\theta \left(\frac{r - c}{r}\right)$ (see Fig. 10). The effect of dealing with the bend results in this manner produced a set of values compatible with the tension results as shown in Fig. 16 $\left(Z_m . \cos\theta . \frac{r - c}{r} \text{ curve}\right)$.

An examination of the combined curves for the tensile and bending tests on the "as received" rod, and the tensile tests on annealed material as shown in Fig. 16 leads to the following conclusions. Mechanical stresses within the glass have a marked effect on the value of $Zc^{\frac{1}{2}}$. Both 3mm and 5mm (when corrected - see Fig. 17) annealed rods give the same value for $Zc^{\frac{1}{2}}$, but the "as received" rod values are differently distributed for 5mm and 3mm rods. In addition it will be observed that the curves of the results for both 3mm and 5mm "as received" specimens pass through the line of the annealed-rod results at two specific points. This will be considered further in the next section.

At this stage it is sufficient to note that inside the neutral zone, i.e., in the zone of tensile stresses, the measured value of $Zc^{\frac{1}{2}}$ is consistently lower than annealed value. Outside the neutral zone, i.e., in the zone of the compressive stresses, the value of $Zc^{\frac{1}{2}}$ is consistently too high. In order to reduce the experimental "as received" $Zc^{\frac{1}{2}}$ values to the annealed $Zc^{\frac{1}{2}}$ values the stress Z has to be adjusted. In the compressive zone Z must be reduced (in the particular case of these rods) by a maximum of 1 - 2 Kgms/mm^2, and increased at the axis of the rod by a maximum of about 1 - 2 Kgms/mm^2. Since these stresses are at the sort of level which might easily be introduced during the cooling stage of the manufacturing process, the curves of Figs 16 and 17 suggest that the values of $Zc^{\frac{1}{2}}$ given by them could be used to give an accurate measure of these actual stresses. Corroborative evidence for this proposal will be given shortly.

In order to obtain consistent values for $Zc^{\frac{1}{2}}$ in tension and bending, as recounted above, it was found necessary to place a different interpretation upon the value of Z used in Eqn. 1.3.1 than had been employed up to that point. It will be recalled that Z was re-defined above as that stress acting locally, immediately prior to fracture, at that point in the specimen where bifurcation of the crack subsequently took place. This simple shift in emphasis allows the diversity in mirror profiles obtained from the various testing procedures to be explained. Some of the most characteristic mirror shapes can easily be obtained by geometrical construction as described in the next section. But first, the modified interpretation of the stress to be used in Eqn. 1.3.1 is supported on several grounds. First, it is apparent

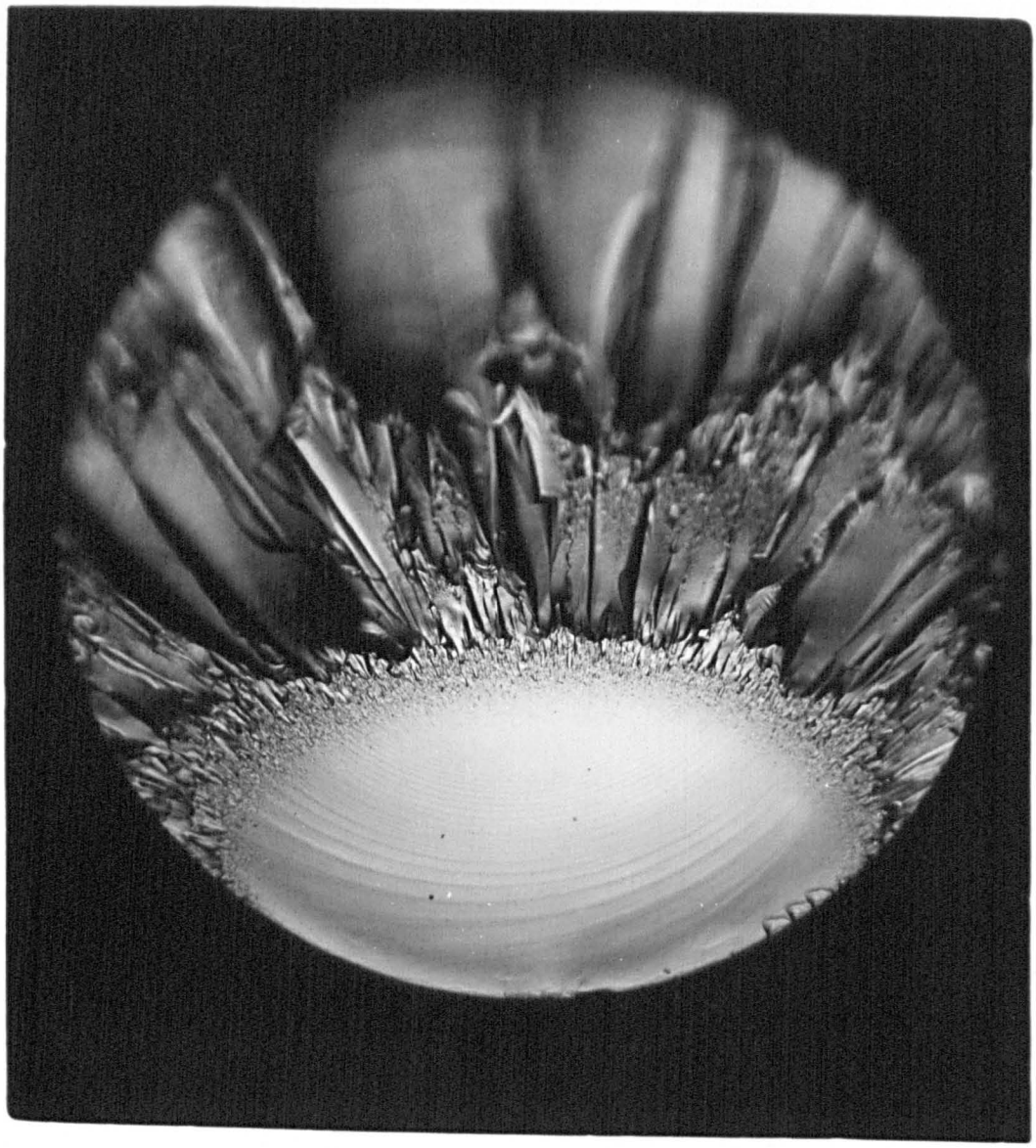

Fig. 18

Showing a D-shaped mirror. Non-annealed X8 rod broken in tension. Magnification x 45

Vertical incident illumination.

from the tensile results of Chapter 2, Section 2.10 that it is the local thermally induced mechanical stresses which have a profound effect on the value of $Zc^{\frac{1}{2}}$. That is, it is the local stress existing prior to fracture at the point at which bifurcation subsequently appears which matters. Second, the results of Section 2.10 indicate that the propagation of the crack does not produce any major change in the distribution of the local stress field during its passage. This shows that the part of the local stress field which is due to the independent mechanical stresses within the rod, is not altered in any important way by the elastic disturbances produced by the propagating crack. Finally, that part of the local stress field due to the externally applied tensile stress would not be expected to change radically during the time of passage of the crack (3 - 5 microseconds). Any such alteration in this stress can only be made by longitudinal stress waves travelling from the crack region to the grips and back. This time is usually much larger than the time required to sever the specimen. On this basis, the interpretation placed on the Z required by Eqn. 1.3.1 is felt to be reasonable.

3.3 Generation of mirror profiles by geometrical construction

The experiments conducted in tension on "as received" 3mm X8 rod and described above, yielded mirrors which had shapes different from those from fibre, or annealed rod, fractures. The profile of an "as received" rod mirror (hereafter called a D-shaped mirror) is shown in Fig. 18 and can be compared with the mirrors observed in the fracture of annealed rods (see Fig. 1). Both these are different in profile from the mirrors obtained from bending breaks and these latter also

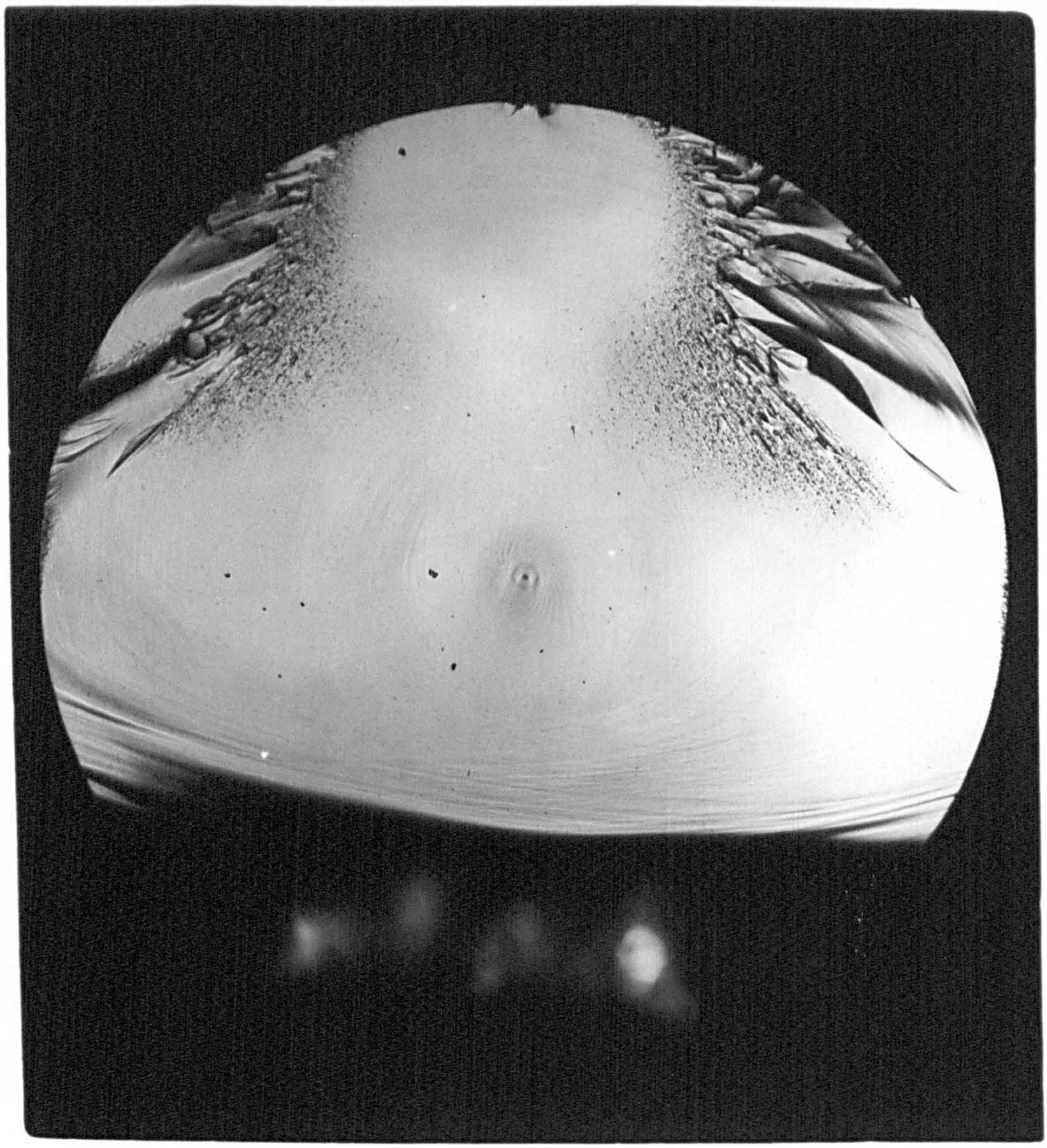

Fig. 19

Showing the phenomenon of "break-through" in the mirror region.
X8 3 mm rod broken in bending. Magnification x 45.
Vertical incident illumination.

have a diversity of shape within their own group. For instance, no complete mirror has been obtained in these experiments greater than 0.5mm in radius from a 3mm rod, or greater than 1mm radius from a 5mm rod when tested in bending. After these distances bifurcation appears to fail to take place in the centre and there is a "break-through" of greater or lesser extent, although there is nearly always successful lateral forking giving rise to "wings" on the fracture surface (see Fig. 19). This type of fracture has been reported in the literature (Shand (3), (4) etc.). One other type of mirror profile produced in bending is the "off axis" break which gives rise to its own characteristic distortion (Fig. 20) and which may also be combined with the "break-through" phenomenon.

All these types of mirror profile may be generated by geometrical construction with a fair degree of success by utilising the changed approach to the meaning of the stress Z in Eqn. 1.3.1.

For any given value of the constant (say 6) in Eqn. 1.3.1 there is a unique set of pairs of values of Z and $c^{\frac{1}{2}}$ which give k as a product. Fig. 21 shows such a set given in the form Z as a function of c. Only combinations of Z and c given by points on this curve will yield a product $Zc^{\frac{1}{2}} = 6$. The curve is unique for any given value of the constant and should be true for specimens of any diameter. The curve of Fig. 21 has been drawn for $Zc^{\frac{1}{2}} = 6$ (the experimentally determined value for X8 glass rods) and as far as $c = 3.0$mm. It is possible to represent on Fig. 21 the tensile stress acting, immediately prior to failure, at all points in a specimen being tested in tension by a line such as AB. The intersection of

Fig. 20

Showing the fracture surface which resulted from a bend test on 3 mm X8 rod when the fracture origin lay off the line of maximum surface stress. Magnification x 45.

Vertical incident illumination.

AB with the curve CD gives the value of c to be expected from failure at this stress level, and it can also be seen that pure tensile tests in general will yield only one value of c to be expected from the particular stress level concerned. This is not surprising, in fact so far this is only a graphical re-statement of the empirical truth of Eqn. 1.3.1. However if the stress distribution is not that due to a tensile test but that due to bending, then a different result is evident.

In the bending case the diameter of the specimen is important since the reasonable assumption will be made that for round rods the neutral bend axis is a plane containing the geometrical axis of the rod. Suppose, for the purposes of illustration, a 5mm rod is placed in bending. It is possible to represent the stress distribution in the rod immediately prior to fracture by some inclined line like EF on the graph of Fig. 21. Clearly a large number of such lines could be drawn through the neutral bend axis, the intercepts of these lines on the principal stress ordinate depending only on the maximum surface stress required to initiate fracture. Such a line as EF is seen to intersect the curve CD in two places, one corresponding to a small value of c , the second intersection to a larger value. This is the first point to be made, that is, the larger mirror radii in bending require surface stress levels in the same range as the surface stress levels required by small mirrors. Therefore in the crack development process the construction indicates that the conditions necessary to produce a small mirror are always satisfied first. Also it will be observed from the diagram that a line drawn through the point representing

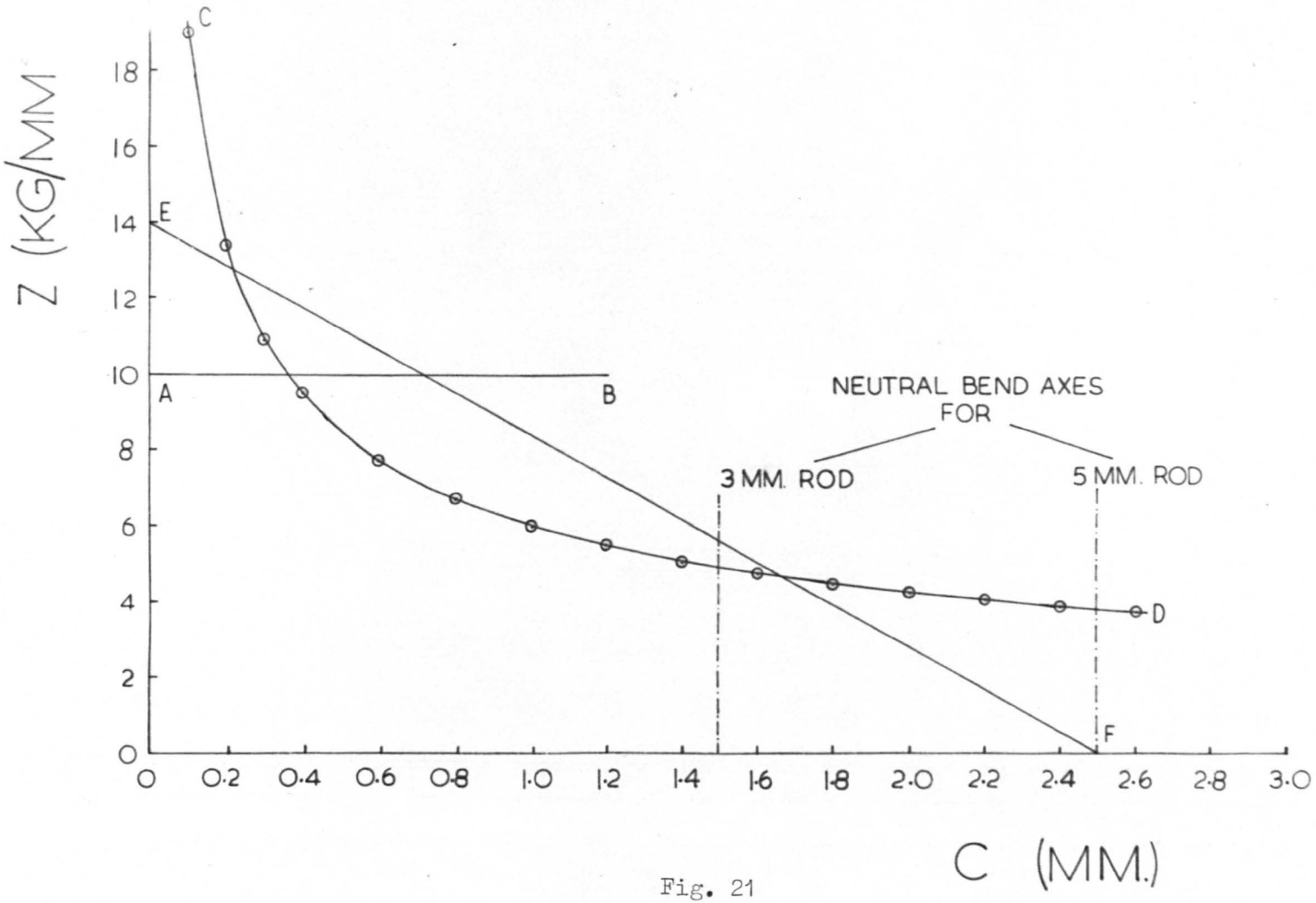

Fig. 21

Showing the breaking stress Z as a function of mirror depth for a value of $Zc^{\frac{1}{2}} = 6$.

the neutral bend axis and at a tangent to the CD curve is the minimum slope at which the $Zc^{\frac{1}{2}}$ product can be satisfied in bending. At surface stress levels below that given by this line the implication is that bifurcation should fail to take place.

In order to generate the complete mirror profile it is necessary to visualise the meaning and construction of this process in three dimensions. The principal stress ordinate can be visualised as being located at the origin of fracture on the circumference of the specimen, but the stress distribution (in the case of bending) is now an inclined plane (not a line) passing through the neutral bend axis. The mirror profile is obtained by rotating the CD curve about the principal stress ordinate and finding the locus of all the points in which the CD curve intersects the EF plane. All the "large-mirror" points should be disregarded as being excluded solutions, and the true mirror profile is given by projecting the locus so found into a horizontal plane. This process is most easily carried out using standard geometrical construction and engineering drawing techniques. A selection of mirror profiles obtained using such techniques is given in Fig. 22. These profiles represent various solutions of the bending case involving one off axis break (cf with Figs 19 and 20).

It is a simple matter to perform the constructions for various stress distributions i.e., tensile stress, tensile stress with paraboloidal stress distribution in the rod, and bending stress. All yield fairly successfully shapes corresponding to those obtained in practice. In addition it will be seen that the tangents to the CD curve through the respective neutral bend axes for rods of

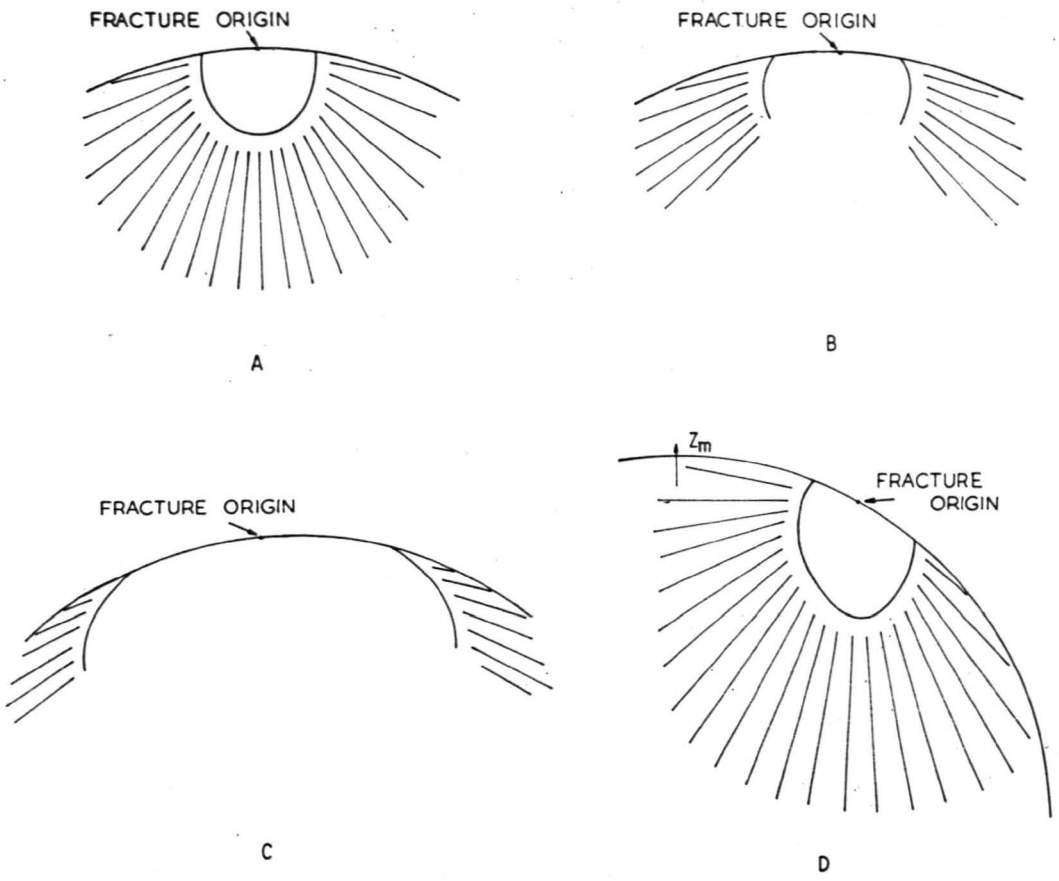

Fig. 22

Sketches of four mirror profiles (bending case) obtained using geometrical and engineering drawing techniques. Arbitrary scale.

various sizes give the maximum values to be expected for the mirror radius of a complete mirror. In particular the CD curve in Fig. 21 drawn for $Zc^{\frac{1}{2}} = 6$ gives,

maximum complete mirror radius = .45 - .55mm for 3mm rods,

and " " " " = .75 - .95mm for 5mm rods.

It can be seen from Figs 16 and 17 that these values are very close to the maximum complete-mirror size obtained in practice for X8 rods tested in bending and having this value for $Zc^{\frac{1}{2}}$.

3.4 Previous observations of a relationship between Z and $c^{\frac{1}{2}}$.

Several workers have previously observed a relationship between breaking strength and the square root of the mirror depth, and have given empirical equations for it. It is interesting to compare the present results with their values.

Levengood (2), using small specimens of sheet glass broken in bending, obtained a value of $Zc^{\frac{1}{2}}$ as follows,

$$Zc^{\frac{1}{2}} = 2.7 \times 10^3 \qquad 3.4.1$$

where Z is the breaking strength in pounds per square inch, and c is the mirror depth in inches.

The value for $Zc^{\frac{1}{2}}$ given above is an average value calculated from all points on the curve, with a variation of $\pm$ 16%. Levengood did not qualify the value of the stress Z to be used as was done in section 3.2 above. Orr (15) has given an empirical equation for this type of fracture which was identical in form to Eqn. 3.4.1 and he reported a variation in the value of the constant from 1.7 to 2.0×10^3 lbs/in .

By using the experimental data given by Terao (12), Levengood computed a value of $Zc^{\frac{1}{2}}$ for rods 5mm in diameter which were broken in bending. Terao plotted the depth of the mirror as a function of the breaking stress, using different rates of loading for two groups of samples. Average values were taken directly from these curves by Levengood and the value of $Zc^{\frac{1}{2}}$ was found to be 1.65×10^3, with a random variation of $\pm 0.1 \times 10^3$ - units as before. There were no apparent effects from variations in the rate of loading.

Cameron (16) has recently obtained results for the value of $Zc^{\frac{1}{2}}$ in bending, tension, and torsion for rods up to 10mm in diameter. Within the limits of experimental error his values are sensibly in agreement with those given so far.

It seems curious however that none of the previous workers using round rod in flexure (i.e., Terao, Cameron, Shand (17)), reported the non-constancy in the value of $Zc^{\frac{1}{2}}$ as measured in the present work and described in Section 3.2. Shand (17), using the value of $Zc^{\frac{1}{2}}$ for round rods in bending to estimate the tensile stress at failure in tests where this would otherwise remain unknown, made the $Z_m \cos\theta$ adjustment described in Chapter 2, Section 2.10 but did not report finding it necessary to make a $Z_m \cos\theta \frac{r - c}{r}$ adjustment to obtain consistent results. Of the other workers Orr would be precluded from the possibility of observing this effect by his use of rectangular specimens and his method of measuring c along the surface of maximum stress.

Orr also confirms that, for flat plate, the local thermally induced mechanical stress in the plate must be added to the stress at fracture

in order to obtain a value for $Zc^{\frac{1}{2}}$ which is in agreement with the value of $Zc^{\frac{1}{2}}$ obtained from strain free material.

It should be noted that Griffith (5) showed from theoretical considerations that the breaking strength Z , depends on the inverse square root of a crack length as follows,

$$Z = \sqrt{\frac{2E\alpha}{\pi c}} \qquad 3.4.2$$

where E is Young's Modulus of the glass,

α is the surface tension of the glass,

and c is one half the crack length on the surface.

Equation 3.4.2 bears a superficial resemblance to Eqn. 3.4.1 but it should be said here that the two equations are not equivalent. Griffith's equation applies to the situation in which a plane, static, pre-existing crack is contained in a brittle medium, and his equation is concerned with determining the conditions for spontaneous expansion of this crack. Equation 3.4.1 is an empirical relationship found to hold for the instantaneous position of a moving non-planar crack at which position the crack is producing mist of a fairly closely defined scale. For these reasons the Griffith relationship (Eqn. 3.4.2) is considered to be different from the $Zc^{\frac{1}{2}}$ functions given by Levengood, Orr and that given in this thesis.

The empirical relationship used in this thesis has the precise form of Eqn. 3.4.1. It was independently discovered during a re-examination of the results taken to examine Smekal's parameter, the "reduced tensile strength". The values of $Zc^{\frac{1}{2}}$ for the glasses used fall in the range 5.5 - 7.5 Kgms/$mm^{3/2}$, that is 1.5 - 2.0 x 10^3 lbs/in 3

These values are in good agreement with those of Orr and Terao. The coefficient of variation of a group of samples (about the mean) is approximately 3%, which is within the estimated maximum experimental error of approximately 5%.

3.5 Previous explanations of empirical fact $Zc^{\frac{1}{2}} = k$

Bateson (18) has developed the relationship $Zc^{\frac{1}{2}}$ = constant, from theoretical considerations, and as he indicates that the value of $Zc^{\frac{1}{2}}$ ought to depend principally on the maximum fracture velocity and the surface tension his work will be discussed in some detail below.

Bateson derived an expression for the velocity of crack propagation in a brittle material on the basis of the distortion energy at the crack surface. By differentiating this expression with respect to time he obtained the acceleration of the crack as a function of the applied stress, crack tip radius and some physical constants of the material. Up to this point Bateson's equation is in general agreement with most other workers. However, Bateson took the result further by assuming that a terminal velocity V_f is reached when hackle* appears and that the

---

* In this thesis a distinction is made between mist and hackle (see Chapter 1, Section 1.2), but it seems clear that Bateson does not make this distinction. The term hackle used in the text is Bateson's term. It is thought that this must have the same significance as the term hackle as defined in Section 1.2 of Chapter 1. The fracture features called mist in this thesis can be shown, by the use of the electron microscope, to be in existence at a very early stage in the development of that feature which is called mirror when observed with an optical microscope.

acceleration of the crack remains constant. Elementary mechanics can be applied and the mirror relationship, $Zc^{\frac{1}{2}} = k$, is easily extracted. Bateson's final equation is given below with slight changes in notation,

$$Zc^{\frac{1}{2}} = \left(\frac{V_f}{V_T}\right)\left[E\,\alpha\,(1+\nu)\right]^{\frac{1}{2}} \qquad 3.5.1$$

where Z is the applied tensile stress,

c is the mirror depth,

E is the Young's Modulus of the glass,

α is the surface tension per unit area of the glass,

V_f is the terminal velocity of the crack,

V_T is the transverse wave velocity in the glass,

and ν is the Poisson's ratio for the glass.

Bateson offers no explanation of the role of terminal velocity in the production of mirror, mist and hackle. It is not clear why the attainment of a terminal velocity by the crack should result in the observed fracture morphology. If the assumptions on which Eqn. 3.5.1 is based are accepted for the moment, the value of $Zc^{\frac{1}{2}}$ as determined experimentally can be compared with the values predicted by Eqn. 3.5.1.

The value of $Zc^{\frac{1}{2}}$ as measured experimentally for X8 glass is approximately 6.0 Kgms/mm$^{3/2}$. The value predicted by Bateson's equation can be obtained by substituting experimental values for E, α, V_f/V_T and ν in Eqn. 3.5.1. Some typical values for these quantities are given in Table 3.5.1 overleaf.

Table 3.5.1

Glass of X8 composition

	Value	Source
E dynes/cm^2	6.5 x 10"	Lab.-bending beam
α dynes/cm	310	Calculation using Dietzel's (19) method
V_f/V_T	.45	Schardin (20)
ν	.25	Schardin (20)

The theoretical value of the constant $Zc^{\frac{1}{2}}$ for a glass of approximately X8 composition calculated from Eqn. 3.5.1 using the values given in Table 3.5.1 is 0.2 Kgms/mm$^{3/2}$. This value is more than one order of magnitude smaller than the experimentally measured value. There is some experimental evidence which suggests that the surface energy of glass at the tip of a running crack may be much greater than that quoted in Table 3.5.1 (Orowan (21)). However, an increase in the quoted value for the surface energy by one order of magnitude will still only yield a value of 0.7 Kgms/mm$^{3/2}$ for the value of $Zc^{\frac{1}{2}}$. Therefore a comparison of the experimental value with the theoretical value shows poor numerical agreement.

It is clear that although Bateson's equation predicts a different value of $Zc^{\frac{1}{2}}$ for different glasses, the actual numerical agreement between experiment and theory is poor. This disagreement is not much reduced by the possibility that the value of the surface energy normally accepted may be in error by one order of magnitude.

Assuming that the experimental measurements are correct, this disagreement between theory and experiment may be due to one, or both, of two reasons. First, it is possible that in the course of the derivation of Eqn. 3.5.1 some condition, invalid in the context of the derivation, has been applied. Second, it is possible that the assumptions on which the theory is based are in error. The first of these two possibilities will now be examined with particular reference to the work of Mott (6), Dulaney and Brace (22), and Berry (23).

Mott has given an equation for the velocity of crack propagation in a brittle medium which Bateson says is equivalent to his own, both in general form and in its numerical evaluation. It seems relevant to make particular note of this since, as has been pointed out by Dulaney and Brace, Mott's theory in its original form cannot predict the entire velocity behaviour of a running crack as it accelerates from rest to terminal velocity owing to a simplifying approximation in the derivation. Because Mott was primarily investigating terminal velocity, he imposed the condition that the rate of change of velocity with crack length was zero. Bateson re-derived Mott's equation in order to compare it with his own equation for this velocity of crack propagation, but in doing so made no mention of the limiting condition imposed by Mott and noted above. The equivalence of Mott's and Bateson's equations seems to imply that Bateson's equation is only true at, or near, terminal velocity.

Dulaney and Brace, and Berry have obtained expressions for the velocity behaviour of a growing crack without recourse to the restriction noted above, and these expressions show that the crack should make a

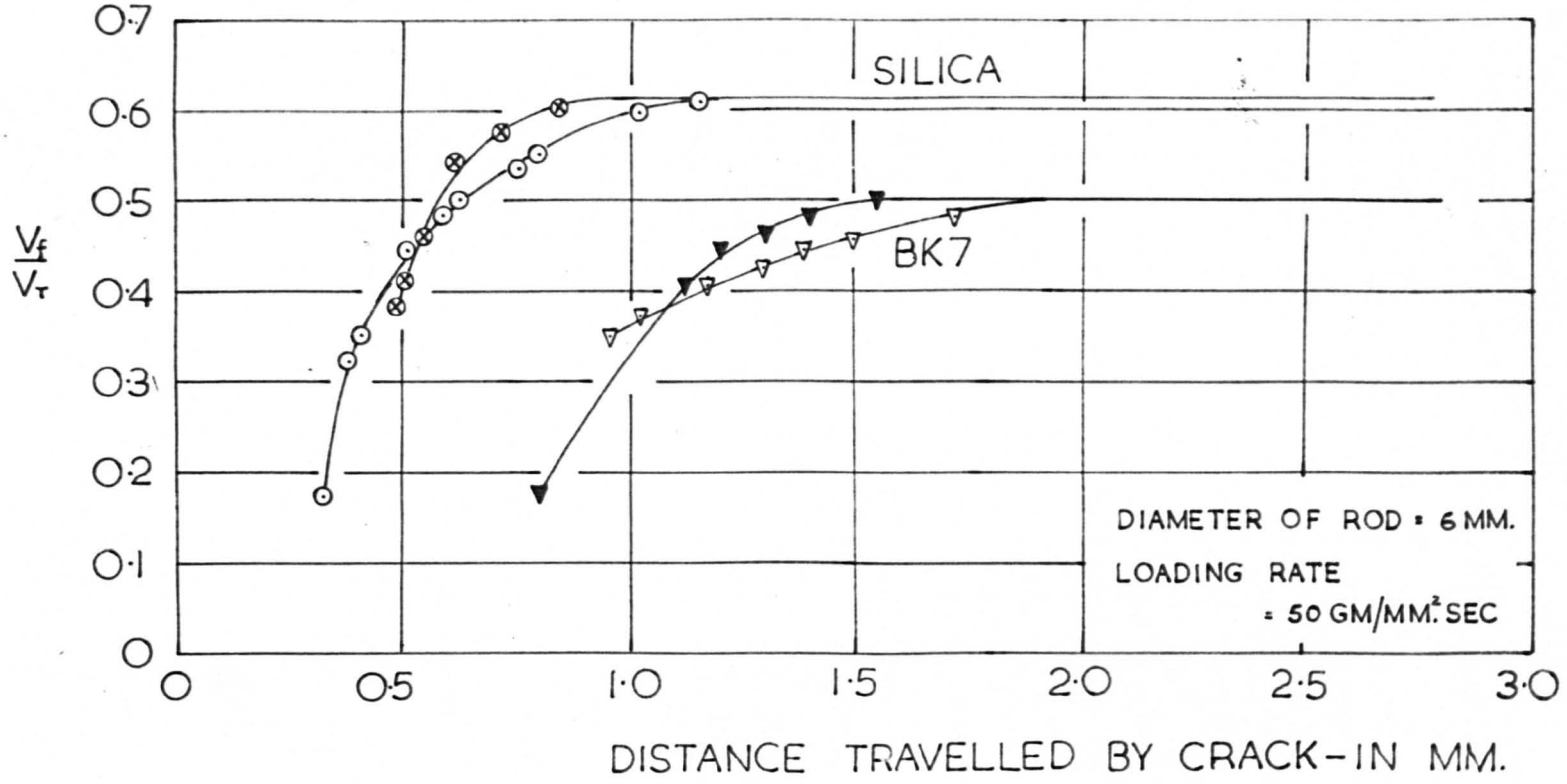

Fig. 23

Showing the relative crack velocity V_f/V_T as a function of the distance travelled by the crack.

hyperbolic asymptotic approach to terminal velocity. Experiments on fracture in perspex (polymethyl methacrylate) support this conclusion. It is also clear that the acceleration of the crack from rest until its velocity reaches a maximum value is anything but uniform. Thus the condition of uniform acceleration required by Bateson's theory for the application of elementary mechanics in order to obtain an expression for the distance moved by the crack to reach maximum velocity, is not fulfilled.

So far it has been concluded that the values of $Zc^{\frac{1}{2}}$ indicated by Eqn. 3.5.1 do not agree with experiment and two possible reasons why this may be so were given above. The first of these has been examined and it has been concluded that the assumption of uniform crack acceleration is an over simplification of the general velocity behaviour of the crack. The second possible reason given above was that the derivation may have been based on wrong physical assumptions.

Bateson's treatment is based on the assumption that a terminal velocity V_f is reached when the hackle portion of the fracture starts. Experiments reported by Dulaney and Brace (22), on fracture in perspex show that the attainment of a terminal velocity and the appearance of hackle may coincide. On the other hand data published by Smekal (24) indicate that a terminal velocity may be attained, and maintained, for some considerable distance before hackle appears, in some cases without hackle appearing at all, as shown by Fig. 23. For this figure, taken from Smekal, information on the temporal behaviour of the fracture process was deduced from fracture surfaces which showed naturally occurring Wallner lines. These features are generally obscured by mist and hackle,

and therefore the fact that a terminal velocity can be shown in Fig. 23 indicates the absence of mist and hackle up to the limit of these measurements. It may be said therefore that Bateson's treatment based on the assumption that a terminal velocity V_f is reached when hackle starts, is based on an assumption which is not generally true.

This concludes the examination of Bateson's derivation of a relationship $Zc^{\frac{1}{2}}$ = constant. This derivation is regarded as being wrong in principle on the grounds of the experimental evidence quoted above. It should be noted here that Bateson clearly realised the shortcomings of his treatment which appears to be one of the few attempts at a theoretical derivation of the mirror relationship available. In Chapter 6 there will be a further very brief consideration of Bateson's equation and the grounds for placing a different interpretation than ordinary surface tension on the term α in Eqn. 3.5.1.

The suggestion has been put forward by Shand (4) that the break-up of the mirror region takes place at a critical stress which is characteristic of the material. He proposed that the first part of the fracture process takes place very slowly and during this time the crack is in quasi-static equilibrium. Jones (25) and Preston (8) have also supported this argument. Shand thought that eventually the crack would reach such a size that the stress at the crack tip would attain a value which would lead to bifurcation. The breaking stress according to Shand is the intrinsic strength of the glass divided by the stress concentration factor of a crack with the dimensions of the mirror surface. Thus in the case of a crack with a depth, or radius, c in the section of a circular rod

of diameter D , the nominal breaking stress can be written as follows,

$$\sigma_a = \frac{\sigma_m}{k} = \frac{\sigma_m \sqrt{\rho}}{f(D, c)} \qquad 3.5.2$$

where σ_a is the breaking stress of the sample,

σ_m is the critical or intrinsic stress of glass,

k is the stress concentration factor,

ρ is the effective radius of the crack tip,

and $f(D, c)$ is a component of the stress concentration factor.

One objection to Shand's idea however, is that the concept of the fracture process being divisible into two distinct phases is an over-simplification of the facts, as is shown by a microscopic examination of the fracture surface. A second objection is that the idea of the slow growth of the initial crack through the mirror region is almost certainly in error (see Fig. 23). Finally, and possibly most importantly, it is not immediately obvious what is meant by the statement that "... the mirror, when large enough, will cause catastrophic failure by exceeding the theoretical strength of the material", (Anderson (26)). It is difficult to see why the stress at the crack tip, at any stage during its growth, is not already equal to, or greater than, the theoretical strength of the material, since bonds are being irreversibly broken. The second and last of these objections taken together raise severe conceptual difficulties, and the lack of success experienced in obtaining a physically plausible estimate of this critical crack-tip stress, promoted a search for the formulation of other criteria for the termination of the mirror region.

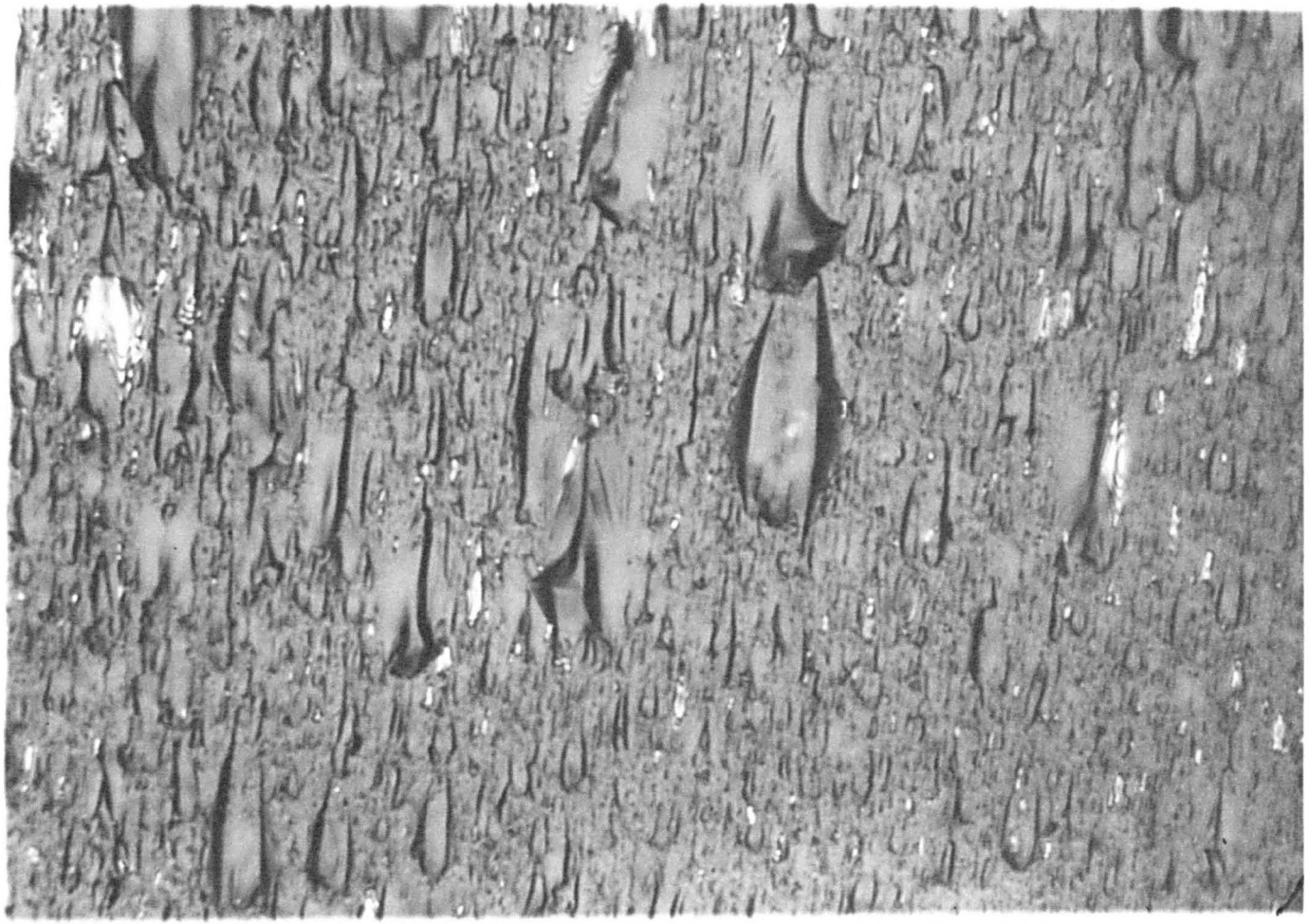

Fig. 24

Typical mist area in X8 glass. Magnification x 920.

PART II

CHAPTER 4 DETAILED STUDY OF THE MORPHOLOGY OF GLASS FRACTURE FACES

4.1 Introduction

The experimental work described in Chapter 2 represents the work performed to measure the value of $Zc^{\frac{1}{2}}$ for various glasses in various experimental situations. The $Zc^{\frac{1}{2}}$ parameter however, by definition, depends upon the presence and full development of the mirror, mist and hackle pattern on the fracture surface. So that although it was possible in the preliminary analysis of Chapter 3 to obtain some useful information, a full interpretation of the factual data collected by the experiments of Chapter 2 awaits an insight into the significance of the mirror, mist and hackle morphology itself. It was therefore felt that the answer to this problem might be found in the features of the fracture surface. In particular an examination of the structure and an interpretation of the mist, which is the point to which the measurement of c is taken, was felt to be most urgently required.

A preliminary inspection of this question revealed an apparent paucity of published information about the actual structure of the mist. Other types of fracture feature have been well documented, for instance Murgatroyd's (11) descriptions of ribs and striae etc., on fracture surfaces produced in complex stress systems. The gross macroscopic appearance of mirror, mist and hackle has also been described many times. However the actual characteristics and micro-appearance of mist seems to have been relatively untouched..

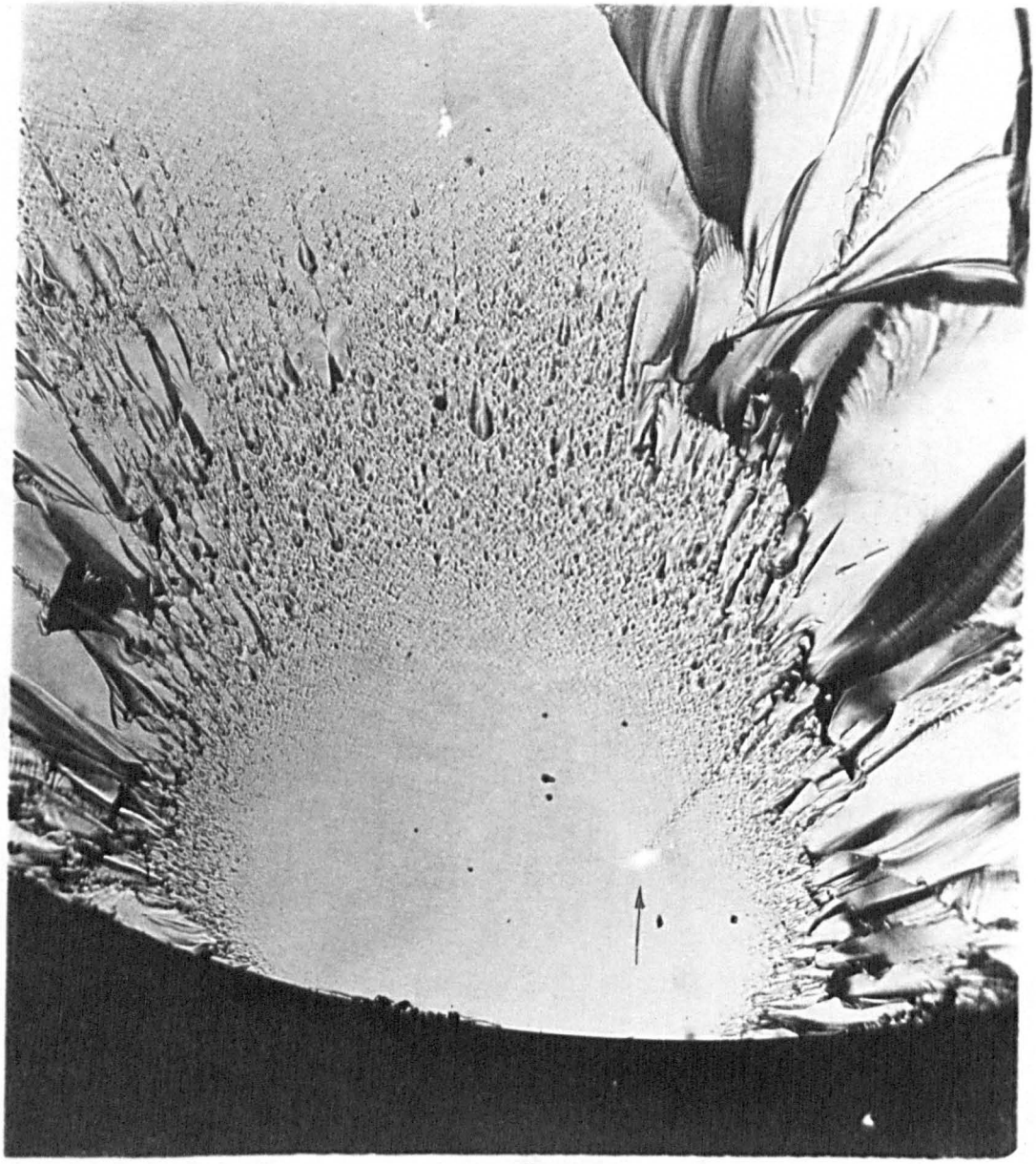

Fig. 25

Inhomogeneity in silica, bending fracture. Magnification x 85.
Transmitted light.

An examination of the mist was therefore undertaken. The main results of this examination to be described below, were the recognition of two basic types of mist feature, or element, and the discovery of the existence of a large number of stopped sub-surface micro-cracks under the fracture surface in the mist region which correlated with the mist elements mentioned above. It is worth-while noting here the difficulties involved in presenting material of this nature where, to avoid ambiguity, descriptions must often be lengthy even when aided by photomicrographs.

4.2 Some experimental observations on the occurrence of mist in glasses

The most frequently observed situation for the development of mist is of course as the middle stage in the development of the mirror, mist and hackle pattern. In this situation the gross characteristics of its morphology can be easily identified. First, where the full specific fracture pattern as typified by Fig. 1 has been developed in the silicate glasses the mist has never been observed to be absent. That is, the transition mirror - hackle has never been observed. Second, there is an increase in size in the mist features from sub-microscopic to macroscopic in a direction away from the origin of the crack. Third, the mist features have clear directional qualities, in this case pointing radially to the origin of fracture. Finally, when observed under an optical microscope the mist has features which are separable as units, yet there is a lateral interdependence of these features which confuses the actual physical extent of any one unit. A typical mist area is shown in Fig. 24.

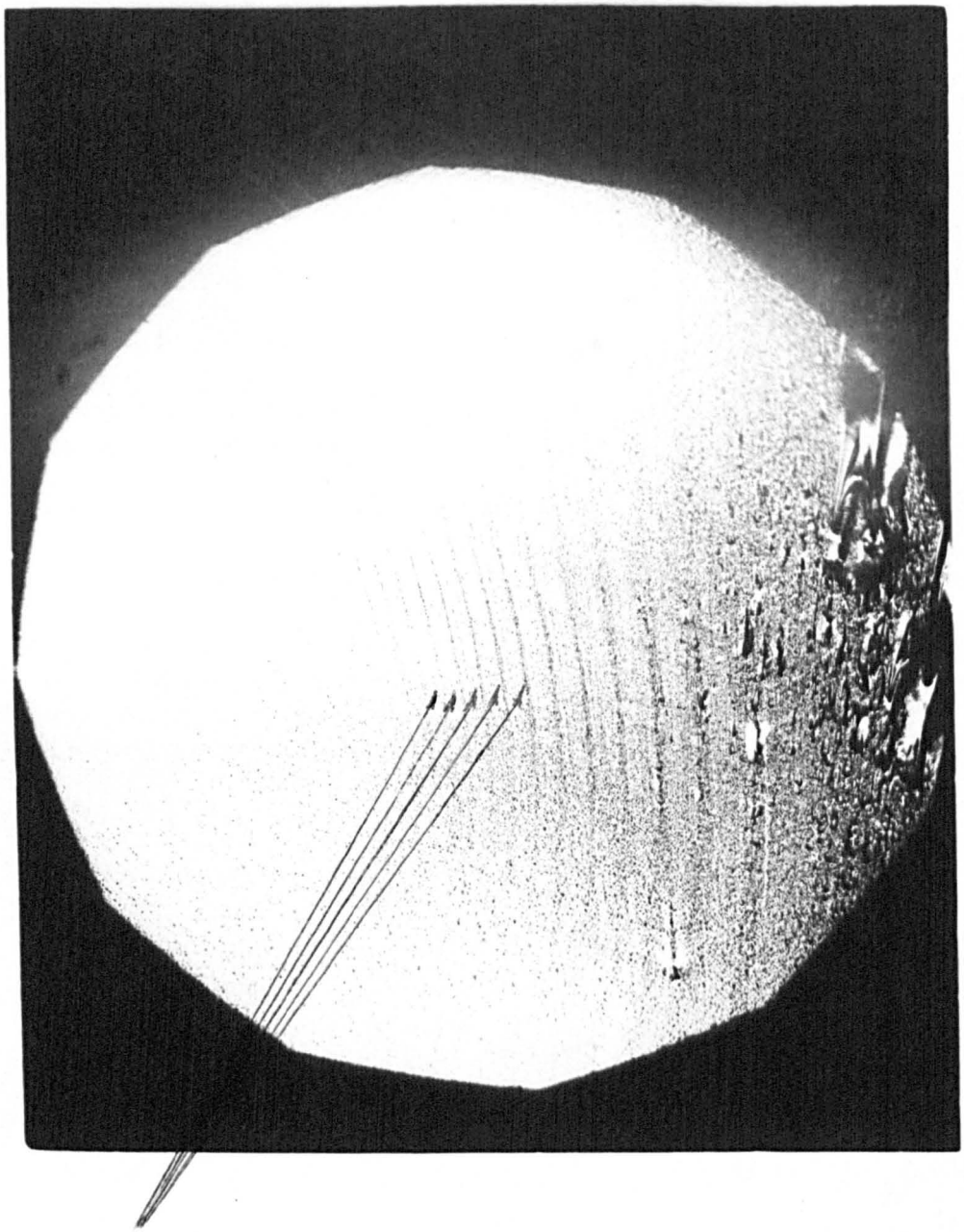

Fig. 26

Mist developed on "wrappings" in lead glass drawn by the Danner process. Oblique incident illumination.

Magnification x 45.

Mist can also develop apparently in isolated situations. Chemical inhomogeneities of the glass and the presence of bubbles interfere with the propagation of a crack in such a way as to influence the resulting fracture morphology. As an illustration of this Fig. 25 shows the presence of a chemical inhomogeneity in silica which has disturbed the advancing crack in such a way that mist formation in that area has set in earlier than it normally would have done, as shown by the position of the rest of the mist. It has been possible to establish in cases like this that the action of the inhomogeneity is to cause a re-entrant angle to appear in the crack front. This re-entrant angle persists for some time and during the greater part of this interval mist is produced by the crack over a local area as shown by Fig. 25. This figure also shows the directional quality of mist referred to above.

Another situation in which mist appears on its own is shown in Fig. 26. Here the mist is developed on "rings" in lead glass. These "rings" have been tentatively identified as being regular regions of chemical inhomogeneity appearing in all the soft glasses drawn by the Danner process. It is understood that in the glass industry these rings are called "wrappings" (Hawkins (27)). It is interesting to note that after following the path of the rings for a short distance the mist trails break free and continue independently for a distance. It is probable that here the action is due to both the formation of a re-entrant angle in the crack front, and the fact that the material of the rings is different from the rest of the glass.

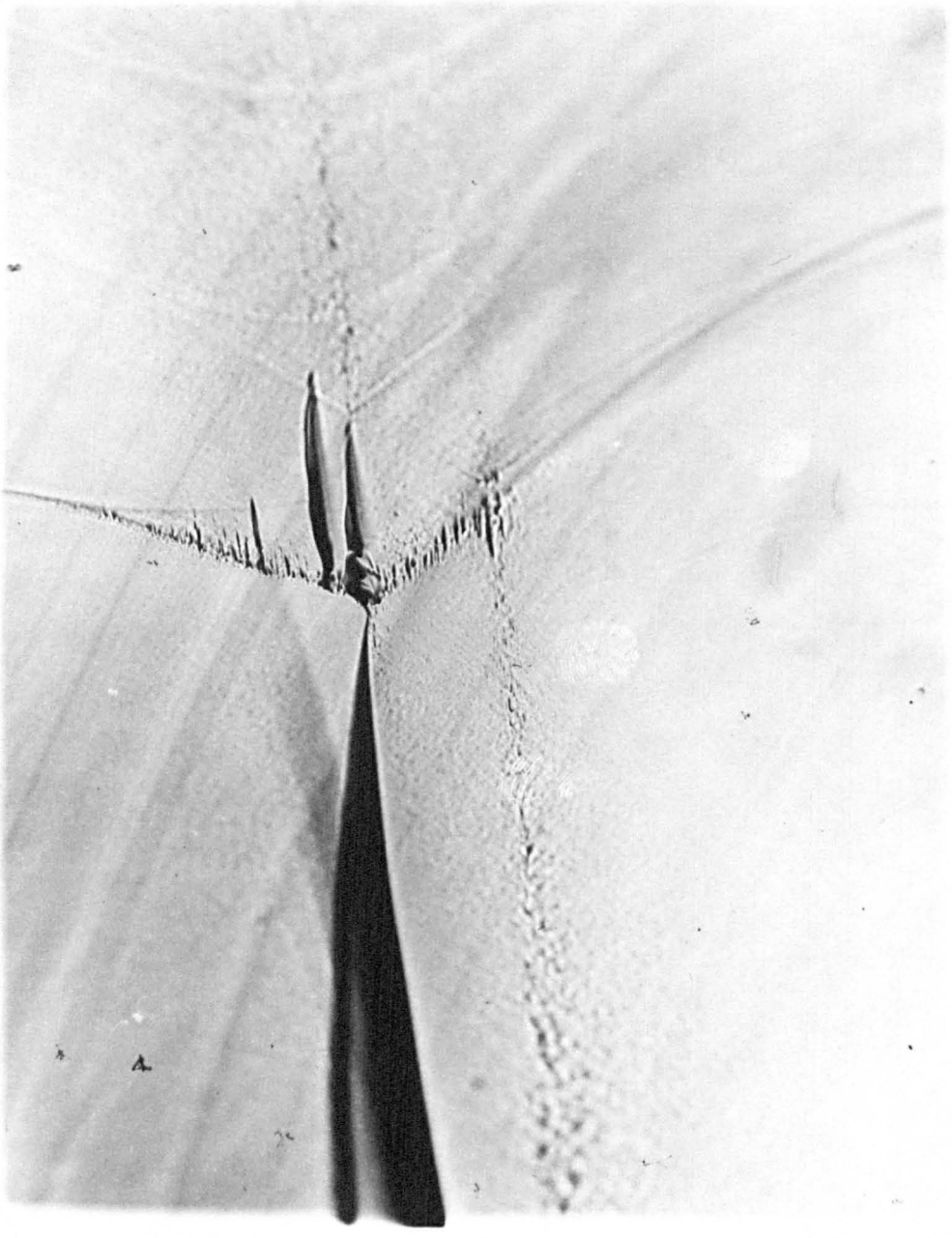

Fig. 27

Area of fracture surface of Pyrex rod broken in bending showing mist along a Wallner line. Magnification x 145. Transmitted light.

Yet another instance of the occurrence of mist on its own is shown by Fig. 27. It is apparent from this photograph that the mist here is the response to a transient condition. The mist area of interest is confined to the Wallner line, that is, to the locus of the intersection of the crack front and a stress wave. It should be noted that the Wallner line itself and the areas of mist on it are not produced instantaneously.

In summary then, the general occurrence and scale of the mist is controlled or influenced by some local condition associated in part with the crack itself and in part with the state or nature of the glass.

4.3 Some experimental observations on the classification of mist features

This section describes the results of a close inspection of the features of the mist region with the aid of a Vickers Projection Microscope and an attempt to classify the mist elements on the basis of two main types. In the course of this work a large number of fracture surfaces was examined, covering the range of useful dry optical magnifications (X5 - X60 objectives) and using a variety of glasses. A number of pairs of fracture surfaces was examined under a low power stereo-microscope. From this preliminary inspection pairs of surfaces, showing complete mirrors of good shape, were selected for a more intensive scrutiny.

It is not a simple matter to record the impressions of a visual inspection of the mist region in even a semi-factual manner. At first sight the mist region has a gross uniformity of appearance which makes it difficult to identify specific areas on matching fracture surfaces.

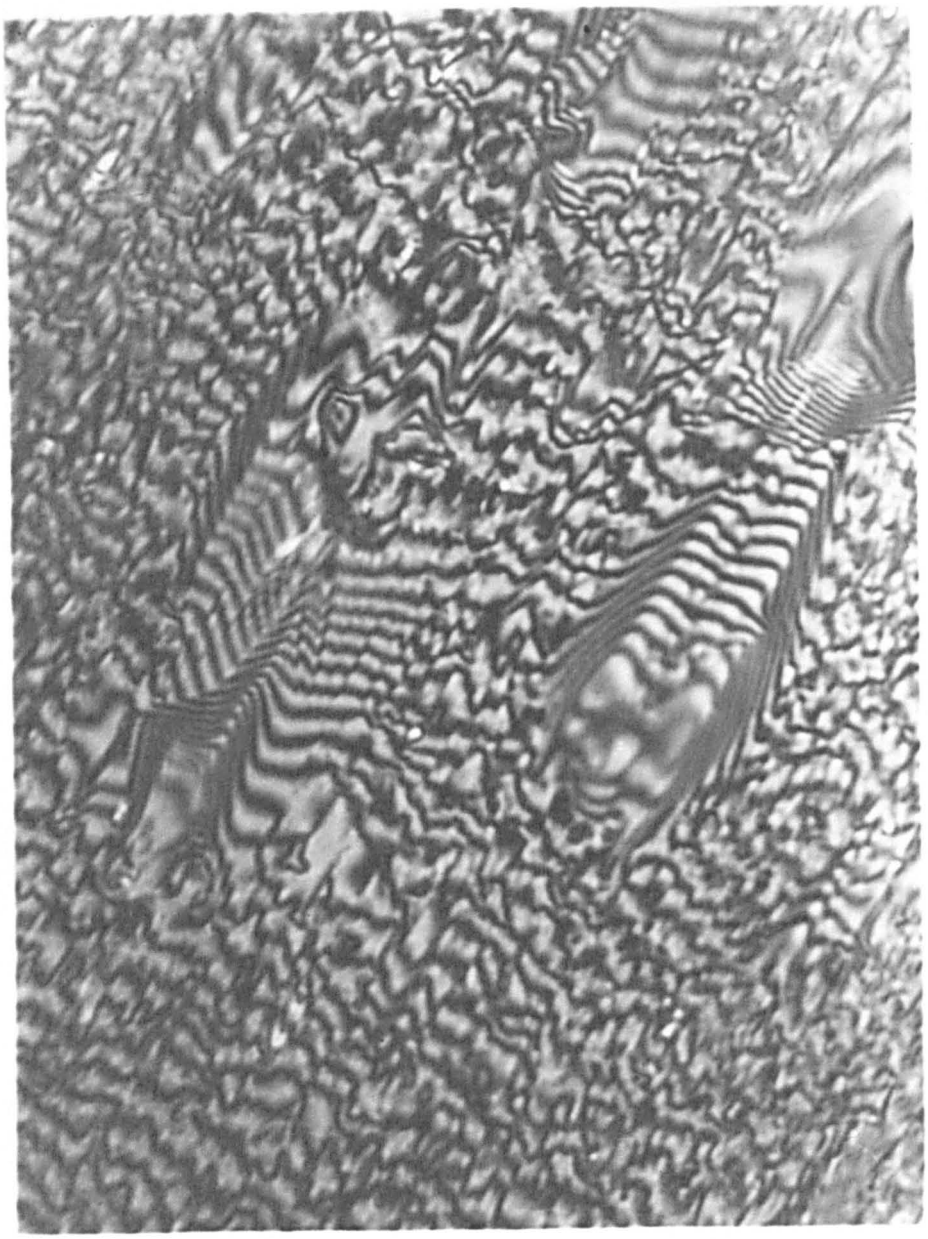

Fig. 29

Photomicrograph showing double-beam interference fringes in the mist zone. Magnification x 1470.

powers of x 40 or x 60 to be used with equal facility. An example of two beam interference fringes obtained between the unsilvered fracture surface and unsilvered reference plate is shown in Fig. 29.
A description of the construction of the interference attachment is given in Appendix II.

Type 2

Type 2 elements in their simple form are also easily recognised but not easily described. Once again a sketch of an idealised version appears in Fig. 28 (i). At the head of the feature is either a depression or a projection of the general shape shown. In the sketch the intention has been to portray a projection. However, matching fracture surfaces should show complementary elevations and depressions in the same areas. Flat mirror smooth areas of the surface are usually present on either side of the frontal feature and extend for some distance in the direction of crack propagation. These two flat areas intersect in the rear of the frontal feature forming a "wake" to it. Stiae are often predominant on the wake as represented in the sketch. In addition, on the middle and outer edges of the mirror - smooth areas, very small mist elements begin to form again as shown in Fig. 28 (i).

The mist region was thus found empirically to be capable of a broad division into two types of mist element, or feature, recognisable by their external appearance. These were Types 1 and 2 as described above. No solution to the formation of these basic features was forthcoming at this stage. An essential clue to the formation of the mist elements specified above as Types 1 and 2 was obtained when the fracture surface was lightly etched, with hydrofluoric acid. The two

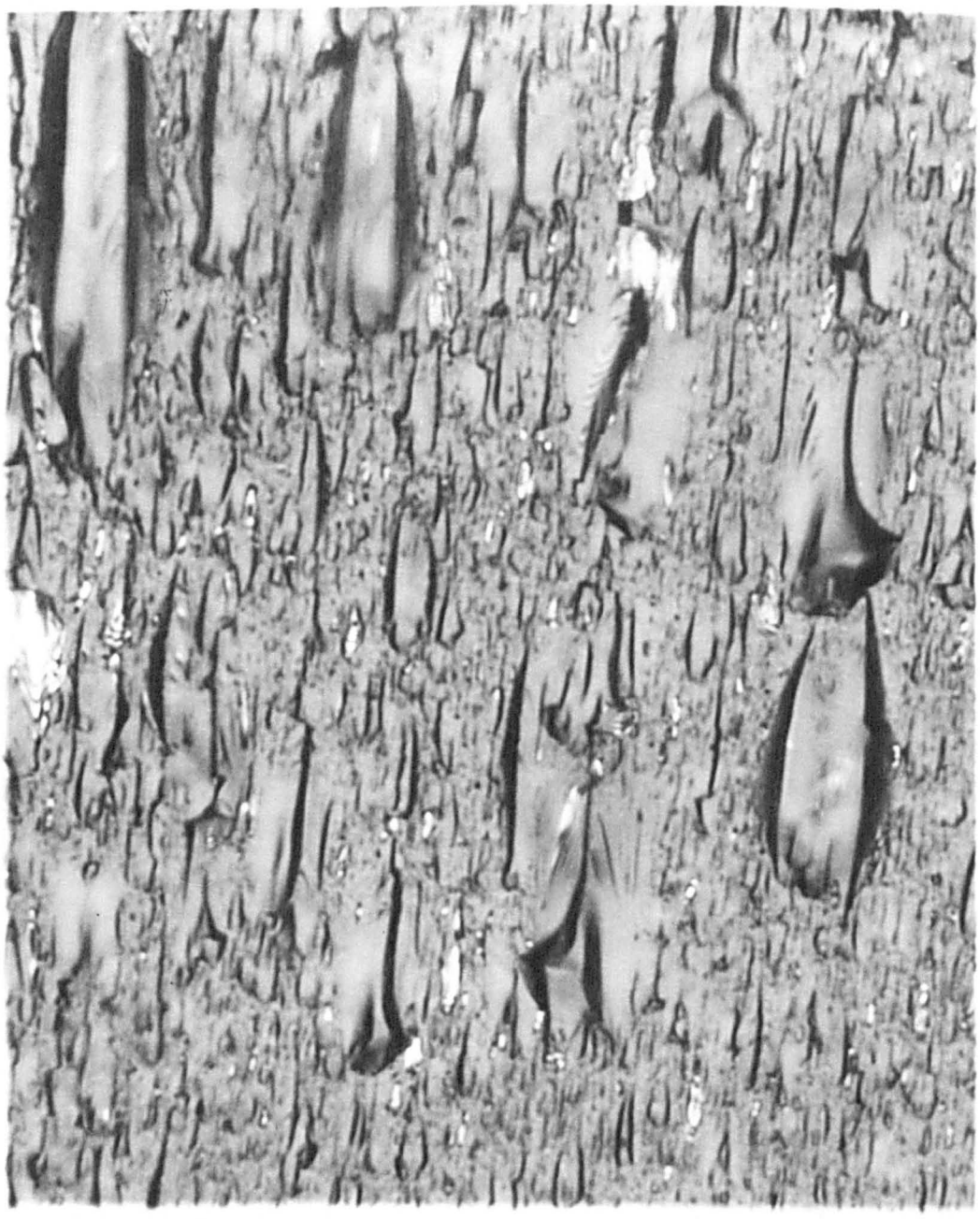

Fig. 30

Photomicrograph of specific mist area in the fracture surface of X8 glass. Normal incident illumination.

Magnification x 1100.

photomicrographs Figs 30 and 31 show the same area of the same fracture surface of an X8 rod. Fig. 30 was taken with normal incident illumination without treating the surface in any way. Fig. 31 shows the same area using dark field illumination after the surface had been etched for 2 mins in 4% (wt) H.F. The area in Fig. 31 is covered with patches of light, some occupying a considerable area. Under the microscope these patches can be identified as sub-surface stopped cracks which have been revealed by the etching. In addition the combined print of Fig. 32 shows the important fact that these patches of light can be correlated with the main fracture features. It should be pointed out that not all the very small patches of light represent cracks, some are reflections from irregular surface features but these are easily recognised under the microscope. In fact the sub-surface micro-cracks are difficult to photograph successfully because of distortions introduced by photographing through the irregular surface features. Preliminary experiments designed to investigate the possibilities of covering the irregular glass surface with some material capable of presenting a smooth surface to the microscope objective and yet not able to penetrate the micro-cracks, were only partially successful.

However it is evident from Figs. 30 and 31, and Fig. 32 that in the mist zone, underlying the features of the fracture surface itself, are large numbers of micro-cracks which have apparently stopped propagating after a short distance. During experiments involving serial etchings of fracture surfaces with very weak HF (< 1% wt) the subjective impression was gained that some of these cracks were

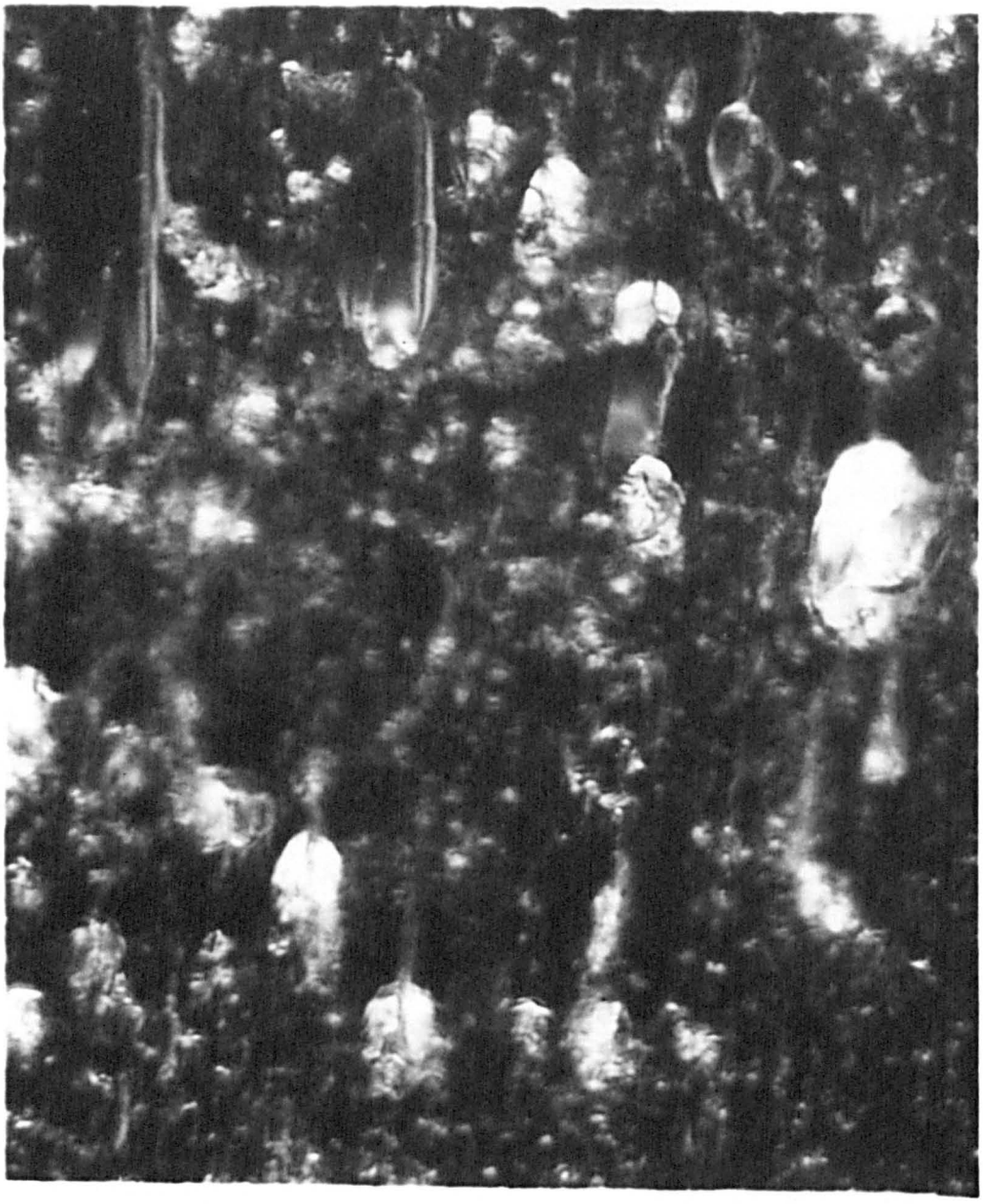

Fig. 31

Photomicrograph of mist area of Fig. 30 etched in 4% (wt) HF and shown under dark ground illumination.

Magnification x 1100.

not penetrated until the etching process had been under way for some time. This implies that some sub-surface cracks have no access to the main fracture surface, and the conclusion to be drawn here is that a secondary nucleation mechanism is in operation. This impression would profit from a closer inspection. The observation of these stopped sub-surface micro-cracks is an important one, for it provides a basis for an explanation of the general appearance of the mist zone and the mist elements identified above as Type 1 or Type 2. It is believed that the presence of such cracks beneath the surface of the mist zone has not been previously recorded in any specific statement.

4.4 Discussion of the formation of mist elements

To a certain extent the problem of deciding which mechanism operates to produce micro-cracks is an academic one. Given the production of semi-independent micro-cracks during the fracture process, and Figs 31 and 32 lend powerful support to the contention that such cracks exist, it is possible to classify and explain in a qualitative fashion the features of the mist region. For the purposes of the description given below a secondary nucleation hypothesis has been assumed. It is necessary to amplify the notion of secondary nucleation to be used here.

For the purposes of the following discussion it will be assumed that by secondary nucleation is meant the generation of an independent crack at a site in the material which is in front of the main fracture. In order that a crack may be initiated at such a site it is necessary that the local tensile stress there should be raised sufficiently

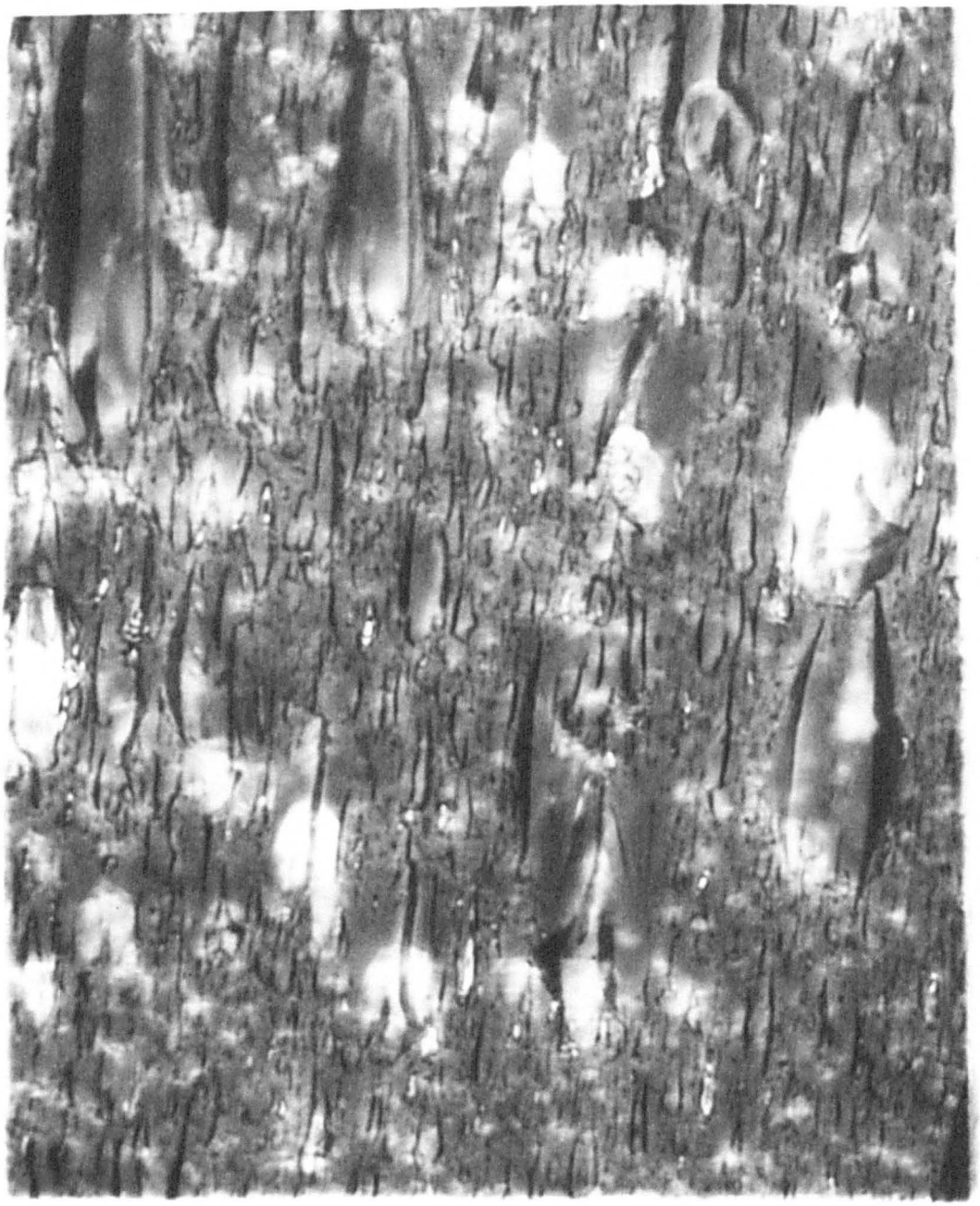

Fig. 32

Combination print using Figs. 30 and 31. Magnification x 1100.
(Fig. 31 is precisely overprinted on Fig. 30)

for the chemical bonds of the material to be broken. In general, it could be reasonably held that in a situation in which fracture has already been initiated by the "worst flaw", the local tensile stress at any other flaw site in the body will not be raised sufficiently to break the bonds of the material by the interaction of any type of stress-raiser located at that site and the local tensile stress arising from the applied load. (This may not be the case in materials in which fracture proceeds so slowly that there is time for an elastic wave to be propagated to the grips and back again). In this limited case it is assumed that in order for secondary nucleation to operate, the stress at any discontinuity must be further raised by the proximity of the main crack. This means in physical terms that the stress raising action of the main fracture at a secondary site is accomplished through the medium of the elastic disturbances generated by the main crack and passing through the secondary sites. In crude terms the secondary site receives the information of the approach of the main crack via the elastic disturbances generated by the latter. Thus it is clear that while the secondary site is importantly affected by the approach of the main crack, the latter is not affected by the presence of the flaw until a crack is nucleated there and an elastic disturbance thereby generated from it. The main crack is therefore physically uninfluenced by the presence and growth of the secondary crack during the time it travels some distance, this distance depending on how far ahead secondary nucleation takes place and the amount by which the secondary site lies off the main propagation plane. For the

purposes of the following discussion, the critical role of the elastic waves generated by the main crack in assisting the nucleation of secondary cracks should be borne in mind. An attempt is made to explain Type 1 features first below.

The evidence of Figs 31 and 32 is accepted as showing that independent cracks are generated during the fracture process. Suppose that at a point just above or below the average plane of fracture propagation and slightly ahead of the average crack front, the local tensile stress is sufficiently high for a crack to be independently nucleated. Then the interaction of this crack with the advancing main-crack front can have a number of results which depend upon the rate of growth of the secondary crack, the velocity of the main crack (assumed for these purposes to be held at a constant value), and the distance ahead at which nucleation takes place. If the rate of propagation of the secondary crack is low, or the distance ahead at which nucleation takes place is small and off the plane of general propagation, then it is possible for the main crack front to overtake the secondary crack before being intercepted by an elastic wave from the secondary crack and while the latter is itself still physically small. The interception of the main crack front by the secondary elastic wave is an important event and is assumed here to lead to the deflection of a local region of the main crack front away from the secondary site. The deflection of crack fronts by elastic waves is a well documented phenomenon, being supported both by naturally occurring Wallner lines on fracture surfaces and the method of modulating fracture surfaces with ultrasonic sound waves described

by Schardin (20). It is also a reasonable assumption that elastic disturbances generated by a growing crack will lead to consistent and similar results from their interactions with a crack front.
The unsupported part of the assumption made above is that the interaction is one which leads to a deflection of the crack front away from the flaw site. The only defence which can be made at present in favour of such an assumption is that empirically this looks to be the action occurring in the material itself and that the explanation of both mist element types is facilitated by accepting this. It is assumed for these reasons that when the main crack front meets the elastic disturbance generated by the secondary crack it is locally deflected away from the flaw. If the physical size of the secondary crack is small, and its expansion velocity below maximum, it ought still to be possible for the main fracture to sever the region above or below the secondary crack. In this way the main fracture, propagating at a high velocity, could out-distance the secondary crack. In this event the propagation of the secondary crack would cease. The digressive portion of the main fracture could then return to the general plane of crack propagation under the influence of the applied tensile stress. The schematic diagram of Fig. 28 (c) is an attempt to represent this process.

Clearly the presence of micro-cracks would be expected, on this hypothesis, under Type 1 features having an upward convexity on the fracture surface as in Fig. 28 (c). The physical extent of such cracks should be very limited. The complementary feature in the

idealised case would not be expected to display them. It can be fairly certainly shown (Fig. 32) that Type 1 features do exhibit very small sub-surface cracks at their head, usually under the convex feature. The above discussion was given in terms of secondary cracks nucleated in front of a main crack. In fact the advancing crack front would not on these arguments have such simple unity, but would be composed of a large number of secondary cracks. In this fact lies a possible explanation for the phenomenon of the multiple start mentioned in Section 4.3. Very often the larger mist elements at an advanced stage in the mist region display the coalescence of a number of small surface strips (now identified with secondary cracks) into the main mist elements. It is conceivable that a group of associated secondary cracks, representing the main crack front at that instant, could be influenced by an advanced secondary crack in the manner described above which concerned a local region of a "solid" crack front. Inspection of the earlier stages of mist formation shows a gradual decrease (in a direction towards the fracture origin) in the number of separate cracks forming the multiple start. In the very earliest mist elements which can be detected with the optical microscope there are very few multiple starts although the external forms of the elements are essentially the same as those depicted in Fig. 28.

Type 2 features are more complex than Type 1 and the corresponding number of distortions from the idealised version is greater. In this case there are two basic ways in which the necessary micro-crack interaction might be brought about.

First, consider the simultaneous nucleation of two secondary cracks, one almost above the other with the plane of general fracture propagation lying between them (see Fig. 28 (ii)). The two cracks are assumed to expand at approximately equal rates and diverge as they propagate. (This is essentially the same assumption as that made above). If the rate of expansion of these two cracks is such that they are overtaken by the main fracture, a pincer movement around and between these two diverging cracks becomes possible, as represented in Fig. 28 (iv). This movement, together with the divergent motion of the seondary cracks, terminates any further growth by them.

Second, consider the nucleation of only one secondary crack, as in Type 1, but at such a distance ahead of the main fracture front that by the time the main fracture arrives at this crack, the fracture fronts of primary and secondary crack are superimposed and expanding at the same rate (Fig. 28 (iii) and (v)). The situation can then develop as described above for double nucleation.

A brief consideration of the three dimensional properties of the crack arrays just described for Type 2 features will confirm that no complete surface of separation exists immediately. The surfaces will tend to stick together. The severance of the surface in the local region between the cracks is accomplished later in shear. Likewise the cracks of the main fracture front, forming the pincer movement, run together in a stress relieved zone. Where the overlapping of the secondary cracks begins, a complex stress system will operate. This is supported by the observation of the frequent presence of striae (which are characteristic features of fracture surfaces produced under

some types of complex stress system) in this area, as indicated in the sketch, Fig. 28 (i). To the sides of this area there are no sub-surface cracks, the stresses are predominantly tensile and ultimately very small mist elements begin to appear again.

Once again, for Type 2 features also, the surface markings are complementary over these local regions on pairs of matching fracture surfaces. However, inspection of the diagrams will show that this time micro-cracks are to be expected under both surfaces in almost identical positions. Furthermore the sub-surface micro-cracks might be physically fairly large in comparison with the surface features. Pairs of optical photomicrographs of the same feature on matching surfaces show just such cracks after the surfaces have been etched in HF (4% wt) for 10 - 20 minutes. Figs. 30, 31 and 32 show the relationship of the sub-surface cracks to the surface features for one of a pair of fracture surfaces.

The material forming the basis of sections 4.2 and 4.3 is, for the greater part, empirical fact. The observation of sub-surface micro-cracks in the mist region, although perhaps not too well illustrated by the photomicrographs at present available, can be easily verified under the microscope. Given the fact of the formation of these cracks, the relationships borne by the mist elements to them and the general form of the mist region can be qualitatively explained. As noted above, it could be argued that the mechanism responsible for the formation of the micro-cracks is an academic question. However the explanation of section 4.4 above is couched in terms of a secondary nucleation hypothesis and a consideration

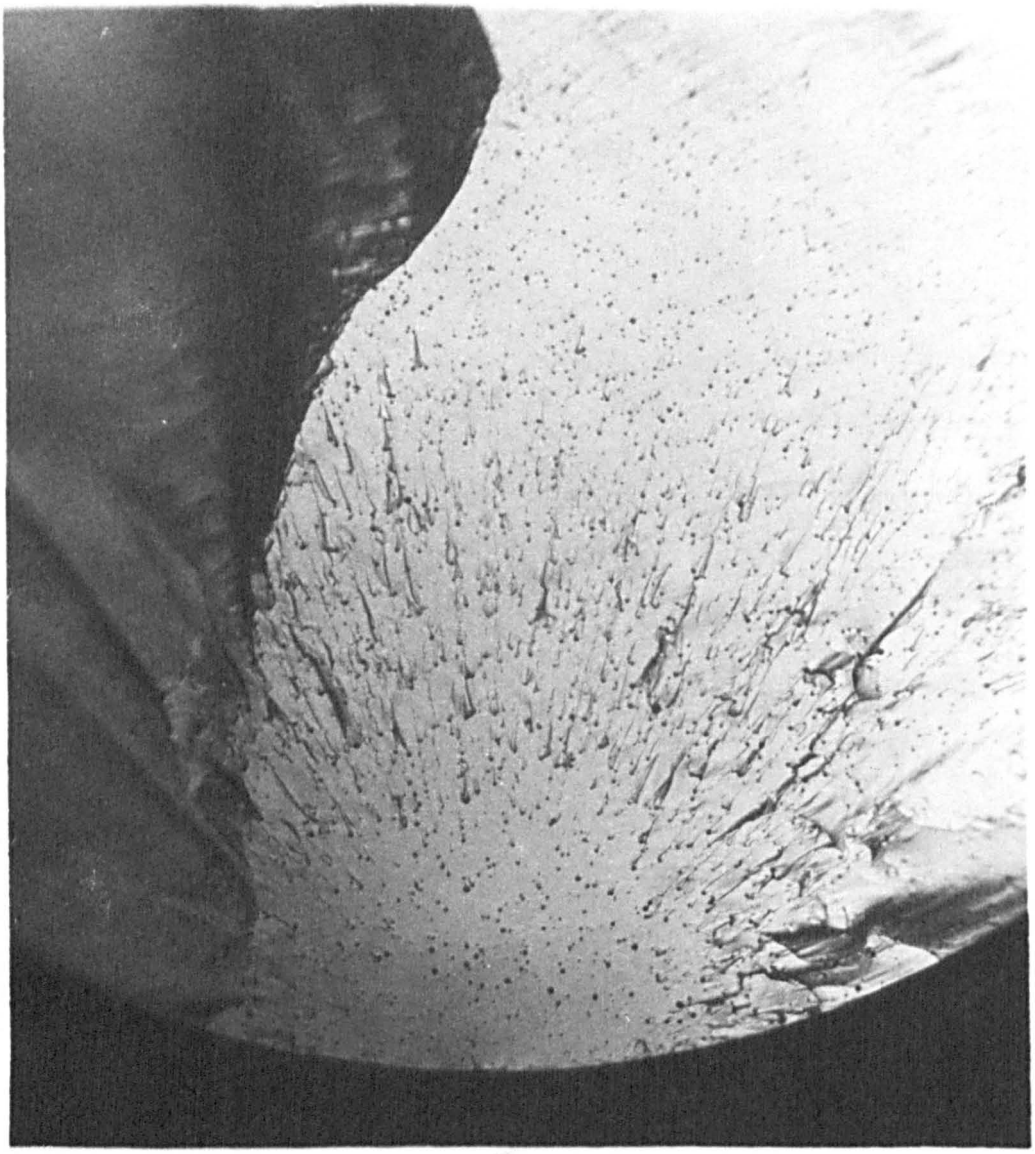

Fig. 33

Fracture surface of satin silica, bending fracture.

Transmitted light. Magnification x 80.

of the possible mechanisms of micro-crack formation is interesting. It should perhaps be emphasised that the following discussion is largely conjecture.

4.5 Discussion of possible mechanisms of micro-crack formation

Three basic ways in which micro-cracks might be caused to appear at the crack front suggest themselves. These will be called the "crenulation", the "forking", and the "secondary nucleation", hypotheses. It will be convenient to deal briefly with the least likely of these three first.

(a) The crenulation hypothesis

The term "crenulation", as applied here to describe the shape of the crack front, is meant to indicate the development of indentations, or sharp notches, in the crack front, the portions of crack front between the notches being arcs of circles with their convex sides facing in the direction of crack propagation. This is the appearance which would be presented to an observer at some point above the plane of crack propagation. For this idea it is necessary to postulate the existence of an array of discontinuities in the material which are able to interfere with the crack propagation process and locally lead to a drop in the velocity of propagation. If the discontinuities are conceived as having a range of effective delaying powers, as for instance the bubbles in the satin silica of Fig. 33, then clearly the more effective discontinuities will achieve the greatest delay in the crack. At some stage during crack propagation the instantaneous crack-front might consist of a few large arcs with small indentations of various sizes upon each individual arc. It is possible to argue

that the faster travelling portions of the crack front, between discontinuities, could than act as semi-independent small cracks at the fracture front. Clearly this hypothesis implies that only a discrete number of micro-cracks can exist at the fracture front at any one time, the total number depending on the density of discontinuities in the material and the total length of the crack front. Another implication is that events at any one place on the fracture surface would be expected to show evidence of having been influenced by immediately preceding events, for instance, the action of a discontinuity on the crack would depend to some degree on the shape of the advancing crack-front at that point, i.e., whether it was an indentation or a protuberance. In fact an examination of Fig. 24 will show that mist features are apparently remarkably uninfluenced by immediately preceding events. Finally the number of separate mist elements would be expected to increase or at least to remain constant. In fact the number of mist elements is apparently reduced as fracture proceeds, at the same time they occupy a greater individual area on the fracture surface.

(b) Forking hypothesis

The term "forking" has been used extensively in the literature to describe that event in the fracture process which has been referred to in this thesis as bifurcation (perhaps loosely) and which is represented by the point X in the schematic diagram of Fig. 2b. The terms forking and bifurcation taken literally are a good description of what appears to happen on a macroscopic scale, but they may well be misnomers for the process itself. It would be very difficult to prove

that the origins of the macroscopic forks are in fact superimposed. It seems just as likely that what are seen on a macroscopic scale as superimposed crack forks, or bifurcations, could develop from single adjacent cracks formed at oblique angles to the general plane of crack propagation. The terms bifurcation and forking could not be correctly applied in these cases. Nevertheless the use of the term forking here is meant to indicate the spontaneous appearance of both superimposed micro-cracks, and single oblique micro-cracks, at the main crack front. These micro-cracks are to be associated with the formation of oblique broken bonds at the crack tip. It is an essential part of the hypothesis that these bonds are broken so that physical continuity of the crack is maintained and the identity of the crack as a single unit is conserved, albeit with a somewhat ragged leading edge. The work of Yoffé (28) and Craggs (29) (discussed later) in predicting a stress distribution at the crack tip with maxima at an angle to the direction of propagation, provides, at least in principle, a possible explanation for the spontaneous appearance of double, oblique, broken bonds at the crack tip. However the work referred to does not make any predictions on what happens to the stress distribution when the crack becomes non-planar and the appearance of pairs of broken bonds has caused the initial lobed stress distribution to collapse. Further, there would seem to be no adequate explanation of the way in which semi-independent cracks could develop simply from the formation of broken bonds distributed along the fracture front.

(c) Secondary nucleation hypothesis

Secondary nucleation was first advanced as an explanation for the mirror, mist and hackle morphology by Smekal (1). As far as the nucleation of secondary cracks is concerned the explanation given below follows Smekal closely.

Smekal invokes the existence of a system of naturally occurring, but unspecified, flaws within the glass. The externally applied stress causes a system of locally increased stresses around each flaw. The important case arises when the number of flaws present is large so that they are densely distributed throughout the material. In this case the crack enters the region of the stress systems of a large number of flaws at the same time. Due to the proximity of the main crack and the local stress fields associated with the flaws, secondary cracks are nucleated at flaws just ahead of the main crack front. However, since the maximum local stress generated at any flaw depends upon its shape, nature, and orientation with respect to the externally applied stress, in general the flaw at which a secondary crack is nucleated will not always lie on the plane of the main crack, but may be to one side of it, either above the plane or below it.

The acceptance of a hypothesis such as this would necessarily involve as an important part some consideration of the secondary nuclei. As far as the silicate glasses are concerned, there would clearly have to be very large numbers of such nuclei normally present in a glass with a similarity of distribution probably unaffected by the manufacturing process or by subsequent treatments. Actual physical foreign particles can perhaps be excluded (although these are accepted

sources of occasional secondary cracks in polystyrene , e.g., Wolock, Kies and Newman (30)), but there seems to be no reason why the nuclei should not be identified with some inherent or characteristic discontinuity of the glassy structure. In addition, the nucleation and propagation of a secondary crack ahead of the "main" fracture front implies the possibility of a period of travel by the secondary crack in a direction opposite in sense to the direction of growth of the main fracture. It is conceivable however that this period of reverse travel could be reduced to a very small amount if the secondary nuclei were "triggered" only a short distance ahead of the "main" crack front. There seems to be no reason why, in the limiting case, nucleation of secondary cracks should not take place almost simultaneously with the arrival of the main crack at the secondary nucleus. It could therefore be quite difficult, with sub-microscopic nuclei, to differentiate between secondary nucleation and forking in practice.

4.6 Discussion of the most probable mechanism of micro-crack formation

There are a number of serious objections to the crenulation hypothesis. Consider a defect array in the material, the individual defects of which array have a range of effective powers for delaying the forward progress of the crack at the site of the defect, (as distinct from a range of effective stress concentration factors as required by secondary nucleation). In the early stages of crack propagation only the most effective defects will achieve any delaying action on the crack. But as propagation proceeds and crack velocity increases, the delaying action of defects of less than maximum effectiveness will be enhanced by the increased crack velocity. It could be argued that,

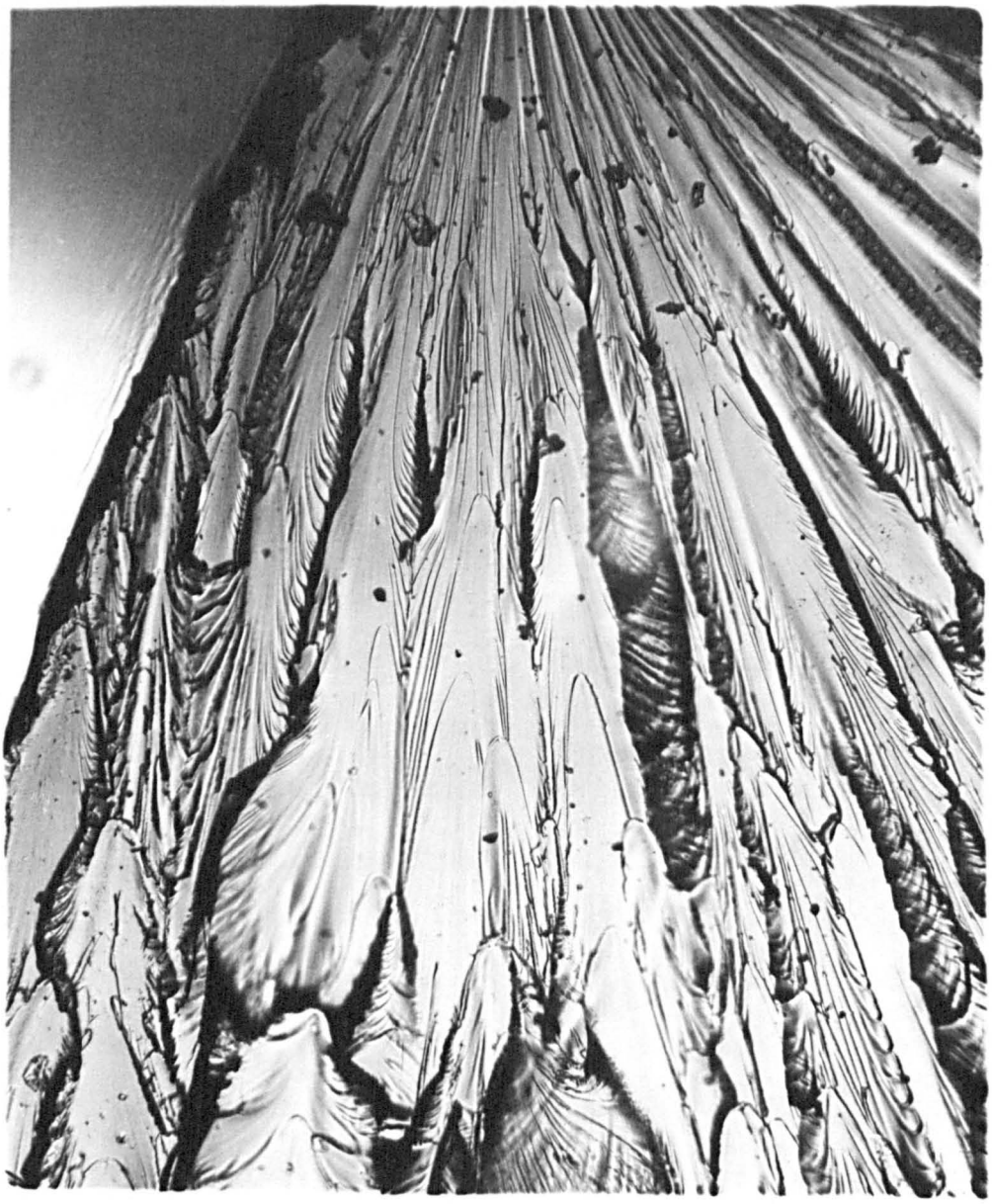

Fig. 34

Photomicrograph of conic figures developed in the fracture surface of "araldite". Magnification x 100.

Transmitted light.

at some stage in the fracture process, the small section of the crack front isolated between closely adjacent defects takes on the properties of a semi-independent crack. This sort of process is apparently responsible for early features in a bubbly glass like satin silica, (Fig. 33). However, for a mechanism of this type to be responsible for the formation of true mist elements, an increase in the number of mist elements exhibited by a fracture surface as fracture proceeded would be demanded. This is in disagreement with the observed occurrence of true mist elements as typified by Fig. 24. Furthermore, the contribution of any individual defect to the fracture process would depend on the shape of the approaching crack-front i.e., whether a "rounded tooth" or a re-entrant angle was approaching the defect. So that in this respect the formation of mist elements might be expected to depend to some degree on the event immediately preceding it. This too conflicts with subjective observation of mist features the formation of which seem to be dependent only on local conditions. The cremulation hypothesis is on the whole regarded as being inadequate in explaining the general occurrence and specific form of mist elements, although it may have limited application in some cases, e.g., the early stages of fracture in satin silica.

It is more difficult to differentiate between a forking hypothesis and a secondary nucleation one. As mentioned above it is conceivable that in the limit the forking hypothesis could be considered similar in effect to a special case of secondary nucleation. With the phenomenological evidence at present available it would certainly be difficult to distinguish between these two. However, in order to

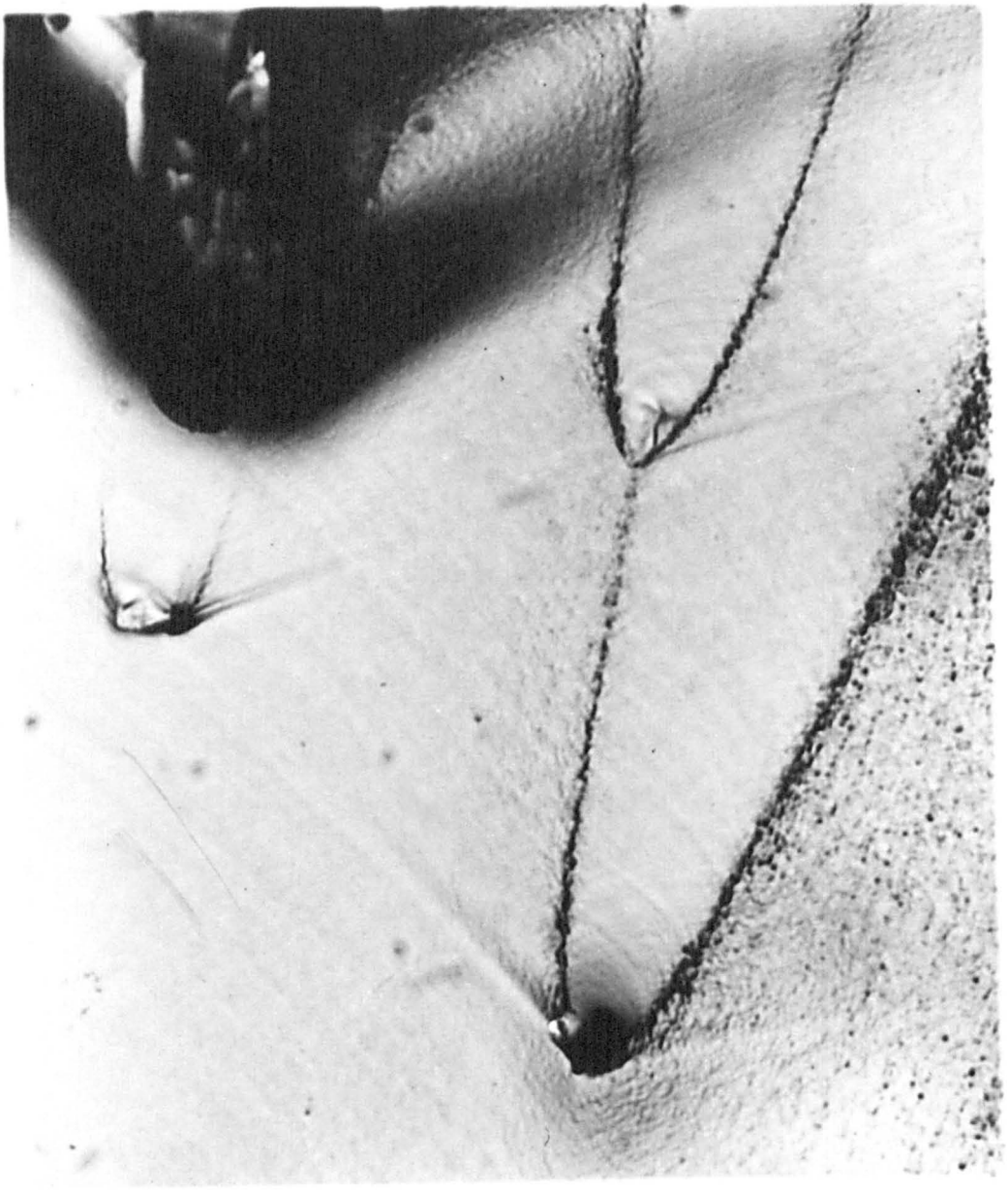

Fig. 35

Photomicrograph of conic figures developed from silica particles in the fracture surface of X8 glass contaminated with fine silica sand. Magnification x 540.
Vertical incident illumination.

achieve an economy in the number of theories concerning the fracture process, it is held that the secondary nucleation proposals would make a more useful working hypothesis for further investigations.

It is widely accepted that the conic figures appearing on the fracture surfaces of certain plastics e.g., polymethyl methacrylate and "araldite", are due to the nucleation of secondary cracks at dirt particles and other defect centres, (see Wolock, Kies and Newman and Fig. 34). Conic figures can only arise when the main crack and the secondary crack mutually interfere in the same plane. The particular type of conic figure ultimately observed on the fracture surface depends upon the relative propagation velocities of the primary and secondary cracks. It is possible to cause conic figures to appear on glass fracture surfaces by mixing into the melted material particles of a comparatively refractory substance and then breaking the composite. For example Fig. 35 shows the effect of silica flour particles on the fracture morphology of X8 glass. Even with these conic figures it will be observed from Fig. 35 that there is no apparent time of reverse travel by the secondary crack as distinct from the observed mechanism in the plastics. This may be merely a result of silica particles having a low stress raising action in X8 glass and a consequent inability to nucleate a secondary crack at a large distance ahead of the main crack front. When the nucleation takes place at a point sufficiently removed from the plane of propagation, no conic figure appears at the head of the feature, as shown by Fig. 36. While it is true that a diligent search of the fracture surfaces of normal glass has given no indication of the presence of secondary nuclei consisting of

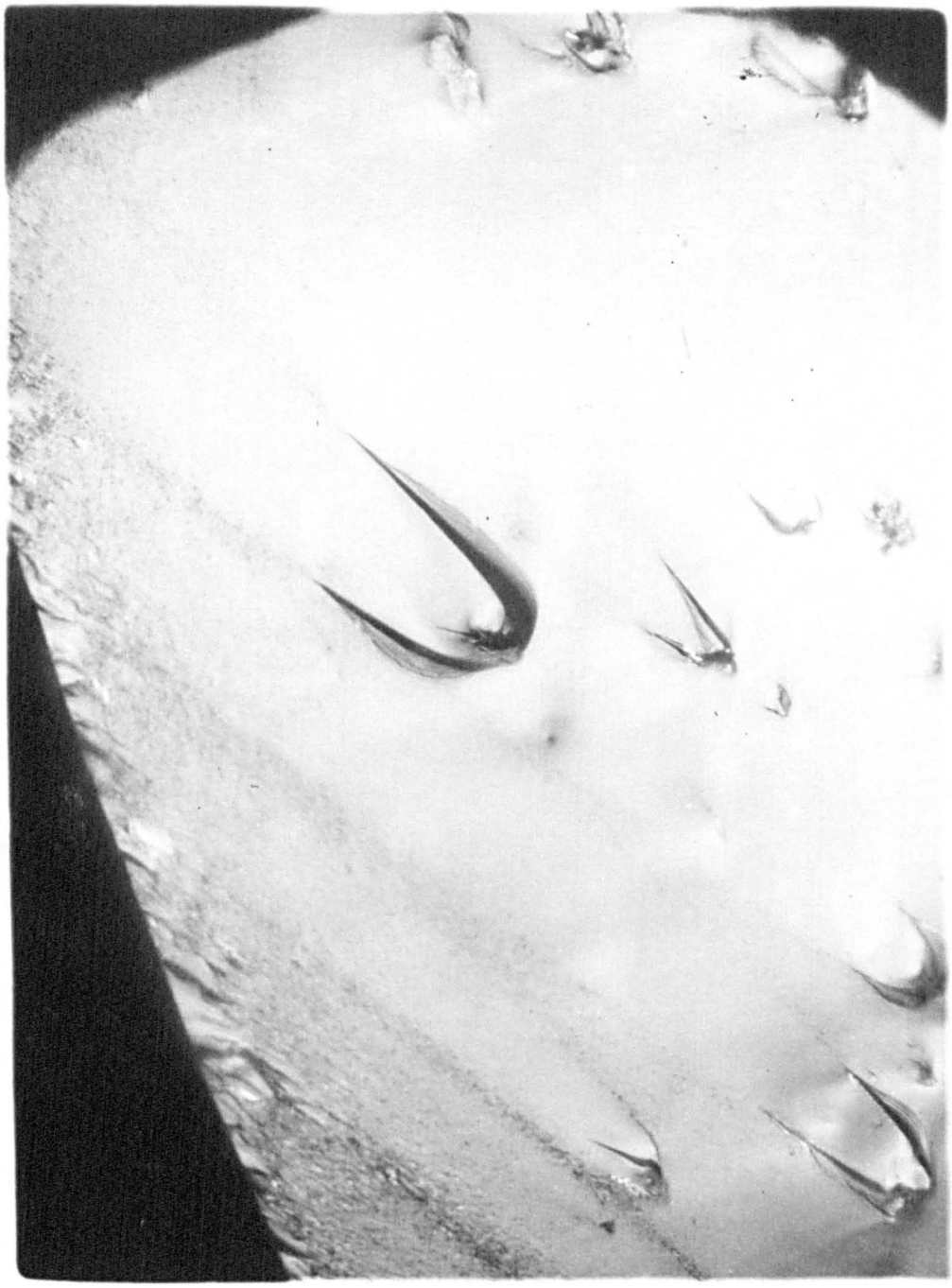

Fig. 36

Photomicrograph of secondary crack nucleation at defect centres lying off the main plane of crack propagation.

Vertical incident illumination. Magnification x 500.

physical foreign particles, or detectable reverse travel by secondary cracks, it is felt that the accepted operation of secondary nuclei in plastics, and the demonstrated possibility of producing conic figures in glass under the correct conditions, recommends that this mechanism should be seriously considered as a useful working hypothesis.

4.7 Summary

This chapter describes the information obtained from a qualitative inspection of the mist zone. Briefly, the result of most importance arising from this inspection is the observation of the existance of large numbers of stopped sub-surface cracks which can be associated with specific fracture surface features in the mist zone. In addition the fracture surface features are found to be capable of a division into two broad groups, Types 1 and 2 as described previously. Using the basic experimental fact of the presence of micro-cracks under the fracture surface it is possible to give a qualitative explanation of the formation of the mist elements in terms of micro-cracks developed at the crack front. Up to this point the conclusions drawn are based on experimental fact. The further discussion of the possible and most probable mechanisms responsible for the formation of micro-cracks at the crack front is largely conjecture but supported wherever possible with factual information.

The multiplicity of sub-surface cracks in the mist zone draws attention to the energetics of the fracture process in addition to providing the basis for an explanation of the morphological appearance of the mist elements. This is the most fruitful observation arising from the inspection of the mist zone. The realisation that these

cracks represent, in total, the dissipation of large amounts of elastic energy during the fracture process was directly responsible for the attempts to formulate a quantitative critical energy criterion for the end of the mist zone which is described in Chapter 6. However, before embarking on this, a general review of some theoretical work relevant to the problem of the significance of the gross morphological pattern of mirror, mist and hackle, will be attempted. This review forms the subject of the next chapter.

CHAPTER 5 REVIEW OF THE THEORETICAL WORK RELEVANT TO THE FORMATION OF THE MIRROR, MIST AND HACKLE MORPHOLOGY

5.1 Introduction

Under this chapter heading it is intended to review briefly previous theoretical work dealing with the development of the fracture process in brittle materials. This work will be examined to see in which way it helps to explain the formation of the gross morphological pattern of mirror mist and hackle observed on glass fracture surfaces.

There have been three main types of approach to the problem of the growth of fracture in a material. First there is the qualitative physical model put forward by Smekal (1) to explain the process for glass only. Second, there is the elasticity - theory approach in which a crack in an infinite elastic medium is extended by finite forces. This theoretical approach has been used by many authors following Griffith's (5), first successful application of the method to the propagation of a static crack. The work of Mott (6), Craggs (29), Yoffé (28), Berry (23), Dulaney and Brace (22), will be considered below. The contributions of this latter group of authors have led to the formulation of a number of equations describing the motion of the growing crack. Third, there is the approach which considers the particulate nature of the material, in which fracture is regarded as a process governed by the probability of failure of interatomic bonds, e.g., Poncelet (31).

5.2 Qualitative physical model due to Smekal

Smekal's model invokes the existence of a system of naturally occurring, but unspecified, flaws within the glass. Smekal indicated how secondary cracks might be nucleated at these flaws just ahead of the main crack under the influence of the stress concentration effects of the flaws themselves, and the close approach of the main crack. This aspect of the model was dealt with in Chapter 4, Section 4.5 (c). Smekal further supposed that the disposition of those particular flaws at which secondary nucleation subsequently took place, would be within a narrow glass layer about the main plane of crack propagation. The effect of a large number of flaws distributed in front of the crack in this manner would therefore be to deflect the crack from its plane of propagation more or less strongly. While the initial crack should proceed perpendicular to the rod axis, it ought not to continue so, but should be deflected from this plane by the action of secondary cracks nucleated at flaws with high stress concentration factors. As fracture proceeds, the area in which noticeably increased stresses around the front of the crack may exist should become larger, and the irregularities in the crack front ought to become rougher the further the crack travels. According to Smekal, the area of increasing roughness surrounding the mirror (i.e., the mist) can be interpreted as visible evidence of the inherent inhomogeneity of glass, the local flaws of which are densely distributed throughout it. Ultimately flaws of very high stress concentration factors can become effective at a considerable distance ahead of the primary crack as soon as the requisite increase of stresses in their vicinity has become effective. Smekal maintained that the

nucleation of secondary cracks at such flaws would lead to the propagation of a series of independent secondary cracks which would run into the primary crack and halt it. Fracture would then proceed along the secondary cracks until the general conditions required for break-up could be again fulfilled and the secondary cracks halted by tertiary cracks. Smekal visualised this process being repeated until the specimen severed.

As far as glass is concerned Smekal's flaw hypothesis provides a plausible physical model for the gross appearance of mirror, mist and hackle. It was of course designed to do just this. Smekal developed, from his qualitative arguments, a quantitative theory leading to the notion of a constant of the material which he called the "reduced tensile strength". The very early phase of the experimental work reported in this thesis was concerned with measuring this quantity as mentioned in Chapter 1, Section 1.3. Although the "reduced tensile strength" was not found to be a useful parameter. Smekal's ideas on secondary nucleation form the major argument in Chapter 4, Sections 4.5 and 4.6 and a discussion of some of the expected results of the operation of a secondary nucleation mechanism will be found there. This model cannot explain the empirical fact expressed by Eqn. 3.4.1. It should also be remembered that the mirror, mist and hackle morphology is not confined to glass, other materials also show very similar features. This fact implies that there is a common explanation uniting the morphologies of such diverse materials as glass, Lithium fluoride, ceramics, rubber at low temperature etc., is it therefore possible that this physical model

can be extended to include these materials without radical modifications? In the case of glass, for which the model was intended, Smekal did not give any explanation for the morphology of specific areas of the fracture surface in terms of his model.

5.3 Applications of the principle of the conservation of energy

The second approach to the fracture process, involving an application of the principle of conservation of energy would appear to be basically above reproach. Griffith (5) was responsible for the original idea in which he suggested that an energy balance condition, between the surface tension of the newly created fracture surface on the one hand and the elastic energy stored in the stress field on the other, was the controlling factor in crack propagation. This idea has exercised a profound influence on the study of fracture processes in general. In its original form Griffith's theory referred specifically to the condition required to initiate the propagation of a static crack under a tensile stress. It has also been applied to other types of stress system with conspicuous success, notably that of cleavage (Benbow and Roesler (32), Gilman (33)). In many studies, the criterion has usually been used to define the critical condition for fracture. More recently some attention has been paid to the behaviour of moving cracks, again using the Griffith approach.

Essentially Griffith's argument was that, not only is it the natural tendency of a deformed system to attempt to reach a state of minimum potential energy, but also that if the material could pass from the unbroken to the broken condition by a process involving a continuous decrease in potential energy, then fracture would occur

spontaneously. However, in forming a crack in the interior of a body composed of molecules which attract one another, work is done against the forces of cohesion between the molecules on either side of the crack. The work done appears as potential surface energy, and if the distance apart of the crack sides is greater than a very small distance which Griffith called the "radius of molecular action", the energy thus described per unit surface area is a constant of the material, namely, its surface tension. Griffith pointed out that, in general, the surfaces of a small newly formed crack cannot be further apart than the radius of molecular action. It therefore follows that the fracture process cannot be quantitatively described unless the law connecting the surface energy with distance of separation is known. In order to make the calculation Griffith assumed a crack with sides separated by a distance greater than the radius of molecular action at all points except near its ends. In this case, the potential surface energy could be identified with the surface tension, and the increase in surface energy due to the spreading of the crack could be calculated.

Griffith performed the analysis for the case of a flat, homogeneous, isotropic plate of uniform thickness containing a straight crack which passed normally through it, the plate being subjected to stresses applied in its plane at its outer edge. Assuming in this case a crack of length $2c$ and a stress σ applied to the material across the direction of the crack, then, using a method due to Inglis (34), it can be shown that the elastic energy of the material differs from that value it would have in the absence of the crack by an amount,

$$\frac{\pi \sigma^2 c^2}{E} \qquad 5.3.1$$

where E is the elastic modulus of the material. Assuming that the propagation of the crack does not cause any major change in shape of the body at its extremities and that the change in elastic energy reappears entirely as potential surface energy, to the energy of Eqn. 5.3.1 may be added the surface energy of the crack,

$$- 4 c T \qquad 5.3.2$$

where T is the surface tension.

The total energy balance, adding Eqn. 5.3.1 and Eqn. 5.3.2 is thus,

$$\frac{\pi \sigma^2 c^2}{E} - 4 c T \qquad 5.3.3$$

Griffith's criterion states that the crack will spread spontaneously if the energy given by Eqn. 5.3.3 increases with increasing c . The condition for this is given by,

$$\frac{\pi \sigma^2 c}{E} > 2T \qquad 5.3.4$$

Therefore the externally applied stress σ which Griffith found is required to fracture the ideal material containing a crack of length 2c is as follows,

$$\sigma = \sqrt{\frac{2 E T}{\pi c}} \qquad 5.3.5$$

Griffith's equation expresses the condition required to extend a static, pre-existing, planar crack in an isotropic material. The analysis requires the conversion of elastic energy into only one new form, that is, potential surface energy. Therefore, although the Griffith equation can be set in a form similar to the relationship expressed by Eqn. 3.4.1, it cannot be, in its original form, an explanation of the empirical observations given by Eqn. 3.4.1.

Mott (6) was responsible for the application of Griffith's methods to the problem of a moving crack in a brittle solid. The decrease in elastic strain energy of the body from its value in the absence of a crack is brought about by re-arrangements in the local stress field around the crack. Material just ahead of the crack tip will become more highly stressed, and material just behind the crack tip will become less highly stressed. This elastic energy is available for conversion into other forms of energy depending on the material and ultimately on the rate of strain energy release. As each bond breaks in the material the two freed particles acquire a velocity away from each-other because of the inbalance produced by the break. This general process results in a series of elastic disturbances travelling away from the crack. The atoms involved therefore acquire a velocity of translation and hence a kinetic energy. Thus it is that immediately the crack begins to propagate with a significant velocity, kinetic energy must be considered as an important factor absorbing part of the elastic energy released by the crack. Mott derived an expression for the kinetic energy associated with a purely brittle crack moving across a plate as follows,

$$- \frac{k \rho V_f^2 \sigma^2 c^2}{2E^2} \qquad 5.3.6$$

where ρ is the density of the material,

V_f is the velocity of crack propagation

and k is a numerical constant.

Adding the energy of Eqn. 5.3.6 to that of Eqn. 5.3.3, the total energy for a moving crack now becomes,

$$\frac{\pi \sigma^2 c^2}{E} - \frac{k \rho V_f^2 \sigma^2 c^2}{2E^2} - 4cT \qquad 5.3.7$$

and by the conservation of energy this is constant, so that the full equation is,

$$\frac{\pi \sigma^2 c^2}{E} - \frac{k \rho V_f^2 \sigma^2 c^2}{2E^2} - 4cT = \text{constant} \qquad 5.3.8$$

Mott was interested only in the terminal velocity of the crack and removed the unknown constant from the right hand side of Eqn. 5.3.8 by differentiating with respect to c and setting the acceleration of the crack equal to zero. This is true only near terminal velocity and the expression for the latter is

$$V_f = \sqrt{\frac{2\pi}{k} \cdot \frac{E}{\rho} \left(1 - \frac{2ET}{\pi \sigma^2 c}\right)} \qquad 5.3.9$$

Mott's equation is the forerunner of a number of derivations for the velocity of a running crack notably by Dulaney and Brace (22), and Berry (23). The derivations of the latter authors have been made without assuming zero acceleration of the crack and as a result their equations are slightly different from Eqn. 5.3.9 viz,

Dulaney and Brace - $$V_f = \left(\frac{2\pi}{k} \cdot \frac{E}{\rho}\right)^{\frac{1}{2}} \left(1 - \frac{2ET}{\pi\sigma^2 c}\right) \qquad 5.3.10$$

Berry - $$V_f = \left(\frac{2\pi}{k} \cdot \frac{E}{\rho}\right)^{\frac{1}{2}} \left(1 - \frac{C_o}{c}\right)\left[1 - (n-1)\frac{C_o}{c}\right] \qquad 5.3.11$$

where n is a numerical factor,

and C_o is half the original crack length,

n and C_o are related by the expression

$$nC_o = \frac{4ET}{\pi\sigma^2} \qquad 5.3.12$$

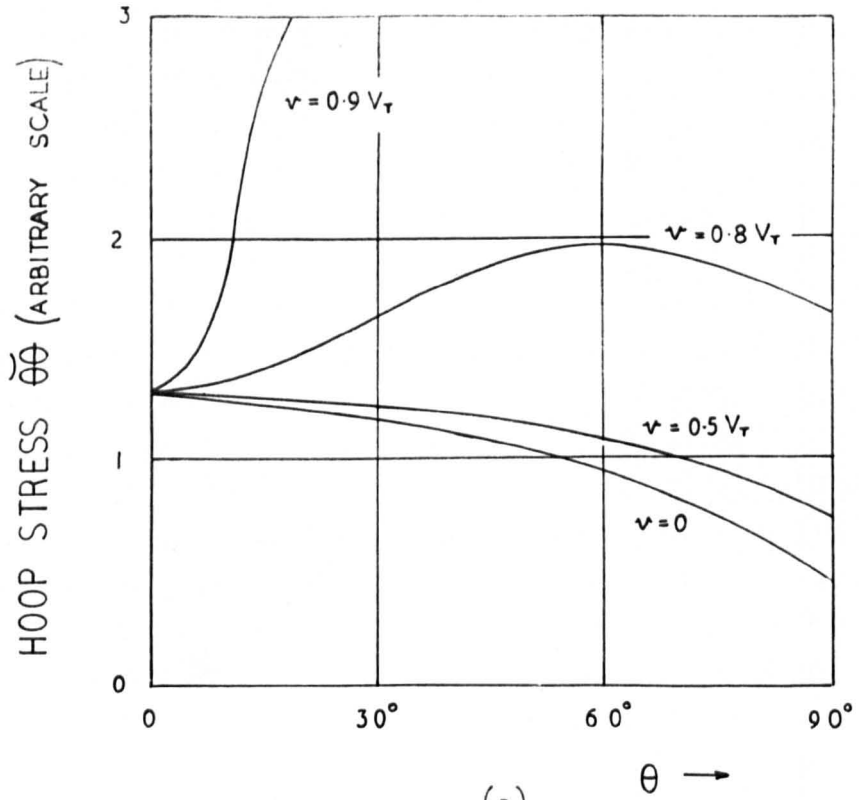

(a)

Showing the relationship between the distribution of the hoop stress $\widetilde{\theta\theta}$, the tip of the crack and the fracture velocity v .

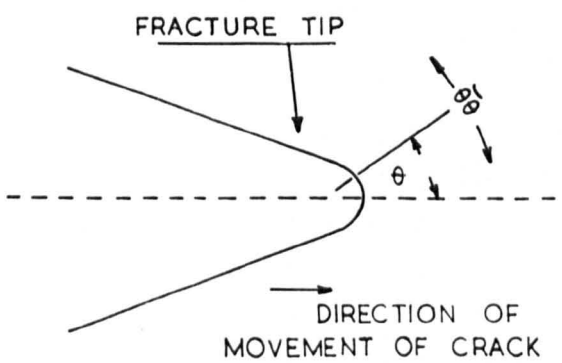

(b)

Illustrating the meaning of the term "the hoop stress at the tip of the crack".

Fig. 37

The equations of motion given above as Eqn's 5.3.9, 5.3.10 and 5.3.11 do not immediately lead to any further understanding of the mirror, mist and hackle phenomenon, for in order to use them, some criterion would have to be assigned to the end of the mirror. It will be recalled that Bateson proceeded in this manner having obtained an equation of motion for the crack as described in Chapter 3, Section 3.5. He had to assume that hackle was produced by the crack on reaching a terminal velocity and that the acceleration of the crack up to this point remained uniform. It was then possible to deduce a $Zc^{\frac{1}{2}}$ = constant, relationship. With the more exact equations 5.3.10 and 5.3.11 the acceleration of the crack cannot be assumed to be uniform. Even assuming the same criterion as Bateson for the onset of hackle, the distance travelled by the crack cannot be extracted, since Berry reports that his velocity equation 5.3.11 when integrated to give a length-time relation for the crack, gives an integration constant which is infinite when the appropriate boundary conditions are inserted.

Craggs (29) and Yoffé (28) have used the Griffith approach with very rigorous mathematical methods to investigate the stresses developed at the crack-tip while the crack is in motion. This analysis yielded a particularly interesting result. Yoffé produced the graph shown here as Fig. 37. It shows the relation, at various fracture velocities, between the hoop stress $\widetilde{\theta\theta}$ very near the fracture tip and the polar coordinate θ. The direction in which the hoop stress acts is shown in Fig. 37 (b). The graph of Fig. 37 (a) shows that at low fracture velocities the maximum hoop stress occurs when $\theta = 0$. (i.e., in the plane of the crack). At a fracture velocity of $v = 0.8\ V_T$, where

V_T is the velocity of transverse sound waves in the material) the hoop stress is at a minimum at $\theta = 0$ but maxima now occur on either side of $\theta = 0$. Yoffé concluded from these results that if the material is such that a crack propagates in a direction normal to the tensile stress, there is a critical velocity of about 0.6 V_T at which the crack tends to become curved. At a lower velocity the crack extends in a straight line, but as the velocity increases the $\widetilde{\theta\theta}$ curve becomes flat and the crack may form branches since nearly equal stresses exist over a wide arc about the head of the crack. At higher velocities the $\widetilde{\theta\theta}$ curve has definite maxima and each branch tends to curve. These are Yoffé's views. Cragg's analysis produces essentially the same mathematical conclusions and also predicts stress maxima above a velocity of about 0.6 V_T. This expectation of the formation of stress lobes at the head of a fast travelling crack could have important consequences if integrated into a general crack development hypothesis. For instance, the conceptual ideas contained in Chapter 4, Sections 4.4 and 4.5 (c) concerning secondary nucleation can be more easily accepted if a stress-lobe mechanism such as that described by Yoffé is in operation. Standing against this work is the fact that the maximum experimental value of the fracture velocity appears to be only about 0.6 V_T for silica, with the soft glasses all rather less than this (Schardin (20)). The numerical experimental values for the maximum velocity are not quite in agreement with theory.

In addition, when a crack forms branches in response to a particular stress distribution at the tip of the crack, it is necessary to know what conditions are required in order that the branches may continue to propagate as separate entities. This condition for the continued

propagation of the crack branches is the required criterion for the termination of the mirror zone. The theories of Yoffé and Craggs, in common with those of Berry, Dulaney and Brace etc., suffer from the disadvantage that the materials considered are ideal. It is difficult to see for instance, whether stress lobes would develop in a real material which deviated from Hookean behaviour. This could have important repercussions when assessing particular physical models for crack propagation.

This disadvantage is shared by Poncelet's (31) theory. Poncelet's approach, relating the rate at which bonds at the crack tip "break", with the stress at the crack tip, does not in itself lead to any radically new predictions concerning the mirror, mist and hackle phenomenon. His work supports Yoffé and Craggs in that it states that broken bonds will appear at an angle to the crack propagation plane, and that the obliquity of such bonds also rises as the stress at the crack tip rises. (There is, however, no specific statement, and it does not appear to be necessary, that the formation of oblique broken bonds is associated with the appearance of stress "lobes" at the crack tip). In addition, Poncelet's theory makes the interesting positive statement that the frequency, as well as the obliquity, of such broken bonds (which Poncelet says lead to crack "divergences") rises as the fracture process proceeds. Qualitative examination of the mist region of glass fracture surfaces indicates that this prediction is not true for glass.

The contributions of Bateson (18), and Shand (4) were considered in Chapter 3, Section 3.5 as explanations of the empirical fact $\gamma = Zc^{\frac{1}{2}}$ = constant. With the exception of Smekal's (1) qualitative explanation, Bateson and Shand appear to be the only workers to propose

a specific explanation of the mirror, mist and hackle phenomenon in theoretical terms. Of the various other fracture development theories reviewed in this chapter it is probably true to say that none is adequate in providing either a complete theoretical or physical model for the fracture process.

The ideas to be discussed in the next chapter contain two main proposals. First, the modifications to the theories of Griffith, Mott Dulaney and Brace, and Berry required for a crack propagating in a real material are discussed. A simple attempt to take these modifications into account by utilising some existing experimental evidence follows. Second, a specific proposal for a criterion for bifurcation is made following on the observations recorded in Chapter 4 Section 4.3.

CHAPTER 6 APPLICATION OF THE MOTT ENERGY-BALANCE EQUATION TO REAL MATERIALS. AN INTERPRETATION OF THE PHYSICAL SIGNIFICANCE OF THE VALUE OF $Zc^{\frac{1}{2}}$

6.1 Introduction

It is intended in this chapter to discuss the energetics of brittle and semi-brittle fracture in real materials, with reference to the basic energy-balance equation for a crack in motion given by Mott (Eqn. 5.3.8, Chapter 5). A simple modification to the surface energy term in Eqn. 5.3.8 is suggested using experimental information given by Roesler (35), Culf (7) and Benbow (36). In addition a criterion for the termination of the mist zone in glass is suggested. When this criterion is used in conjunction with the modified Mott equation, it will be shown that a relationship between the breaking strength of a specimen and the square root of the mirror depth of the form $Zc^{\frac{1}{2}}$ = constant is predicted which yields a numerical value for $Zc^{\frac{1}{2}}$ not incompatible with experiment. As a result of this agreement an interpretation of the significance of the value of $Zc^{\frac{1}{2}}$ is proposed. A short discussion of the possibilities of extending these arguments to other materials follows and using the experimental information provided by Benbow (36) and Schardin (20), the value of $Zc^{\frac{1}{2}}$ for polymethyl methacrylate to be expected from the theory is given. The chapter closes with a summary of the results of this investigation into the significance of the mirror, mist and hackle morphology and associated phenomena. Some suggestions for further work are given.

6.2 Discussion of the fracture energetics of real materials

In principle it should be possible to write a balanced energy equation for the fracture process. Excluding systems in which fracture takes place in such a manner that the forces acting at the grips do work during the fracture process, the energy used in achieving a fractured state is ultimately all derived from the elastic strain energy stored originally in the body. In such a case the uncertainties arise when the attempt is made to write mathematical expressions for the absolute amounts of such energy released, and the proportions of it transformed by the various energy dissipative mechanisms available in the material. It will be useful to give Mott's total energy expression (Eqn. 5.3.7, Chapter 5) again here in order that the terms in it may be discussed with more convenience,

$$\frac{\pi \sigma^2 c^2}{E} - \frac{k \rho V_f^2 \sigma^2 c^2}{2E^2} - 4 c T \qquad 6.2.1$$

The expression of the elastic energy term in the form

$$\frac{\pi \sigma^2 c^2}{E} \qquad 6.2.2$$

originally due to Inglis (34), is for an open, straight-edged crack in a thin elastic plate of infinite extent. The crack is supposed to be planar and the tensile stress, applied at infinity normal to the long axis of the crack, must remain constant during crack propagation. At late stages in the crack propagation process for glass the cracks are narrow and at the point of interest definitely non-planar. In addition the change in strain energy given by expression 6.2.2 represents the change in the total strain of the body. This introduces an additional

complication since the other terms in expression 6.2.1 are concerned primarily with local conditions immediately around the crack. However Irwin and Kies (37) have analysed the propagation of a semi-brittle crack across a plate and estimate that even then the change in strain energy due to the presence of the crack is,

$$\frac{\pi \sigma^2 c^2}{E} \times K \qquad 6.2.3$$

where K is a factor associated with the plate dimensions. The form of the expression for the elastic energy term depends on the stress and displacement fields around a moving crack. These fields are not known but are usually assumed to be the same as around a static crack. This assumption is supported by a series of photographs taken by Wells and Post (38), of a moving crack in a photoelastic material. These photographs are interpreted as showing that the dynamics and static stress fields do not differ significantly for a crack moving through a thin plate. For these reasons it is proposed that, as far as real materials are concerned, the elastic energy term may be retained unmodified.

The kinetic energy term in 6.2.1 i.e.,

$$-\frac{k \rho V_f^2 \sigma^2 c^2}{2E^2} \qquad 6.2.4$$

depends on the stress and displacement fields around a moving crack in the same way as the elastic energy term, and can be supported by the same arguments. In addition, it contains the interesting numerical factor k, the value of which depends on the extent to which the material surrounding the crack contributes to its kinetic energy.

According to Hiorns and Venables (39) k can be assigned a value approximately equal to unity. Unfortunately their reasons for making this statement are not given. Equations 5.3.9, 5.3.10 and 5.3.11 of Chapter 5 make it clear that as the crack grows very large the crack velocity approaches a terminal value given by

$$V_f = \left(\frac{2\pi}{k}\right)^{\frac{1}{2}} \left(\frac{E}{\rho}\right)^{\frac{1}{2}} \qquad 6.2.5$$

Equation 6.2.5 apparently offers a useful method of determining the value of k since

$$\left(\frac{E}{\rho}\right)^{\frac{1}{2}} = V_L \qquad 6.2.6$$

where V_L is the velocity of longitudinal sound waves in the material. Experimental values are available for the quantity V_f/V_L. Equation 6.2.5 predicts that k should have a value,

$$k = 2\pi \left(\frac{V_L}{V_f}\right)^2 \qquad 6.2.7$$

However setting k in Eqn. 5.3.8 equal to the value given by Eqn. 6.2.7 will show that the kinetic energy term becomes, in this case, equal to the rate of release of elastic energy without further considering that energy used in forming fresh fracture surface. Clearly either the expression for the rate of release of elastic energy is incorrect at the terminal velocity of the crack, or the k appearing in Eqn. 5.3.8 does not have the same significance as that k in Eqn. 6.2.7. The numerical value to be assigned to k will be considered further shortly.

It is worthwhile considering here the nature of the kinetic energy represented by Mott's term. Ideally the term should be a measure of the velocity of recession of the crack walls and the quantity of material

involved in this movement. In view of the connotations normally placed on kinetic energy in physical processes, the question here is whether the kinetic energy term can be regarded strictly as an energy "sink" or whether it may also act as an energy "source" as far as crack tip phenomena are concerned. There is little doubt that, in a situation in which fracture takes place without the assistance of external work on the body during the fracture process, the energy required for fracture is all derived from the elastic strain field around the crack tip. Also all the elastic strain energy liberated by the passage of the crack must be dissipated by one mechanism or another. Either the processes mentioned above or transformation into elastic disturbances, heat, sound etc. It is quite probable that the amount of kinetic energy acquired by the crack walls is not completely described by Mott's expression. This is a feature of all the mathematical quantities appearing in the expression 6.2.1 and is not in question here.
The point to be considered here, is whether some of the energy acquired by the crack walls by virtue of their relaxation can in some way reappear at the crack tip thereby upsetting the energy balance there.
The author's opinion is that this is not possible in view of the fact that recessional velocity of the crack walls at the crack tip depends only upon the product of the local elastic strain and the velocity of sound in the material. The motion of the crack walls does not cease until the bulk elastic strain of the specimen is relaxed, it is therefore difficult to see how this could affect crack tip phenomena.

The surface energy term in the expression 6.2.1 also provides interesting material for discussion. If the structure of a solid is known, the surface energy can be estimated from the number and strength of the chemical bonds broken to provide new surface. This calculation usually provides an overestimate of the total surface energy since there is some rearrangement in the surface layer with partial saturation of the broken bonds. Thus to find an estimate for the surface energy requires a correction which is difficult to make for glass since the unknown surface re-arrangement may have a decisive effect on the value of T. Attempts to measure the surface energy of glass experimentally have previously been made on glasses in the molten state ordinarily in contact with air. The more reliable data place values for commercial glasses between 200 and 400 dynes per cm when extrapolated to room temperature. Generally speaking the method of determining surface energy using molten material is not satisfactory. Those chemical constituents of the glass which tend to lower the surface energy will accumulate at the surface under these conditions of increased ionic mobility. There are also severe difficulties inherent in obtaining a chemically clean surface. Surface energy is also a property of rigid glass although not subject to direct measurement. Recently experiments have been devised in an attempt to estimate the surface energy of rigid materials and these have led to some interesting results of paramount importance to the arguments to be proposed shortly.

Roesler (35) showed that cone fractures, produced by pressing small steel indenters into the glass surface, could be made stable i.e., propagated at an arbitrarily slow speed. His experiments demonstrated

the truth of the functional form of the Griffith energy balance theory, but the numerical value of the surface energy so found was much larger than a true surface tension should be. Observations showed that when the force was removed from the indenter the cracks in the glass did not quite close up, suggesting that plastic deformation had occurred. Thus it is apparent that even in brittle materials such as glass the fracture process may involve the dissipation of energy in forms other than the kinetic energy and true surface energy as considered above. This immediately suggests that the attempt should be made to take into account this extra energy dissipated by the inclusion of another term in the energy expression 6.2.1. The energy measured in experiments such as Roesler's has been called the fracture energy and it has the dimensions of a surface energy. The experimental fracture energy will always include the true surface energy since this of course is by definition associated with the passage of a crack. The difference between the total fracture energy and the true surface energy is spent irreversibly in a number of dissipative processes which depend upon the material concerned. The nearer the material is to the ideal material considered by Griffith, Craggs etc., the nearer the value of the fracture energy should approach the true surface energy. Conversely, in a material which deviates markedly from the ideal elastic solid, the fracture energy may be very large indeed and the proportion of it representing true surface energy may be insignificant. Theory gives no answer at present to the problem of whether the fracture energy is constant, but in order to take account of the multitude of dissipative processes operating during fracture by a quantitative term in expression 6.2.1, it must be considered a constant

of the material. It is proposed that the symbol γ represent the fracture energy and that this should have the dimensions of surface energy. The quantity γ thus represents the elastic energy supplied by the body to form unit area of new fracture surface. The energy balance expression 6.2.1 becomes,

$$\frac{\pi \sigma^2 c^2}{E} - \frac{k \rho V_f^2 \sigma^2 c^2}{2E^2} - 4 \gamma c \qquad 6.2.8$$

If Griffith's ideas are applied to the energy balance expression 6.2.8 the crack can continue to propagate provided that the rate of change of elastic energy with increasing c is greater than or equal to the rate at which it can be converted into the principal new forms, i.e.,

$$\frac{d}{dc}\left(\frac{\pi \sigma^2 c^2}{E} \geq \frac{k \rho V_f^2 \sigma^2 c^2}{2E^2} + 4 \gamma c\right) \qquad 6.2.9$$

$$\text{or} \quad \frac{2 \pi \sigma^2 c}{E} \geq \frac{k \rho V_f^2 \sigma^2 c}{E^2} + 4 \gamma \qquad 6.2.10$$

It will be observed from the form of Eqn. 6.2.10 that the fracture velocity has been tacitly assumed to have attained a constant value. There is strong experimental evidence to suggest that the crack reaches terminal velocity at an early stage in its propagation (see Smekal (24)). However this point will be discussed further later. An examination of Eqn. 6.2.10, also shows that unless V_f is able to achieve very large values, the rate of release of elastic energy (under given conditions) can ultimately rise to values greater than can be accommodated by the kinetic energy and fracture energy terms. Since it is a matter of experimental experience that V_f is in fact limited it is clear that the rate of release of elastic energy can rise to values which cannot be dissipated by one crack alone.

Suppose that it is possible to ignore the phenomenological fact that as fracture proceeds the crack is no longer a single, smooth, planar crack. Then it is likely that at some stage of the fracture process the rate of release of elastic energy will be so great that it becomes energetically possible to support the propagation of <u>two</u> complete cracks. If this is true then the condition to be satisfied at point X in Fig. 2 (b) is an energy one, and it represents that point at which the rate of release of elastic energy is such that the propagation of two cracks (F' and F" - Fig. 2 (b)) becomes energetically feasible. For this condition which represents the condition for bifurcation Eqn. 6.2.10 can be re-written,

$$\frac{2\pi\sigma^2 c}{E} = \frac{k\rho V_f^2 \sigma^2 c}{E^2} + 8\gamma \qquad 6.2.11$$

Equation 6.2.11 contains terms in $\sigma^2 c$ and can be transposed for $\sigma c^{\frac{1}{2}}$ as follows,

$$\sigma c^{\frac{1}{2}} = \left[\frac{8\gamma E^2}{2\pi E - k\rho V_f^2}\right]^{\frac{1}{2}} = Zc^{\frac{1}{2}} \qquad 6.2.12$$

Equation 6.2.12 embodies the proposed criterion for the point X in Fig. 2 (b) representing the termination of the mirror and mist regions. In this respect it is slightly different from the criterion used to obtain the numerical values for $Zc^{\frac{1}{2}}$ in which the depth of the mirror was taken to an arbitrary point in the mist zone because of irregularities in the hackle arc. The essence of the proposed criterion is contained in the difference between Eqn. 6.2.10 and Eqn. 6.2.11 in which the elastic energy released by the propagation of a crack through the material is required to provide fracture energy as defined previously for <u>two</u> cracks and not one. Some of the physical approximations made in the erection of

Eqn. 6.2.12 need to be examined further and this is done below. A numerical evaluation of Eqn. 6.2.12 can now also be attempted using commonly accepted experimental values for the quantities contained in it. This value will be compared with the results of the present experiments.

6.3 Discussion and evaluation of Eqn. 6.2.12

Equation 6.2.10 was derived by assuming that the velocity of fracture has a constant value. There is strong experimental evidence which supports this assumption (Smekal (24)). However the mere fact that this appears to be the case experimentally need not mean that the velocity in any one material is limited to the value measured experimentally for it. Theoretically it is possible that the velocity of crack propagation could approach the transverse wave velocity in the material, although Craggs maintains that the crack would divide long before this due to the formation of stress lobes at the crack tip. In a real material the fracture velocity might be limited by the action of the physical mechanism responsible for aiding the crack to propagate. For instance, if the crack propagation process in any material is accomplished by the action of independent cracks generated at secondary nuclei, it is conceivable that this could lead to an early limitation to the fracture velocity. This can be seen from the form of the energy expression 6.2.8. From this expression it can be seen that the kinetic energy term has the theoretical property of being continuously variable up to a fixed maximum value by virtue of the V_f quantity contained in it. It should be noted that while the crack velocity V_f is increasing Eqn. 6.2.10 does not follow from Eqn. 6.2.9 since the acceleration must be included in this case. This maximum value may never be attained however if stress

conditions at the crack tip necessary for the nucleation of secondary cracks are satisfied first. There is thus the possibility that the maximum fracture velocity theoretically attainable may never be reached, and the velocity may be confined to an artificially low value due to the prior satisfaction of conditions necessary for secondary crack nucleation and the alternative opportunities for energy dissipation these provide. This point might be better illustrated by considering briefly the increase of the kinetic energy associated with the crack during the process of crack propagation first, in an ideal elastic medium and second, in a medium which contains a system of stress raising flaws but is otherwise ideally elastic.

In an ideal elastic medium it can be assumed that the only energy quantities involved in the crack propagation process are, the elastic strain energy released by the passage of the crack, the kinetic energy associated with the recessional velocity of the crack walls and surrounding material, and the potential surface energy of the new surface. In this case the potential surface energy is the true surface energy not the fracture energy. The Griffith criterion, given by Eqn. 5.3.5, governs the condition necessary to extend the incipient flaw. Once a crack is in motion the excess elastic energy released by the crack leads to an increase in the velocity of crack propagation and thus to an increase in the amount of energy dissipated as kinetic energy. It is possible that the crack velocity in the ideal material in this way ought to approach the velocity of sound in the material. It is also possible that for an ideal material there is a real limit to the crack velocity which is less than the velocity of sound in the material due to the development of stress lobes at the crack tip as suggested by Yoffé and Craggs. In either case

the crack velocity should increase smoothly up to these maximum values. In fact the experimentally determined crack velocity in real materials is much less than either the velocity of sound in the material or the numerical estimate provided by Yoffé and Craggs. In order to see a possible reason for this, consider the second material containing a system of stress raising flaws.

In this case the initial extension of the flaw and the subsequent early acceleration of the crack would probably follow a closely similar pattern of development to that of a crack in the first material. However, if it is assumed that at some early stage in the crack propagation process, the stress field at the crack tip is such that the local stress at the flaws ahead of the crack tip reaches the bond strength of the material, then under what conditions can the incipient cracks continue to propagate? An essential condition is that there must be sufficient local elastic energy to support momentarily the propagation of two cracks. If the elastic energy release is only low then the acceleration of the secondary crack is slow and it may be possible for the main crack to overtake it and terminate its propagation. If however the rate of release of elastic energy is relatively high then the secondary crack may continue to propagate and accelerate at the expense of further acceleration by the main crack. The latter is envisaged as either maintaining a constant velocity or even suffering a slight velocity reduction for a short time as a result. The energy dissipated by the propagation of the secondary crack is at the expense of further increase in the kinetic energy of the main crack. If the secondary crack is energetically able to continue to accelerate, it is reasonable to suppose that this process could be

repeated, the stress field at the head of the secondary crack now initiating other incipient cracks at flaw sites. It is conceivable that in this way, by the continuous creation of new crack surface ahead of the main crack front, the fracture velocity could be kept down to an artificially low value.

The value to be assigned to k in the kinetic energy term has been discussed already. As previously stated, Hiorns and Venables have placed the value of unity upon it without stating their source. Numerically, for a glass of soda- lime - silica composition (Schardin (20) glass No 24), Eqn. 6.2.7 yields an extreme value of 78. In the numerical evaluation of Eqn. 6.2.12 below two values for k will be used, one of unity following Hiorns and Venables and one somewhat less than the extreme value yielded by Eqn. 6.2.7 in accordance with what has been said previously.

Roesler (35) showed how experiments on cone cracks in glass could be used to determine the fracture energy. Culf (7) has made a large number of determinations of the fracture energy γ for glass using steel indenters pressed into the glass surface in a hydraulic press. The experimental arrangement allowed the surrounding medium to be varied from liquids to dry gases. Compared with an energy of 3,200 to 4,300 dynes/cm in air (at various humidities), the fracture energy became 7,600 dynes/cm under gaseous nitrogen and 7,800 dynes/cm under gaseous carbon dioxide. A brief consideration of the consequences of using these values for fracture energy (i.e., values obtained from experiments on slow crack propagation) in a situation applying to the propagation of fast cracks will be left until later.

Because of the high value for the fracture energy found by Culf for tests under nitrogen and carbon dioxide, the value for the fracture energy to be used below has been set at 8,000 dynes/cm.

Thus for a soda-lime-silica glass (Schardin glass No 24), substitution of the following numerical information in Eqn. 6.2.12

$E = 7.2 \times 10^{11}$ dynes/cm^2 $\quad V_f = 1.5 \times 10^5$ cm/sec

$\gamma = 8{,}000$ dynes/cm $\quad \rho = 2.57$ gms/cm^3

yields a value of $\sigma c^{\frac{1}{2}} \doteqdot 3$ for $k = 1$

and $\sigma c^{\frac{1}{2}} \doteqdot 4.5$ for $k = 50$.

The correspondence between the experimentally obtained values of $Zc^{\frac{1}{2}}$ for glasses, and the values given by the energy equation as written above, is encouraging notwithstanding the approximations applied.

It is worthwhile examining here what has been said so far about the energy approach as an explanation for the mirror, mist and hackle phenomenon in glass.

First, it has been proposed that the balance between elastic energy released, and kinetic energy and fracture energy together, controls the fracture process. This is not a new concept even when applied to fast moving cracks of the type being considered, (Cameron (16)). However, a specific proposal was made that an important stage in the fracture process for glass is reached when the elastic strain energy released is sufficient to enable two cracks to propagate separately. Further, the onset of hackle as previously described is considered to be a manifestation in the fract surface of the satisfaction of this condition. Finally, the energy balance equation has been re-arranged incorporating this condition to give a numerical estimate for the value of $Zc^{\frac{1}{2}}$ for a glass.

The limitations imposed by using the fracture energies found by Culf for slow fractures in a fast crack environment should be discussed. This is a difficult topic to treat at the present time. It might be expected that effects like plastic deformation, for which the time of passage of the crack through an elemental volume of the material would be all important, should be more severe for slow cracks than for fast cracks in the same material. Hence the fracture energy of a slow crack would be expected to be higher than for a fast crack. However, this results in an anomalous situation, for the fracture energies found by Culf could on this argument, be associated with the quasi-static cracks considered by Griffith in the derivation of Eqn. 5.3.5 Chapter 5. Griffith checked the value of Eqn. 5.3.5 experimentally and theoretically using artificially induced cracks in the walls of glass tube and bulbs and a value for the surface energy obtained by extrapolation from experiments on molten glass. The expression originally given by Griffith (5), was,

$$\sigma = \sqrt{\frac{2 E T}{\pi \nu c}} \qquad 6.3.1$$

where ν is Poisson's ratio for the glass. Eqn. 6.3.1 should be compared with the corrected expression given later by Griffith and written as Eqn. 5.3.5, Chapter 5. They differ only in the presence of the quantity ν. However the numerical and experimental check referred to above was performed with Eqn. 6.3.1. Griffith found experimentally that the value of $\sigma c^{\frac{1}{2}}$ for the propagation of artificially induced cracks in tubes and bulbs was about 240 $lb/in^{3/2}$. The following data concerning the glass he used was given by Griffith,

$$E = 9.01 \times 10^6 \text{ lbs/in}^2$$
$$T = 3.1 \times 10^{-3} \text{ lbs/in} \qquad \nu = 0.251$$

Substitution of these values in Eqn. 6.3.1 yields a value of 266 lbs/in $^{3/2}$ for $\sigma c^{\frac{1}{2}}$ and excellent agreement with experiment. The same information substituted in the modified Eqn. 5.3.5 yields a value of only 133 lbs/in$^{3/2}$ for $\sigma c^{\frac{1}{2}}$, and shows a discrepancy between the later theory and experiement. The value of $\sigma c^{\frac{1}{2}}$ obtained from Eqn. 5.3.5 when the value of T previously used is replaced by Culf's value for γ is 500 lbs/in$^{3/2}$. This result is not much more incompatible with Griffith's experimental value than the 133 lbs/in$^{3/2}$ found as described above. The stress at the tip of the crack is given by Griffith as,

$$\sigma_m = \frac{2\ \sigma c^{\frac{1}{2}}}{\rho^{\frac{1}{2}}} \qquad 6.3.2$$

where σ_m is the stress at the crack tip,

and ρ is the radius of curvature at the crack tip.

Following Griffith, and taking a crack tip radius of 2×10^{-8} in, the theoretical crack tip stress predicted by Eqn. 6.3.2 is 3.4×10^{6} lbs/in^2 for $\sigma c^{\frac{1}{2}} = 240$ lbs/in$^{3/2}$, and 1.9×10^{6} lbs/in^2 for $\sigma c^{\frac{1}{2}} = 133$ lbs/in$^{3/2}$. This already represents stresses of 0.4E and 0.2E respectively.

The stress resulting from using Culf's experimentally measured value for the fracture energy in Eqn. 5.3.5 as a substitute for T is approximately 0.75E. The only way in which the latter result can be made to be physically reasonable is to abandon the concept of an elastic crack, and assume that the tip of the crack does not reduce to atomic dimensions but is somewhat "blunted". This is a reasonable assumption in view of the nature of the fracture energy term, that is, one compounded principally of true surface energy and energy dissipated in plastic deformation.

Thus it may be said that, if the fracture energies measured by Culf have more valid application to slow cracks than to fast cracks, such cracks

are probably not true elastic cracks. This approach can only be made physically consistent by an adjustment of the crack tip radius from a value of about 2×10^{-8} in. to about 25×10^{-8} in. (i.e., 60 Å). This question clearly needs very careful consideration and cannot satisfactorily be answered with the evidence at present available. For the moment, although the application of Culf's measured fracture energies to fast cracks is not positively supported by a consideration of quasi-static crack energetics, the idea is not rejected by it either.

One more point should be mentioned here before attempting an extension of the ideas proposed in section 6.2. That is, Bateson's Eqn 3.5.1 (Chapter 3) should be re-examined in view of the form of Eqn. 6.2.12, to which it bears a resemblance. Using Culf's value for fracture energy as given above instead of the surface tension, Eqn. 3.5.1 predicts a value of 1 $Kg/mm^{3/2}$ for $Zc^{\frac{1}{2}}$. The numerical values given by the equation are therefore still too low despite the general similarity between Eqns 3.5.1 and 6.2.12. The general observations concerning the physical assumptions made by Bateson and discussed in Chapter 3, Section 3.5 are still valid. It is suggested that the correspondence between the equations is a fortuitous one.

6.4 Extension of the energy hypothesis

So far the energy hypothesis, as embodied in Eqn. 6.2.12 has given encouraging numerical agreement with experiment. The approach to the bifurcation condition in glass also explains the source of the energy responsible for the propagation of the micro-cracks observed in the mist region. In the mist region the rate of release of s train energy is greater than that required for the propagation of one single crack but not yet sufficient to support the propagation of two independent

cracks. The result is the propagation of semi-independent micro-cracks which can be used to explain in a qualitative fashion the micro-structural aspects of the mist region. However, if the energy balance approach is to be really useful in explaining the appearance of morphological transition zones on fracture surfaces, it ought to be applicable to materials other than the inorganic glasses.

The value of $Zc^{\frac{1}{2}}$ according to Eqn. 6.2.12 is proportional to the square root of the fracture energy where this term has tacitly been given the properties of a constant of the material. In addition, when the minimum requirement for bifurcation was self-evidently the propagation of two cracks (F', F" - Fig. 2 (b)) instead of one, the condition required to satisfy this could easily be inserted in Eqn. 6.2.10. In contrast any energy dissipating process which produces only a qualitative change in the appearance of the fracture surface cannot be treated in the same simple way. When elastic energy in excess of that required to balance the basic equation is available, the mechanisms employed by the material to dissipate this will depend solely on the nature of the material itself. The particular morphological appearance of the fracture surface will depend to a very great extent on the modes of operation of those mechanisms. Thus, in glass, the energy argument gives no information on the way in which new surface area is to be created and what will be the result of the creation of such new surfaces on the external appearance of the fracture surface. In materials other than glass it is even more difficult to say, merely from a consideration of their physical properties, which processes will be important at any particular stage in the fracture process as dissipators of energy. Non-isotropic

substances will demand different considerations again. For example the body centred cubic crystal α - Fe posesses a theoretical surface energy of 1400 dynes/cm for the (100) cleavage plane and 5,300 dynes/cm for the (111) cleavage plane (Gilman (33)). A crack propagating in the (100) plane could dissipate five times more fracture energy by producing clearage steps with side faces in the (111) plane. Thus quite small cleavage steps could dissipate as much energy as the main crack surface in the (100) plane. On the other hand, a crack propagating primarily in the (111) plane would not find cleavage steps a satisfactory way of dissipating excess elastic energy. It is not intended to propose that these particular processes actually operate during fracture in α - Fe , this is merely offered as an illustration of the type of problem which might be encountered. Haneman and Pugh (40) have recently published some interesting results of work performed on n-type single crystal Germanium. These tests were performed in tension and bending with the (111) plane of the crystals perpendicular to the tensile forces. In both cases the same result was observed on the fracture surface. Fracture took place in the (111) plane and a transition zone was apparent on the fracture surface centred about the origin of fracture which was on the original free surface of the specimen. The transition zone consisted of the production of large numbers of "tear" lines or cleavage steps starting together and distributed along the arc of a circle. Haneman and Pugh found that the product of the breaking strength and the square root of the distance from the origin to the arc was a constant with a value of about 3.3 $Kg/mm^{3/2}$. They drew attention to the correspondence between this relationship and the empirical relationship found for glass,

but sought to explain the phenomena in terms of a critical velocity condition quoting Shand (4), Bateson (18) and Mott (6) in support. This idea has already been discussed in Section 3.5 and rejected. Using the ideas developed so far in this chapter the production of cleavage steps would be identified with a critical energy condition. According to Gilman (33) the theoretical surface energy of Germanium is 726 dynes/cm for the (111) plane and about 1000 dynes/cm for (100) and (110). What the fracture energy for Germanium is in the (111) plane is unknown at the present time, but if it is a constant of the material, a $Zc^{\frac{1}{2}}$ dependence would be expected for any transition zone in accordance with the form of Eqn. 6.2.12. The criterion for cleavage step production in this case is that the rate of release of strain energy reaches a critical value for the (111) plane. In one sense this might be regarded as a similar stage to that for glass during which mist is produced. If the fracture energy of the (111) plane in Germanium and the fracture velocity in the same plane were known, the numerical evaluation for Eqn. 6.2.12 could again be checked and compared with Haneman's and Pugh's result. A point which has been made above and which was also remarked upon by Haneman and Pugh is that arguments in terms of quantities of energy do not explain events on an atomic scale. That is, it is still necessary to discover the physical mechanism which is responsible for the energetically feasible cleavage steps becoming a physical reality. In the past the production of cleavage steps in crystalline materials has been identified with the intersection of screw dislocations by the crack (Gilman (33)). Haneman and Pugh claimed that this was not the mechanism responsible in this instance since etch pits did not appear when the material was etched

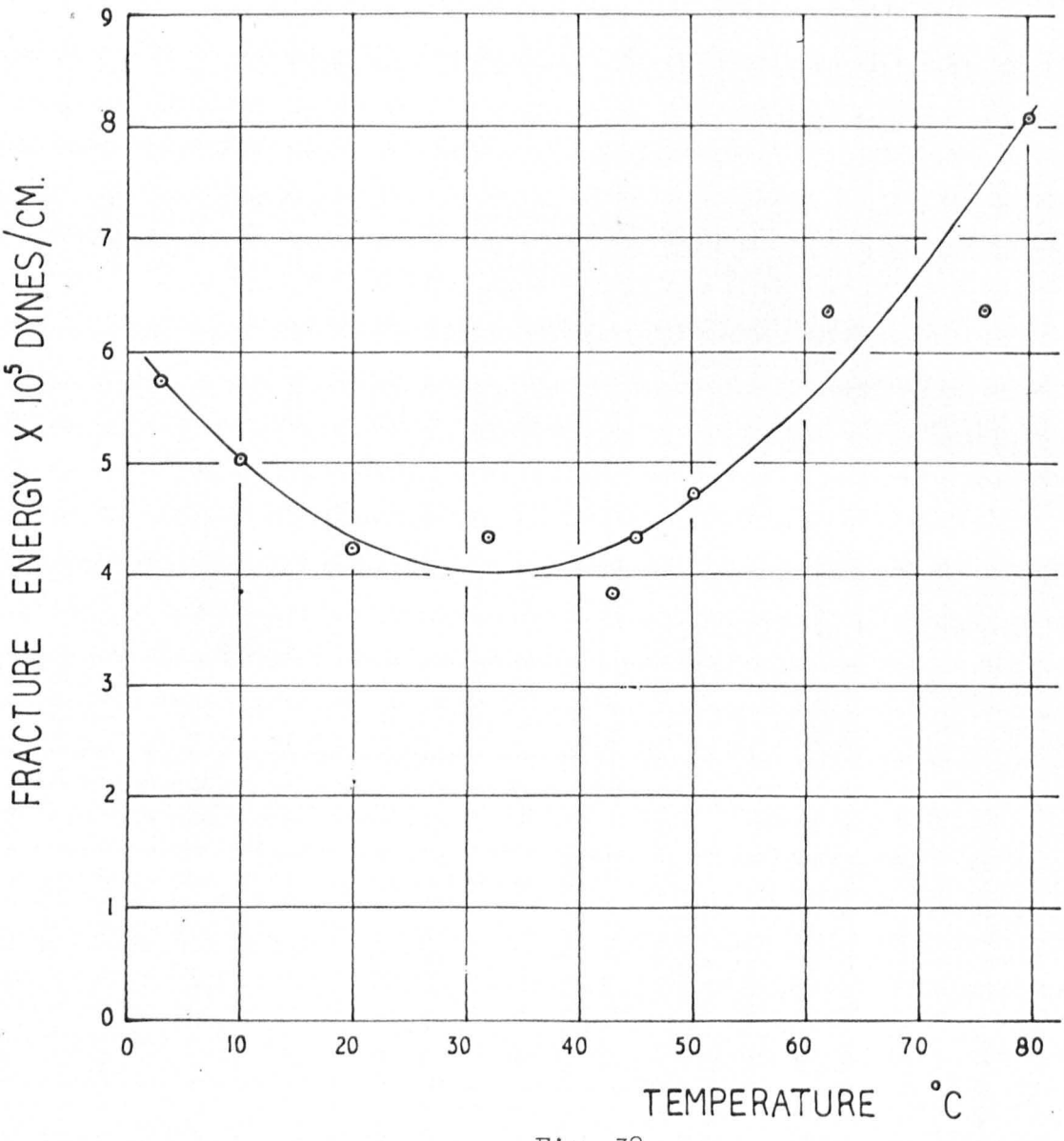

Fig. 38

Showing the fracture energy of perspex as a function of temperature.

with a suitable etchant. However it is not certain that stress induced dislocations (as opposed to grown-in dislocations) can be revealed in this way.

One material which shows a sequence of morphological characteristics on its fracture surfaces similar to those of glass is perspex (i.e., polymethyl methacrylate). There is also a considerable body of useful data already available concerning its physical, and fracture, properties. Benbow (36) has published data for the fracture energy of perspex as a function of temperature between $0^{\circ}C$ and $80^{\circ}C$. This information was again derived from a study of the propagation of stable cracks. Essentially, the apparatus used by Benbow consisted of a wedge used for opening the crack gradually and a system of clamps designed to render the crack directionally stable. Benbow's results are given in graphical form in Fig. 38. It should be stated here that Svensson (41) also reported a variation in the value of the fracture energy for perspex with temperature, but not of this form.

The correspondence between the form of the curve of Fig. 38 and that of Fig. 14 giving $Zc^{\frac{1}{2}}$ for X8 glass as a function of temperature, is quite striking within the temperature limitations of the respective figures. Using Benbow's figures for the fracture energy of perspex at room temperature it is possible to predict a value of $Zc^{\frac{1}{2}}$ for perspex using Eqn. 6.2.12 and assuming that the crack reaches a bifurcation condition in the same way as a glass fracture. The values for the other quantities given below are taken from Schardin's published data.

γ = 4.2×10^6 dynes/cm (at 20°C)

E = 5.35×10^{10} dynes/cm^2

ρ = 1.18 gms/cm^3 $\qquad$ V_f = 300 - 650 m/sec

$Zc^{\frac{1}{2}} \div 5$ Kg/mm$^{3/2}$ $\qquad$ for k = 1

$Zc^{\frac{1}{2}} \div 6$ Kg/mm$^{3/2}$ $\qquad$ for k = 50.

This is an interesting result, for it predicts a value of $Zc^{\frac{1}{2}}$ of the same order as that for glass despite the fact that the two materials have very different properties.

6.5 Summary and suggestions

The work described in this and the preceding chapters comprises an investigation into the observation of the empirical relationship $Zc^{\frac{1}{2}}$ = constant, the value of this constant, and the significance of the mirror, mist and hackle pattern. The first part of the investigation consisted of a series of experiments conducted in tension and bending on a number of silicate glasses, but principally X8, which produced a body of information on the value of the constant in the mirror relationship mentioned above. The immediate result of this accummulation of numerical data, was to suggest a way in which the different mirror shapes, empirically observed to be characteristic of certain experimental stressing systems, could be predicted and drawn. The suggestion basic to these proposals was that the interpretation to be placed upon the quantity Z in the mirror relationship is that of the local tensile stress, existing immediately prior to fracture, at that point in the body where bifurcation of the crack subsequently takes place. A wider interpretation of the numerical results could not be made until the physical significance of the mirror, mist and hackle

phenomenon had been attempted. Part two of the experimental work was concerned with this problem. Examination of the features of the mist area disclosed the existence of very large numbers of stopped sub-surface micro-cracks below the fracture surface which could be correlated with specific fracture surface features. Subsequently it was found possible to subdivide the constituents of the mist features into two groups, and explain, in a qualitative manner, how these arise due to the interactions of groups of micro-cracks developed at the crack front. The observations of the multiplicity of these micro-cracks in the mist region drew attention to the large amounts of excess elastic energy dissipated in this way. This chapter has been mainly concerned with a simple discussion of the energetics of brittle and semi-brittle fracture for real materials, culminating in an attempt to formulate a theoretical equation for the mirror relationship. Such an equation has been proposed, based on the work of Griffith and Mott and the values of $Zc^{\frac{1}{2}}$ predicted by it agree well with experiment. The mirror, mist and hackle phenomenon has its equivalent in materials other than the silicate glasses, and it is thus to be expected that the theoretical equation should be capable of accounting for these cases too. The numerical value of $Zc^{\frac{1}{2}}$ for perspex has been calculated as predicted by the equation and at the present time experiments are being conducted to determine this value empirically.

The present form of Eqn. 6.2.12 indicates that the value of $Zc^{\frac{1}{2}}$ should depend principally on the fracture energy. It is in this area that further work is most urgently required. That is, it is necessary to show conclusively that the value of $Zc^{\frac{1}{2}}$ depends upon the fracture

energy. In order to do this it may be necessary to measure both the fracture energy and the value of $Zc^{\frac{1}{2}}$ on material taken from the same production batch. This could be particularly important for the polymers where a change in the structure and molecular weight is reflected by a change in the fracture energy. The amount of information at present available concerning the fracture energy of various materials is very small and it may be necessary to embrace more types of material. Some experiments are being performed at present in this laboratory in an attempt to measure the value of $Zc^{\frac{1}{2}}$ for perspex as a function of temperature in order to compare this with Benbow's fracture energy curve given as Fig. 38. It should also be profitable to attempt to induce cone cracks in glass at various elevated temperatures.

If the value of $Zc^{\frac{1}{2}}$ does indeed depend on fracture energy, one outstanding problem which remains is why the value of $Zc^{\frac{1}{2}}$ is higher for silica than for X8 and lead glasses. At present this can only be explained by assuming that the crack does plastic work to a constant and fixed distance from its tip irrespective of the glass in which the crack propagates. In this way more work could be associated with fracture in silica than with the other silicate glasses. However this explanation is clearly unsatisfactory, conflicting as it does with the observation that cone cracks in the soft glasses remain open while those in silica do not (implying in the latter case that little plastic deformation has taken place). Furthermore the explanation would have to be confined to the silicate glasses and could not be generalised to include other materials.

Apart from the primary problems there are a number of subsidiary problems associated with the formulation of Eqn. 6.2.12. One of these is the question of what value should be assigned to the constant k in Mott's kinetic energy expression.

The energy hypothesis gives no indication of the type of morphological transition boundary to be expected in any particular material. Some materials will clearly have many more energy dissipating mechanisms available than others and additional complications may arise when the material is non-isotropic. The development of a particular morphological feature may also depend to some extent on the degree of chemical homogeneity or structural perfection possessed by a particular sample when compared with the ideal structure for the same chemical composition. As an example, consider perspex which shows a morphology in which conic figures are typically developed as a result of secondary cracks generated at defect sites. Acrylates in general with a filler added display conic figures in profusion with particles of filler at the foci of the conics. It is therefore fair comment to say that in all probability the secondary nuclei responsible for the development of conic figures on fracture surfaces in commercial perspex are not an intrinsic part of the structure of perspex. If this is so, a refinement of the manufacturing process might eradicate these defect centres and with them the conic figures. A different fracture morphology would be expected from such a refined material.

Within the narrower limits of the mirror, mist and hackle phenomenon in silicate glasses there are some interesting untouched problems. The presence of stopped micro-cracks below the surface in the mist region was demonstrated and the main mist features were explained qualitatively in terms of the interaction of groups of micro-cracks at the head of the crack. It was suggested that secondary nucleation at unspecified defect sites was responsible for the formation of these cracks, but this is conjecture with very little positive supporting evidence as far as glass is concerned. Also arising directly out of the presence of the micro-cracks, is the fact that very little is known, either theoretically or experimentally, about the properties of crack arrays of the type which must result from the presence of many small cracks at the head of the fracture.

Appendix I

A calculation concerning the position of the neutral zone in "as received" glass rod assuming that a paraboloidal temperature distribution develops in the rod during cooling from its softening temperature and finally, as a result of this, a paraboloidal stress distribution develops in the rod.

An essential condition is also that the body should be in mechanical equilibrium under the action of the internal stresses. For this, the sum of the tensile stresses inside the neutral zone must be equal to the sum of the compressive stresses outside the neutral zone.

In Fig. A1 below, a longitudinal section through a length of glass rod is represented. Only the one half of the section is drawn so that CD represents one free surface and OX is the geometrical axis of the rod. The intersection of this section with the neutral zone cylinder is represented by the dashed line EF . A parabola OLP is drawn on the figure representing the thermally induced stress distribution in the rod, so that the stress normal to any point on MQ is given by the length of the line normal to MQ from that point to the curve OLP . Within the area A such stresses have been defined as tensile stresses by the same token within the area B the stresses are compressive. The neutral point is represented by L .

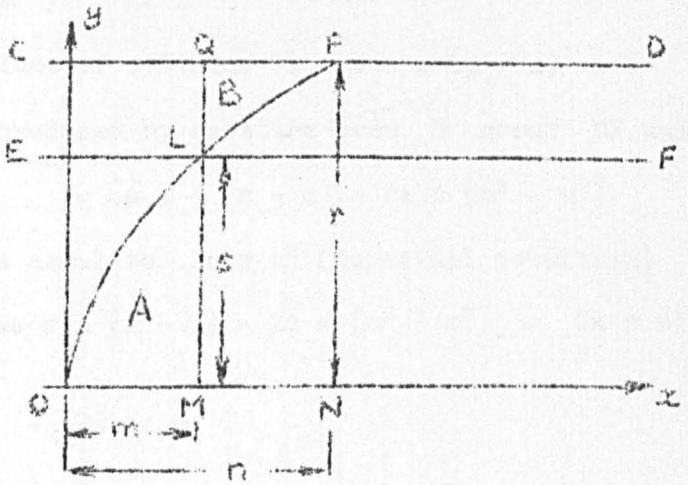

Fig. A1

The general equation of the parabola OLP is $y^2 = 4a\,x$.

Volume described by area A in rotating parabola about OX

$$V_A = \pi \int_0^m y^2\,dx$$

$$= \pi \int_0^m 4a\,x\,dx = 2a\,\pi \left[x^2 \right]_0^m$$

$$= 2a\,\pi\,m^2$$

Volume traced out by parabola between ON by rotating about OX is similarly,

$$= 2a\,\pi\,n^2$$

∴ Volume between M - N

$$= 2a\,\pi\,n^2 - 2a\,\pi\,m^2$$

$$= 2a\,\pi\,(n^2 - m^2)$$

Volume of cylinder of length $(n - m)$ with radius y

$$= \pi\,y^2\,(n - m)$$

when $x = \mathbf{n}$ $y^2 = 4a\,n$

$\therefore$ Volume of cylinder $= 4a\,\pi\,n\,(\mathbf{n} - m)$

$\therefore$ Volume produced by rotating area B about OX axis is,

$$= 4a\,\pi\,n\,(n - m) - 2a\,\pi\,(n^2 - m^2)$$

and this is equal to $2a\,\pi\,m^2$ (essential condition)

i.e., $4a\,\pi\,n\,(n - m) - 2a\,\pi\,(n^2 - m^2) = 2a\,\pi\,m^2$

$\therefore$ $n^2 - 2m\,n = 0$

and $2m = \mathbf{n}$

when $x = \mathbf{n}$ $y = r$

$\therefore$ $r^2 = 4a\,n$

when $x = m$ $y = s$

$\therefore$ $s^2 = 4a\,m$

but $n = 2m$

$\therefore$ $r^2 = 8a\,m$

and $s^2 = 4a\,m$

i.e., $r^2 = 2s^2$

and $s = \dfrac{r}{\sqrt{2}}$

The distance from the geometrical axis of the rod to the neutral axis is $\dfrac{r}{\sqrt{2}}$ approximately.

Appendix II The Linnik (42) interference microscope

The Linnik (42) interference microscope is a valuable, but apparently not well known, application of Michelson's interferometer to the study of the microtopography of surfaces. The special features of Linnik's instrument are as follows. First, it allows high power objectives to be used with ease. Second, a thin film interference pattern of a surface can be secured without the necessity of placing a reference flat near the surface. The essential Linnik arrangement is shown diagrammatically below.

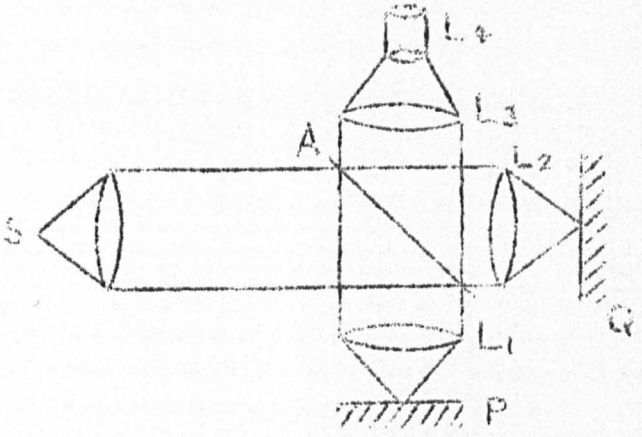

Diagram 1

The light source S is placed at the focus of a lens set to project parallel light on a beam splitter A . The beams from A pass to two microscope objectives L_1, L_2. The surface under study is P, and Q is a reference plate. The lenses L_1, L_3 and L_4 constitute a microscope. The distance between L_1 and P is adjusted so that P is in good focus. Q is brought to the correct plane to be in focus for the equivalent microscope L_2, L_3 and L_4 . Therefore not only is the object P in view but in addition, localised interference fringes are superposed on the image and thus give a contour pattern referred to the flat Q .

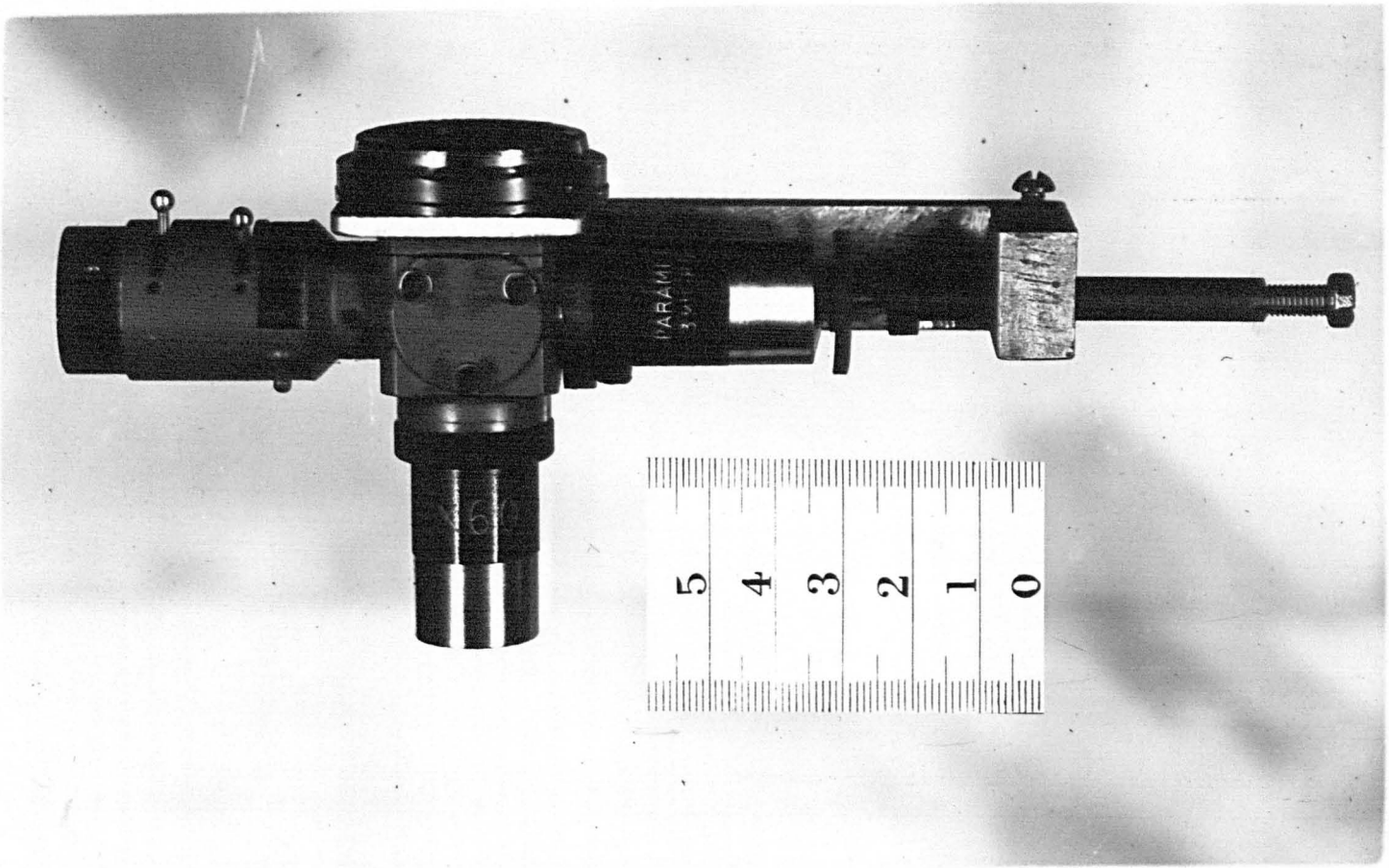

Fig. 39

Photograph of the double objective Linnik interferometer. Scale shown is in centimeters.

The instrument as constructed for use in the present studies was conceived and made as a microscope attachment, see Fig. 39. In the construction, a Beck vertical illuminator was used as the basic unit. The Beck illuminator has a lens and double iris train in an arm leading to the beam splitter which is housed in a central hollow metal cube of 1" sides. From the central cube there exist three convenient light exits in the correct positions as required by Diagram 1 above. The first is the normal one carrying the objective L_1 . Vertically above this the second exit communicates in the normal way with the main microscope barrel. The third exit, opposite the light source, in the Beck system is usually blocked by an inclined dark plate designed to eliminate light rays transmitted from the beam splitter when the instrument is used conventionally. This plate was removed and the entrance provided with a screwed sheath enabling a second objective L_2 to be added to the assembly. It only remained necessary to provide some convenient method of independent adjustment for the comparison plate Q . This was accomplished by adding a light metal beam to the beam-splitter housing, extending some 5 cm beyond the end of the objective L_2 . The end of this beam carried a hollow barrel pointing towards the objective L_2 and mounted on its optic axis. A sliding piston inserted in the barrel carried the comparison plate at its front end, and could be advanced towards L_2 by a screw thread pushing from the rear. Withdrawal of the comparison plate from L_2 was effected by a spring loading arrangement inside the hollow barrel. In this way the comparison plate could be advanced without rotation, thus preserving the angular relationship of the plate Q with the surface P .

In order to obtain the best results with this instrument the total light paths of the split rays must be equal. In a laboratory instrument such as this it was not possible to match carefully the objectives L_1 and L_2 . Nor was it possible to use the ideal beam-splitter i.e., a cube made from two right angled prisms with the interface silvered to split the light into two beams of equal intensity. Instead a half silvered microscope cover slip was used. It is possible to see fringes even when the light paths are not exactly equal by using monochromatic light sources having sharp spectral lines, e.g., low pressure sodium or mercury vapour lamps. However one of the conditions for achieving good contrast of the fringes is that the reflected rays from P and Q should be equal in intensity. This means that uncoated glass objects should be compared with a plain glass plate. The image intensity with such combinations is far too low to be useful when the illuminant is a low pressure vapour lamp. Consequently a high pressure mercury vapour lamp must be used or a high intensity white light source. It can be shown that for the mercury lamp high pressure broadening of the spectral lines causes the fringes to be obscured. For white light of course fringes will only be seen very close to the zero path difference condition. Provided that the discrepancy between the path lengths is not too great it can be accommodated by partly unscrewing one of the two objectives depending on which arm contains the shorter path length. This is the method adopted in the present instance. The path length is increased until, using white light, the central black fringe appears in the middle of the field of view. The use of the high pressure mercury vapour lamp combined with suitable filters, under these conditions, yields an extensive area of sharp fringes with maximum contrast.

REFERENCES

1.	Smekal. A	J. Soc. Glass Technol.	20	432	1936
2.	Levengood. W.C	J. Appl. Phys.	29	820	1958
3.	Shand. E.B	J. Amer. Ceram. Soc.	37	559	1954
4.	" " "	" " " "	37	52	1954
5.	Griffith. A.A	Phil. Trans. A.	221	163	1920
6.	Mott N.F	Engineering	165	16	1948
7.	Culf. C.J	J. Soc. Glass Technol.	41	157	1957
8.	Preston. F.W.	J. Soc. Glass Technol.	10	234	1926
9.	Poncelet. E.F	J. Soc. Glass Technol.	42	279	1958
10.	Andrews. E.H	J. Appl. Phys.	30	740	1959
11.	Murgatroyd. J.B	J. Soc. Glass Technol.	26	156	1942
12.	Terao. N	J. Phys. Soc. Japan	8	545	1953
13.	Timoshenko. S	"Strength of Materials" Part I Chapter VI D. Van Norstrand Comp. Inc.			
14.	Stirling. J.F	J. Soc. Glass Technol	39	134	1955
15.	Orr. L	Private communication			
16.	Cameron. N.M	T. and A.M. University of Illinois Report No 242 April 1963			
17.	Shand. E.B	J. Amer. Ceram. Soc.	42	474	1959
18.	Bateson. S	Phys. Chem. Glasses	1	139	1960
19.	Dietzel. A	Quoted by Stanworth "Physical Properties of Glass" p. 195			
20.	Schardin. H	Review article in "Fracture" Ed. Averbach et. al Wiley			1959
21.	Orowan. E	Nature	154	341	1944
22.	Dulaney. E.N and Brace. W.F	J. Appl. Phys.	31	2233	1960
23.	Berry. J.P	J. Mech. Phys. Solids	8	194	1960

24.	Smekal. A	Glastech. Ber.	23	186	1950
25.	Jones. G.O	J. Soc. Glass Technol	83	120	1949
26.	Anderson. O.L	Review art. in "Fracture" Ed. Averbach et. al. Wiley			1959
27.	Hawkins. F.S	(General Electric Co., Ltd.)	Private Communication		
28.	Yoffé. E.H	Phil. Mag.	42	739	1951
29.	Craggs. J.W	J. Mech. Phys. Solids	8	66	1960
30.	Wolock. I., Kies. J.A., and Newman S.B	Article in "Fracture" Ed. Averbach et. al. Wiley			1959
31.	Poncelet. E.F	Stanford Research Institute Lab. Tech Report 001 - 60			1960
32.	Benbow J.J. and Roesler. F.C	Proc. Phys. Soc. B	70	201	1957
33.	Gilman. J.J	Article in "Fracture" Ed. Averbach et. al			Wiley 1959
34.	Inglis. C.E	Trans. Inst. Naval. Arch. (London)	55	223	1913
35.	Roesler. F.C	Proc. Phys. Soc. B	69	981	1956
36.	Benbow. J.J	Proc. Phys. Soc.	78	970	1961
37.	Irwin. G.R and Kies. J.A	Welding Res. Suppl.	31	95	1952
38.	Wells. A.A and Post. D	Proc. Soc. Exptl. Stress Anal.	16	69	1958
39.	Hiorns. F.J and Venables. J	British Coal Utilisation R.A. Bulletin	25	369	1961
40.	Haneman. D and Pugh. E.N	J. Appl. Phys.	34	2269	1963
41.	Svensson. N.L	Proc. Phys. Soc.	77	876	1961
42.	Linnik.	See "An Introduction to Interferometry" by Tolansky.S (Longmans) p.113			

Postscript

It was mentioned in the discussion that experiments were being conducted to test the prediction made from Eqn. 6.2.12 that the value of $Zc^{\frac{1}{2}}$ for perspex should be about 5 - 6 $Kg/mm^{3/2}$. These experiments have been made by Mr. W. Brearley of these laboratories assisted and directed by the author. A detailed account of the work will not be given here. Briefly, the tests were carried out in tension, at first at room temperature, using specimens cut from cast perspex sheet 1 cm thick. Rectangular bars measuring 1 cm x 1 cm x 10 cm were cut from such sheet. The central region of each bar was reduced to 2 - 3 mm by turning in a lathe fitted with a four jaw chuck, using a cutting tool shaped to cut a smooth, curved, necked-section with a curvature of about 2.5 cms radius. Specimens tested without further treatment to the necked section failed at such low stress levels that bifurcation could not be induced in specimens of this diameter at the neck. However, successful bifurcation of the crack was finally induced in these samples by hand polishing the machined region with fine emery paper followed by jeweller's rouge. About a dozen specimens from which a value of $Zc^{\frac{1}{2}}$ could be obtained were tested at room temperature using this procedure. The value of $Zc^{\frac{1}{2}}$ thus determined varied from about 7 - 12 $Kg/mm^{3/2}$. This is a value in reasonable agreement with that expected from Eq. 6.2.12.

In view of Benbow's results for the value of the fracture energy of perspex as a function of temperature (as given in Fig. 38) Mr. Brearley then endeavoured to obtain the value of $Zc^{\frac{1}{2}}$ for perspex as a function of temperature. This work had to be abandoned because it was discovered that the fracture morphology of perspex changes rapidly

over the range 0 - 80°C and a $Zc^{\frac{1}{2}}$ measurement was rendered impossible. There also appears to be a fracture morphology change at low temperatures (about - 190°C), but it is possible that this change is associated more with the presence and action of internal flaws in the perspex than with changes in the physical and chemical properties of the material. At low temperatures the resulting fracture surface shows that the secondary cracks originating at internal flaws have travelled nearly equal radial distances in every direction from any one flaw. Thus instead of the elongated conic figures observed on the fracture faces of specimens tested at room temperature, the low temperature tests produced a fracture surface entirely covered by a cell-like structure of polygons with the flaws at the centres of the polygons. This indicates that at low temperatures failure occurs by a number of cracks being generated simultaneously, or in rapid succession at a number of separate sites on one plane in the specimen. If this is indeed the mechanism, this draws attention to the problem of measuring the fracture velocity in materials like perspex in which some stage of the fracture process is accomplished by the nucleation of secondary cracks at flaw sites. In these cases the time taken to sever the specimen depends upon the distance between the flaws, the velocity of propagation of the secondary cracks and the velocity of sound in the material.

During this experimental period Mr. Brearley and the author also constructed a number of machines designed to deliver a tensile impact blow to a specimen. Ostensibly the purpose here was to attempt to deal with the change in fracture properties of perspex at high temperatures by delivering a tensile load at high loading rates. In fact no

perspex specimen was ever tested in such a machine but each machine was tested using X8 glass specimens in rod form since the behaviour of this material and its $Zc^{\frac{1}{2}}$ value was by now well documented for normal loading rates. The devices are mentioned here for their own intrinsic interest and the possibility that in the future they could be used to provide more information on the fracture process. The first group of machines were all essentially pendulums. The bottom end of the pendulum was designed so that it would fall "astride" the specimen which was mounted horizontally at the bottom dead centre of the pendulum swing. The pendulum could by this means be made to deliver a tensile blow to a tup fixed to the end of the glass specimen. Such a blow according to Kolsky (P1), generates a steep fronted stress wave travelling up the specimen in which the peak value of the stress σ_m is given by

$$\sigma_m = \rho V_L v_o \qquad \text{(Pa)}$$

where ρ is the density of the material,

V_L is the velocity of longitudinal sound waves in the material,

and v_o is the "particle" velocity acquired by the rod end as a consequence of being struck.

This stress falls away exponentially from the peak value in a manner given by the equation

$$\sigma = \rho V_L v_o \exp - \frac{A \rho V_i t}{M} \qquad \text{(Pb)}$$

where σ is the stress in the rod at the struck end at time t,

A is the cross-sectional area of the rod,

M is the mass of the striker,

and t is the time elapsed after the impact.

The mass of the striker therefore determines only the "flatness" of the exponential tail to the stress pulse and not its peak value.

Some of the difficulties of impact testing lie in the fact that stresses are usually difficult to determine since multiple reflections of the stress wave often take place within the specimen before the local stress achieves a sufficiently high value to cause fracture. In the author's experiments this difficulty was thought to be avoided. The specimens were made in the form of long rods (1 metre) of 3 mm or 5 mm diameter cane. This length of cane was placed horizontally on rollers and otherwise unconstrained. One end carrying the tup was placed at the bottom dead centre point for the fall of the pendulum. The mass of the striker (M in Eq. Pb) was usually made sufficiently large that the stress fell away from the peak value only very slowly i.e., the exponential "tail" was quite flat. The specimen was predisposed to fracture at a point near the tup by damaging it there quite severely with a glass knife. Upon striking the tup with the pendulum a steep fronted stress wave was generated in the glass rod. If the passage of the stress pulse generated a crack at the glass-knife-damage fracture could be completed before the head of the stress pulse arrived back at this point again. (This is because of the relative magnitude of the quantities involved, viz. the length of the specimen was effectively 2,000 mm while the specimen thickness was only 3 - 5 mm . The velocity of crack

propagation is approximately 2/5 of the velocity of longitudinal sound waves in the material). In the event of fracture occurring, part of the exponential stress "tail" would be reflected by the new free crack-surface and returned to the striking element. The tup, plus a short length of the specimen was in this way struck from the rod-end by the pendulum and was caught in a bag. The rest of the rod in this case stayed quite still. If, however, fracture was not initiated, the stress pulse returning from the distant end of the rod was able to reach the striker of the pendulum. This stress pulse, returning as a wave of compression, in effect carried the information to the pendulum that the distant end of the rod was unconstrained. The whole rod was therefore caused to move in the direction of its length by the striker. While this was usually catastrophic as far as preserving the rod intact was concerned the system had the overwhelming advantage that "successful" and "unsuccessful" tests could be clearly differentiated. Also, in the event of a successful test, the stress at which failure occurred could be simply determined to within 4% or 5% by using Eqn. Pa provided that the mass M was large enough for the exponential stress tail to be considered flat. Tests made with the pendulum machines indicated that the value of $Zc^{\frac{1}{2}}$ for X8 rod tested in this way had the same value as that obtained in normal loading rate tensile tests.

The statement was made in Chapter I, Section 1.2 that a crack nucleated at a local flow on the surface propagates perpendicularly to the tensile axis for a distance depending on the severity of the surface flaw. The impact experiments make it clear that the flaw size is in fact of only secondary importance. The mirror size in impact tests

is a function of the striker velocity (i.e., the peak stress value) and not a function of the severity of the damage as in normal tensile tests. In impact tests the surface damage serves merely to initiate fracture, bifurcation is determined by the general stress level existing in the specimen which in turn is dictated by the striker velocity. This supports the assertion made in Chapter 3, Section 3.2 that it is the local stress level which is important. It is felt that further impact tests of this type could yield very useful information about the degree of interaction of a crack with a stress field by using pulsed stress techniques.

These further experiments indicate that the experimental value of $Zc^{\frac{1}{2}}$ for perspex agrees very well with the value predicted by Eqn. 6.2.12. An attempt to follow the variation of $Zc^{\frac{1}{2}}$ for perspex with temperature failed because of the change in fracture morphology of perspex with temperature. However the agreement of the experimental values for $Zc^{\frac{1}{2}}$ for glass and perspex with the values for $Zc^{\frac{1}{2}}$ predicted by Eqn. 6.2.12 is thought to be sufficiently good to warrant further investigation along the lines discussed earlier.

References

(P1) Kolsky H. "Stress waves in solids" Clarendon Press